

Abstracts of Poster Presentations at the Canadian Society For Pharmaceutical Sciences (CSPS) Symposium

June 11-13, 2024 – Edmonton, Alberta, Canada



Functional group transfer oligodeoxynucleotide probe for site-selective internal modification of RNA; application to tritium labeling and functional modulation of RNA with a diverse molecule

Shigeki Sasaki

Nagasaki International University

Purpose. Since site-specific chemical modification of RNA affects RNA function and biodistribution, it is desirable to develop efficient methods. The aim of this study is to develop a selective modification method using oligonucleotides.

Method. We have developed a method that allows chemical modification of the predetermined internal position of RNA based on the formation of a hybridized complex with artificial nucleic acids (Figure 1). This method is used to introduce the pyridinyl keto group onto the 4-amino group of cytidine or the 6-amino group of adenosine.

Results. The modified structure can be reduced with NaBT_4 to produce specifically tritium-labeled nucleic acids, which are useful for studying the biodistribution of nucleic acid therapeutics.¹ In addition, a variety of molecules can be conjugated to the pyridinyl keto group by the click reaction.² Chemical modification of mRNA is expected to affect its function, such as translation.

Conclusion. This paper presents some examples of the application of the functional group transfer oligodeoxynucleotide probe.

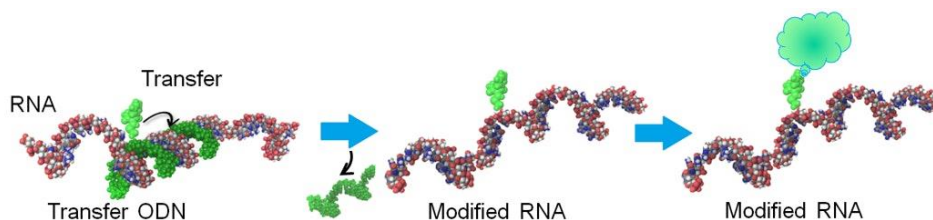


Figure 1. Functional group transfer for the internal modification of RNA

References

Chem. Pharm. Bull. 2023, 71 (1), 64-69.

Chem Pharm Bull 2022, 70 (7), 498-504.

Design and synthesis of Polo like and phosphoinositide-3- kinase inhibitors as anticancer agents.

Tabassum Khan¹, Mrunal Jadhav¹

¹SVKM's Dr. Bhanuben Nanavati College of Pharmacy

Purpose: Kinases are important in various cellular processes, any alteration or mutations in kinases which may cause gain or loss of function can cause cancer. Polo like Kinases (PLKs) and Phosphoinositide-3-Kinase (PI3K) are under evaluation as potential targets for designing anticancer drugs. This research focuses on design and synthesis of entities targeting kinases, implicated in cancer.

Methods: In the present work we designed a series of compounds containing 2,4-diaminopyrimidine and benzimidazole scaffolds as PLK and PI3K inhibitors by using in-silico computational chemistry approaches. The synthesized compounds were purified by chromatography and identity was confirmed by IR, Mass and NMR spectroscopy. They were evaluated for their physiochemical and molecular properties in-silico using Quik Prop. Biological evaluation of these compounds by MTT assay was conducted in human ovarian cancer (SKVO3), leukemia (THP1) and C6 cell lines, followed by *in vitro* enzyme inhibition assay.

Results: Molecular docking of the designed compounds with PLK and PI3K showed that the compounds formed favorable interactions with the amino acids in the hinge region such as Cys133, Leu59, reported to be responsible for PLK inhibition and Val 851, Tyr 836, Trp 780 and Asp 810 responsible for PI3K inhibition. The docking scores of the synthesized compounds was found to be in the range of -5.1 to -8.0 Kcal/mol and -4.98 to -7.86 Kcal/mol for PLK and PI3K respectively. The compounds adhered to Lipinski's rule of five and biological evaluation of these compounds by MTT assay indicated the compounds exhibited concentration dependent cytotoxicity. Compound 8 (4-(4-Ethyl-piperazin-1-yl)-6-methyl-pyrimidin-2-ylamine), compound 16 (6-Methyl-N4-propyl-pyrimidine-2,4-diamine) and compound 27 ((4-Chloro-phenyl)-(5-methyl-1H-benzimidazol-2-ylmethyl)-amine) exhibited inhibition of PLK and PI3K with low IC₅₀.

Conclusion: These compounds have encouraging binding affinity to PLK and PI3K and good *in vitro* cytotoxicity making them strong leads for development of anticancer entities via PLK and PI3K inhibition.

Computational Modelling of The Mode of Binding of the SGLT2 inhibitors, Ertugliflozin and Dapagliflozin with the human Cardiac Sodium Ion Channel Nav1.5.

Arkapravo Chattopadhyay¹, Peter Light², Khaled Barakat¹

¹Faculty of Pharmacy and Pharmaceutical Science, University of Alberta, Edmonton, Alberta, Canada, ²Department of Pharmacology, Faculty of Medicine and Dentistry, University of Alberta, Edmonton, Canada

Purpose: Sodium-Glucose Co-Transporter 2 (SGLT2) activity promotes reabsorption of glucose in the kidneys. Four SGLT2 inhibitors have been approved as anti-diabetics drugs, namely Canagliflozin, Dapagliflozin, Empagliflozin and Ertugliflozin. Except Ertugliflozin, all other SGLT2 drugs are highly cardioprotective. Our recent results indicate that Empa-, Dapa- and Canagliflozin inhibits the late component (late I_{Na}) of the human cardiac sodium channel (hNav1.5) that may underlie the unexpected cardio protection afforded by these drugs. However, Ertugliflozin does not inhibit late I_{Na}, despite being almost structurally identical to Dapagliflozin. Therefore, this current study is focused on investigating the molecular interactions of Dapa- and Ertugliflozin SGLT2 inhibitors within the structure of hNav1.5.

Methods: Starting from the available cryoEM structure for the hNav 1.5 (PDB ID: 7DTC), we constructed the full-length hNav 1.5 channel. Missing loops were modeled using the Swiss-Model server. Dapagliflozin and Ertugliflozin were docked within our previously¹ identified binding sites. Docked poses were then subjected to MD simulations of length 70 ns. Subsequent analyses performed included RMSD, Clustering analysis, hydrogen bond analysis, atomic correlation and binding affinity prediction using the MMGBSA method.

Results: Our data shows that both compounds have an average RMSD value within 2 Å and binding affinities within -32 to -34 kcal/mol. In the presence of both drugs, inactivation gate motifs (IFM) exhibit a strong affinity for alanine 1328 and asparagine 1661. Additionally, both drugs form hydrogen bond interactions with different residues during the simulations. This suggests that our analysis is not sufficient to differentiate the effects of each drug and the inhibition of the late sodium current, I_{Na}, can be due to allosteric effects mediated by conformational changes upon compound binding.

Conclusion: Classical MD simulations may not be suitable to address the impact of Dapagliflozin and Ertugliflozin on the late sodium current; thus, we aim to employ multiscale modeling, extending the time and length scales for a more comprehensive study.

References: Philippaert K Circulation. 2021 Jun;143(22):2188-2204

Transformations in the pharmaceutical regulatory system: opportunities and challenges

Fahad S. Aldawsari

Saudi Food and Drug Authority (SFDA), Riyadh, Saudi Arabia.

Background. A typical pharmaceutical regulatory system comprises conventional activities such as medicine registration, surveillance & pharmacovigilance and laboratory compliance testing. However, there have been recent safety issues in medicines that have influenced society, in which common regulatory activities were not effective enough in mitigating these risks. In addition, new technological and digital tools are gaining attention in stimulating the existing regulatory system as well as establishing new regulatory opportunities.

Purpose. To investigate the new trends in medicines regulations among the world's leading regulatory systems in order to identify learning opportunities for pharmacists and also to provide academia with insights in order to update appropriate curriculums accordingly.

Methods. Thorough analysis of the announced strategic plans for regulatory systems in the countries of the United States, European Medicines Agency, Japan and Saudi Arabia was performed. In addition, scanning for the published research studies from those authorities was also attempted in order to identify research directions and potential areas for enhancing pharmacists' skills.

Results. Three key areas for the new era of medicine regulations were identified, namely: digital health, partnership/collaboration and regulatory-driven scientific research. Moreover, special focus was given to biopharmaceuticals within the context of these areas owing to the future of medicinal therapeutics, taking the COVID-19 pandemic as a drive for this wave.

Conclusions. The new generation of pharmacists are encouraged to broaden their knowledge on the use of scientific tools (e.g. artificial intelligence, data analysis, and biostatistics), and how to incorporate these concepts within the essence of the pharmaceutical sciences arena. Academia is encouraged to embed these areas of learning into their curriculum for better preparation of pharmacists to embark the challenges in regulatory ecosystem.

Biomolecule-inspired PROTACS as potential cancer therapeutic agents

Bhuwan Prasad Awasthi¹, Jennifer I. Brown¹, Petar Iliev¹, Brent Page¹

¹University of British Columbia, Vancouver BC

Purpose: Proteolysis targeting chimeras (PROTACs) are a cutting-edge technology that facilitate the degradation of target proteins in cells and tissues. These heterobifunctional molecules consist two major parts, 1. A ligand that binds to a protein of interest and, 2. A moiety that recruits an E3 ubiquitin ligase, which are linked together with a chemical spacer. Under physiological conditions, these molecules increase interactions between the target protein and the E3 ligase, subsequently increasing protein ubiquitylation followed by proteasomal degradation. As a process of degradation, the protein unfolds and releases the PROTAC molecule allowing the process to repeat. Thus, PROTACs induce catalytic protein degradation and have demonstrated robust biological responses. Our aim is to develop novel PROTACs with anti-cancer activity by using biomolecule ligands.

Method: In my work, I have appended thymidine to the PROTAC structure to generate targeted degraders of thymidine-metabolizing enzymes. These were selected based on well-established metabolic pathways, combined with *in silico* modelling and ease of access using medicinal chemistry techniques. Current work is focused on demonstrating the efficacy of our top PROTAC compounds in cell-based assays.

Results: We have synthesized 15 new thymidine PROTACs with the aim to target and degrade thymidine kinase 1 (TK1), an enzyme essential for DNA synthesis. Disrupting thymidine synthesis and activation is one of the proven, oldest strategies for cancer treatment,

utilized by classic anti-cancer drugs such as methotrexate and 5-fluorouracil. Biochemical assays will be done with the synthesized compounds to check its degradation ability and further modifications will follow.

Conclusion: This presentation focuses on the synthetic approach for producing bio-inspired PROTACs designed to target TK1 and will provide brief introduction on optimization of PROTACs using medicinal chemistry and chemical biology approaches. It will also discuss anti-cancer activity of top compounds and comment on the feasibility of this strategy to other potential targets.

Development of Small Molecule Therapeutics Targeting a Novel Driver of Breast Cancer Metastasis

Jonas E. Olsen¹, Paul Mellor², Henok Sahile¹, Danielle Hanke¹, Deborah Anderson², Brent D. G. Page¹

¹Faculty of Pharmaceutical Sciences, University of British Columbia, Vancouver, BC, Canada, ²Saskatchewan Cancer Agency, University of Saskatchewan, Saskatoon, SK, Canada

Purpose. Breast cancer is the second most common cancer in Canadian women, making up 25% of all cancer diagnoses. While current breast cancer treatments are very effective in early stages, the 5-year survival rate drops down to 30% when the cancer metastasizes to distant organs. Collaborative efforts have identified and validated chloride intracellular channel 3 (CLIC3) as a new driver of breast cancer metastasis. Following a high-throughput *in silico* screen, we have identified several compounds that act as moderate inhibitors of CLIC3 enzymatic activity in biochemical settings (IC₅₀ values \approx 50 μ M). Our ongoing efforts have sought to optimize the activity and pharmacokinetic properties of these compounds to produce safe and effective new therapeutic agents that target metastatic processes in breast cancer.

Methods. A robust medicinal chemistry platform has been employed to produce novel small molecule CLIC3 inhibitors, using *in silico* docking, synthetic chemistry and assessments in enzymatic and cell-based assays. This process has facilitated the execution of structure-activity relationship studies, which has informed the design of further analogues. *In vitro* pharmacokinetic profiling has also been performed, including solubility, metabolic stability, plasma protein binding and intestinal permeability.

Results. We have produced a lead series of inhibitors that are ~50-fold more potent than initial hits, with our top compound having an IC₅₀ of just 1.7 μ M *in vitro*. Additionally, top compounds significantly reduce metastatic phenotypes in breast cancer cell lines at low micromolar concentrations. We have also demonstrated our top compound has good metabolic stability, but has strong plasma protein binding and limited intestinal permeability.

Conclusion. A promising series of CLIC3 inhibitors has been identified, which is being optimized for their activity as anti-metastatic agents. We will continue to advance these compounds towards advanced preclinical testing, with the ultimate goal to improve survival rates and quality of life for breast cancer patients.

Studying the binding modes of SHP2 allosteric inhibitors

Maryam Jama¹, Michael Overduin², Khaled Barakat¹

¹Faculty of pharmacy and pharmaceutical sciences, ²Faculty of Medicine and dentistry

Purpose: Src homology region 2 (SH2) containing protein tyrosine phosphatase 2 (SHP2) is an oncoprotein and an emerging target for cancer treatment¹. Current research is focused on developing SHP2 allosteric inhibitors such as SHP099 for better selectivity and specificity². Despite extensive efforts, allosteric inhibitors targeting SHP2 have not yet made it to the clinic, primarily due to the inhibitors lacking a defined binding mode that targets SHP2's oncogenic form³. This study aimed to investigate the binding mode of SHP099 along with a SHP2 inhibitor (C8) identified by our team. Our ultimate objective is to optimize the structure of SHP2-specific allosteric inhibitors to create improved therapeutic agents for SHP2 driven cancers.

Method: The crystallized structure of SHP2 and SHP099 was used for molecular modelling. The off-target SHP1/SHP099 complex was generated by superimposing the SHP2 co-crystal structure. Next, docking simulations were performed to select the SHP099/C8 poses with the highest docking scores within SHP1 and SHP2. The protonation state of SHP099 was adjusted to study the protonation effect on binding. Next, molecular dynamic (MD) simulations were run on the generated complexes, followed by clustering, energy decomposition and trajectory analyses. Finally, after selecting the dominant conformation from the clustering analyses, the binding modes of C8 and protonated state of SHP099 were studied.

Results: All complexes remained stable during the MD simulations. The free binding energy calculation revealed C8 to have a lower binding affinity to SHP1 compared to SHP2 (Table 1). Furthermore, C8 binds to the same pocket as SHP099 but with different key residues contributing to the total free binding energy. Lastly, the protonated amine group of SHP099 enhanced its binding affinity to SHP2 (Table 1).

Conclusion: Our study demonstrates that C8 binds selectively to SHP2 and the protonated amine group of SHP099 is important for its stability and binding to SHP2.

Protein Complex	Free binding Energy (kcal/mol)
SHP2 protonated SHP099	-60.2166 ± 3.1672
SHP2 unprotonated SHP099	-33.1621 ± 4.0424
C8 SHP2	-45.4346 ± 3.9165
C8 SHP1	-16.3058 ± 3.0383

References

1. Pádua, Ricardo AP, et al. "Mechanism of activating mutations and allosteric drug inhibition of the phosphatase SHP2." *Nature communications* 9.1 (2018): 4507.
2. LaMarche, Matthew J., et al. "Identification of TNO155, an Allosteric SHP2 Inhibitor for the Treatment of Cancer." *Journal of medicinal chemistry* 63.22 (2020): 13578-13594.
3. Song, Yihui, et al. "A multifunctional cross-validation high-throughput screening protocol enabling the discovery of new SHP2 inhibitors." *Acta Pharmaceutica Sinica B* 11.3 (2021): 750-762.

Development of a novel inhibitor of the oncogenic transcription factor STAT5

Danielle Hanke¹, Melanie McDonald Lopez², Siya Malhotra², David A. Frank², Brent D.G Page¹

¹University of British Columbia, Vancouver, BC, ²Emory University, Atlanta, GA

Purpose. The Signal Transducer and Activator of Transcription (STAT) proteins are a family of proteins that are notoriously difficult drug targets, as they lack a traditional enzyme active site where small molecule inhibitors would typically bind. However, aberrant STAT activity drives the development and progression of several cancers and inflammatory diseases. Therefore, inhibiting STAT proteins would open a breadth of possibilities for novel therapeutic agents. The STATs have been the target of many drug development endeavours, but none have uncovered potent and selective STAT inhibitors that have progressed through clinical trials. This research project employs innovative new strategies such as thermal stability assays to identify small molecule inhibitors that target STAT proteins directly.

Methods. A high throughput screen (HTS) was conducted on ~33 000 chemical compounds to search for direct inhibitors of STAT1 protein. Further thermal stability assay experiments were performed to validate promising hit compounds. Chemical optimization was conducted on top hits to synthesize a small library of compounds which were further tested in cellular assays to assess STAT binding

and inhibition.

Results. Three top hit compounds were identified from the HTS and validation experiments based on their ability to stabilize STAT1 towards thermal denaturing. These hits were diversified and optimized using medicinal chemistry techniques to create a library of ~80 chemical compounds for further biochemical testing. Among these top compounds was BP170, which unexpectedly acted as a potent and selective inhibitor of STAT5, not STAT1, activity in cellular assays.

Conclusion. Discovering ways to target “undruggable” proteins such as the STATs will broaden the therapeutic horizon for many diseases. We hope that through mechanistic studies and further optimization of BP170 we will be able to further improve the potency and selectivity of our promising STAT5 inhibitor scaffold to ultimately have applications as a novel cancer therapeutic agent.

Synthesis and biological evaluation of novel FOXM1-targeting PROTACs in ovarian cancer cells

Antonio Vega-Medina¹, Makenzie Vorderbruggen², Erika Loredó-Calderón¹, Bahar Mahani¹, Catalina Muñoz-Trujillo², Adam Karpf², Carlos Velázquez-Martínez¹

¹Faculty of Pharmacy and Pharmaceutical Sciences, University of Alberta, 2-081 Katz Group Centre for Pharmacy and Health Research, 11315 - 87 Ave NW, Edmonton, AB, Canada, T6G 2R3, ²Eppley Institute for Research in Cancer and Allied Diseases, Medical Center, University of Nebraska, 601 S. Saddle Creek Rd, Omaha, Nebraska, United States. 68106

FOXM1, an essential transcription factor regulating cell replication, is implicated in cancer initiation and progression, correlating with poor patient prognosis¹. Proteolysis targeting chimeras (PROTACs) represent a novel class of anticancer agents designed to degrade specific proteins via E3 ubiquitin ligase recruitment². In this study, we investigated three novel FOXM1-targeting PROTACs (compounds 12, 15, and 18), containing linear hydrocarbon chain linkers of varying lengths (5, 7, and 9 carbon atoms), alongside the parent FOXM1 inhibitor, TFI-10³, in high-grade serous ovarian carcinoma cells (OVCAR4). Cell proliferation assays (MTT) and western blot analysis were employed to assess drug efficacy. Our results demonstrate that FOXM1-targeting PROTACs exhibit superior efficacy in reducing OVCAR4 cell viability compared to TFI-10, with minimal impact on normal ovarian cells (FT282 C11). Additionally, these PROTACs effectively suppress FOXM1 expression and downstream targets CCNB1, PLK1, and AURKB in OVCAR4 cells. Notably, other FOX family members (FOXA1, FOXK2, and FOXO3A) showed modest reduction with PROTAC treatment. Overall, TFI-10-based PROTACs display potent anticancer activity in OVCAR4 cells, with a preference for FOXM1 downregulation. Furthermore, our preliminary structure-activity relationship (SAR) analysis suggests a correlation between increased hydrocarbon chain linker length and enhanced potency.

References

1. Breast Cancer Res 2023 25:76
2. Front Chem 2021 9:707317
3. Eur J Med Chem 2021 209:112902

The oxidation of fenamic acid NSAIDs by neutrophil myeloperoxidase produces toxic reactive metabolites that induce leukemic cell death

Newton Tran¹

¹Faculty of Pharmacy and Pharmaceutical Sciences, Katz Group-Rexall Centre for Pharmacy and Health Research, University of Alberta, Edmonton, Alberta, T6G 2E1 Canada

Purpose: The interactions between peroxidase enzymes and fenamic acid NSAIDs cause the formation of reactive oxygen species, potentially leading to toxic side-effects [1]. The aim of this study was to investigate the bioactivation of N-phenylanthranilic acid (NPA) and four drug analogues: flufenamic acid (FFA), mefenamic acid (MFA), meclofenamic acid (MCFA), and tolfenamic acid

(TFA) via myeloperoxidase (MPO). The heme enzyme MPO is known to catalyze oxidation reactions of numerous xenobiotics into reactive metabolites [2]. We hypothesized that the enzymatic oxidation of these compounds by MPO will result in reactive metabolites that lead to cell toxicity in leukemia cells.

Methods: To test our hypothesis, we used biochemical approaches where purified MPO from human neutrophils was used for UV-vis spectrophotometry, liquid chromatography-mass spectrometry (LCMS), and electron paramagnetic resonance (EPR). In addition, *in vitro* studies were performed with HL-60 promyelocytic leukemia cells, which are high in MPO content, to analyze the cytotoxic potential of these reactive metabolites. Anti-DMPO immuno-spin trapping was also utilized to detect protein-free radicals.

Results: UV-vis spectrophotometry studies revealed that MPO catalyzed the oxidation of all fenamic acid NSAIDs. LCMS analysis of the oxidized products displayed the formation of dimers, hydroxylated, and quinoneimine species, although, glutathione conjugates were only detected for NPA, MFA, and TFA. EPR spin trapping with DMPO using reduced glutathione (GSH) revealed the formation of glutathionyl radicals (GS[•]) in a linear concentration-dependent manner for all compounds. We also detected the formation of protein-free radicals in HL-60 cells through immunoblotting. Lastly, all fenamic acid NSAIDs demonstrated cytotoxicity in HL-60 cells.

Conclusion: These findings revealed a correlation between pro-oxidant metabolite reactivity and cytotoxicity caused by fenamic acid NSAIDs. Further studies are required to investigate the cytotoxic potential in leukemia cells that highly express MPO, which may present a novel approach in the MPO-dependent targeted killing of leukemic cells.

References

- [1] Cho, T. and Uetrecht, J. (2017) How reactive metabolites induce an immune response that sometimes leads to an idiosyncratic drug reaction. *Chem Res Toxicol*, American Chemical Society 30, 295-314
- [2] Morgan, A. G. M., Babu, D., Michail, K. and Siraki, A. G. (2017) An evaluation of myeloperoxidase-mediated bio-activation of NSAIDs in promyelocytic leukemia (HL-60) cells for potential cytotoxic selectivity. *Toxicol Lett*, Elsevier 280, 48-56

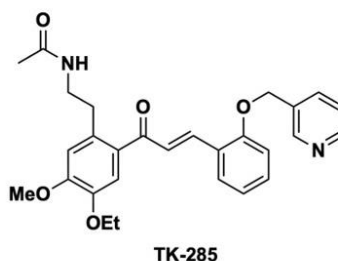
From target molecule identification to PROTAC: Lessons learned from the spacer diversification

Yoshiharu Iwabuchi¹

¹Tohoku University

PROTAC (Proteolysis Targeting Chimera) is an emerging modality in current medicinal chemistry, featuring a chimeric molecule consisting of a ligand for a protein of interest (POI) and a ligand for ubiquitin ligase linked by a spacer, which induces polyubiquitination and proteasomal degradation of POI via the ubiquitin-proteasome system, an intracellular proteolysis pathway¹.

In this presentation, we will discuss our findings on the importance of the spacers through the identification of the target protein of TK-285, a chalcone derivative that expresses anti-inflammatory activity,² and the acquisition of PROTACs that degrade the protein.



Design and development of 2,4-diaminopyrimidines and pyrazoles as aurora kinase inhibitors in cancer

Tabassum Khan¹, Kaksha Sankhe¹

¹Department of Pharmaceutical Chemistry, SVKM's Dr. Bhanuben Nanavati College of Pharmacy, Mumbai, Maharashtra, India

Purpose: Aurora kinase (*AURK*) is a serine/threonine protein kinase that is essential for mitosis, and its overexpression is linked to cancer, highlighting its role as an oncogene. This work aims at development of heterocyclic *AURK* inhibitors as potential leads in cancer therapeutics.

Methods: A series of 2, 4-diaminopyrimidines and pyrazoles were designed using Glide Maestro, Schrödinger and synthesized using conventional and microwave methods. The molecular docking, ADME properties and drug likeliness was determined using Maestro, QikProp, Schrödinger. Their cytotoxicity was evaluated by *in-vitro* assay in ovarian cancer (SKOV3), brain cancer (C6), and leukaemia (THP-1) cell lines followed by *in-vitro* *AURKA* and *AURKB* kinase inhibition of the most active compounds.

Results: Among the synthesized molecules, **2j**, **2l**, **2p**, **9a**, and **10a** showed dose-dependent cytotoxicity in. **2l** and **9a** showed potent activity against SKOV3, IC₅₀ of 0.49±0.001 and 0.019±0.015 µM respectively. **2j**, **2l**, **2p**, **9a**, and **10a** displayed better inhibitory activity against THP1, IC₅₀ of 16.59±0.039, 0.18±0.026, 1.26±18.201, 0.64±56.358, and 0.084±0.030 µM, respectively. **2l**, **9a** and **9b** show promising activity in C6. **2j**, **2l**, **2p**, **9a**, and **10a** were selected for *AURKA* and *AURKB* inhibition assays.

Conclusion: Compounds **2p** and **9a** inhibited *AURKA* at 10µM was 68.14 and 55.64% IC₅₀ of 1 and 2 µM, respectively compared to standard Barasertib with 78.42% inhibition (IC₅₀- 0.6 µM). **2j** and **2p** inhibited *AURKB* with 56.36 and 56.39% inhibition, IC₅₀ of 4 and 2 µM, respectively, compared to Barasertib with 68.62% inhibition (IC₅₀- 0.7 µM). The 2, 4-diaminopyrimidines and pyrazoles based small molecules have emerged as attractive leads for further development as effective *AURKA* and *AURKB* inhibitors in cancer therapeutics.

Revisiting classic dihydrofolate reductase inhibitors as potential next-generation anticancer agents

Ujjwala Karmacharya¹, Merlyn Emmanuel¹, Jennifer Brown¹, Rosanne Persaud², Karla C. Williams¹, Brent Page¹

¹University of British Columbia, Vancouver, BC, ²Admare BioInnovations, Vancouver, BC

Purpose: Dihydrofolate reductase (DHFR) is a classic anti-cancer, immunomodulatory and anti-microbial drug target that enables folate metabolism and production of nucleic acid building blocks, such as thymidine. DHFR inhibitors include some of the earliest cancer therapeutic agents (i.e. methotrexate and pyrimethamine). Despite its long-term success, methotrexate is associated with poor patient response rates, due to both innate and acquired resistance mechanisms. Our current work is focused on applying state-of-the-art chemical biology techniques to this classic drug target, to furnish new inhibitors (degraders) of DHFR for potential use as next-generation cancer therapies.

Methods: A series of pyrimethamine analogues were designed and docked into the DHFR active site using GLIDE (Schrödinger). Several analogues were synthesized by adapting established protocols and assessed for DHFR inhibition in cell-free enzymatic assays. Cellular DHFR engagement was confirmed by leveraging DHFR's auto-regulatory mechanism, where it binds to its own messenger RNA and releases it upon inhibitor binding inducing translation. Thus, acute DHFR accumulation served as a readout of cellular target engagement. Impairment of cancer cell viability was established using different breast cancer cell lines.

Results: A series of 36 pyrimethamine analogues were produced and evaluated using *in vitro* and cell-based assays, leading to the identification of a top ten compound series. Among these, two compounds stood-out as potential lead candidates, which engaged DHFR in cells at concentrations as low as 1 nM, where they also elicited a growth arrest phenotype in breast cancer cell lines. These top compounds continue to be explored and we hope to further validate their promise as potential cancer therapeutic agents.

Conclusion: Revisiting classic DHFR inhibitors through a modern chemical biology lens has illuminated that several pyrimethamine analogues have promising anti-cancer activity in preliminary studies. These compounds will be further evaluated with the ultimate goal of producing novel, safe and effective cancer therapies.

Design, synthesis, and cytotoxic evaluation of novel EGFR inhibitors: fused derivatives of 4(3H)-quinazolinone and 1, 3, 4-oxadiazole.

Tabassum Khan¹, Rupali Likhar²

¹Department of Pharmaceutical Chemistry and Quality Assurance, SVKM's Dr. Bhanuben Nanavati College of Pharmacy, ^{2b}Department of Pharmaceutical Chemistry, LSHGCT's Gahlot Institute of Pharmacy, Navi Mumbai, India

Purpose: The purpose of this study was to employ molecular docking techniques to design novel EGFR (Epidermal Growth Factor Receptor) inhibitors and subsequently assess their potential cytotoxic effects. By leveraging computational methods, new compounds were synthesized with the aim of targeting EGFR, a key protein implicated in cancer progression. This project aimed to design, synthesize, and evaluate a series of 4 (3H)- Quinazolinone-1, 3, 4 oxadiazole fused heterocyclic derivatives as potential leads of anti-cancer agents.

Method: In this study, Autodock 4.0 was employed to design EGFR inhibitors. Based on the docking results, 54 compounds were selected for laboratory-scale synthesis. The synthesized compounds were characterized using various spectroscopic techniques, including IR, ¹H and ¹³C NMR, and Mass spectroscopy. Pharmacological evaluation included cytotoxic activity assessment using SRB (Sulforhodamine B) and MTT (3-(4, 5-Dimethylthiazol-2-yl)- 2, 5- diphenyltetrazolium bromide) assays. The compounds were tested against lung cancer cell line A-549 and breast cancer cell line MCF-7. Compounds exhibiting GI₅₀ values ≤ 10 µg/ml and IC₅₀ values ≤ 10 µg/ml were considered to have good antiproliferative activity. The best four compounds were evaluated for EGFR enzyme inhibition.

Results: The compounds displayed good binding energy, formed hydrogen bonds, and engaged in pi interactions with the target EGFR. The synthesized compounds had desirable physical properties, high purity (>99%), and demonstrated significant cytotoxicity against selected cancer cells. Compound C11 demonstrated the highest EGFR inhibition with an IC₅₀ value of 1.3 µM, closely resembling the IC₅₀ value of the standard drug Erlotinib. Compound C42 also showed significant inhibition with an IC₅₀ value of 3.07 µM.

Conclusion: The synthesized compounds were novel EGFR inhibitors and displayed potent cytotoxic effect, highlighting their potential as promising lead candidates for further development as anti-cancer agents.

Studying the binding affinity of T cell immunoglobulin and mucin domain-containing protein-3 (TIM-3) with its ligands through binding assays and molecular modelling

Ashira Manzoor¹, Azeez Adeniyi¹, Abidemi Kaffo¹, Tae Chul Moon¹, Khaled Barakat¹

¹University of Alberta, Edmonton, AB

Purpose: TIM-3 is an immune checkpoint receptor that is expressed by T cells. It has four ligands Gal-9, PtdSer, CECAM1, HMGB1. Binding affinity and binding mode of TIM-3 to its ligands are not well-known. Only affinity of un-glycosylated TIM-3 to Gal-9 was reported to be 28 nM. This research aimed to measure binding affinities of TIM-3 to its ligands through biochemical binding assays and characterize their interactions through molecular modelling.

Methods: Biochemical binding assays were used for measuring the binding kinetics of TIM-3 to its ligands. Gal-9, HMGB1, CECAM1 were coated onto ELISA plate. Biotin tagged rhTIM-3-6His-Avi-tag was added and detected with Streptavidin-HRP. We also predicted binding interactions of TIM-3 and Gal-9 through docking and MD simulations. Top hits from docking were subjected

to short MD simulations, leading to the selection of a final set of four models. The shortlisted models were further subjected to extended MD simulations up to 200 ns. Best model was selected based on binding free energy calculation using MM-PBSA method.

Results: A dose-dependent manner was observed in binding of TIM-3 to its ligands. Gal-9 showed strongest binding with $K_D = 0.177 \mu\text{M}$. While HMGB1 and CECAM1 showed weak binding with $K_D = 3.56 \mu\text{M}$ and $11.448 \mu\text{M}$, respectively. In terms of predicted interactions, final TIM-3 and Gal-9 model from four models were selected based on their MM-PBSA predicted energies, yielding a binding affinity of $-86.988 \pm 11.396 \text{ kcal/mol}$ compared to $33.662 \pm 8.658 \text{ kcal/mol}$ when there is no glycosylation. Residues PHE-18 and ARG-68 from TIM-3 and residues His-61, Glu-85 from Gal-9 contributed the most in these interactions. Glycan presence enhanced TIM-3 binding to Gal-9.

Conclusion: Our study confirms that HMGB1, CECAM1 and Gal-9 indeed interact with TIM-3. Glycosylated TIM-3 interacts with Gal-9 with high affinity compared to other ligands. This study predicted first known geometry of TIM-3 and Gal-9 interaction and glycans effect.

Does it bind? A focused look at cutting-edge target engagement techniques in medicinal chemistry research

Riley Prout-Holm¹, Daniel Everton¹, Petar Iliev¹, Danielle Hanke¹, Jonas E. Olsen¹, Jennifer I. Brown¹, Adam Frankel¹, Brent D. G. Page¹

¹University of British Columbia, Vancouver BC

Purpose: The popularization of personalized medicine and targeted drug therapies has ushered in a new frontier in drug discovery research, where direct evidence of drug-target interactions has become a critical aspect of modern drug discovery pipelines. The cellular thermal shift assay (CSETSA) has arguably become the most widely accepted technique for measuring direct interactions between experimental inhibitors and their cellular targets, or “target engagement”. This assay measures thermally induced protein aggregation in the presence and absence of potential inhibitors as an indicator of binding. While this technique can be applied to many protein targets, new techniques are emerging that facilitate higher-throughput workflows and can better analyze interactions with non-traditional drug targets. This presentation will highlight some of the cutting-edge target engagement assays being developed in the Page Lab.

Methods: Target engagement technologies using non-thermal stimuli have been developed, using salinity stress, mutation-induced instability, and other conditions. The ability of established and experimental inhibitors to bind their intended target results in stabilization towards these stressors and allows soluble proteins to persist as a measurement of target engagement.

Results: This presentation will focus on our recently developed *in vitro* and cell-based target engagement assays and their applications within our drug discovery projects. These assays have enabled more rapid screening of compounds for cellular target engagement and helped produce novel chemical compounds that elicit the expected phenotypic responses for target binding. Examples include recently published isothermal ligand-induced resolubilization assay (ILIRA) and other recent developments.

Conclusions: While modern target engagement techniques have critically transformed aspects of the early drug discovery process, further development could facilitate high-throughput target engagement screening approaches that will facilitate drug discovery efforts.

Designing a Multi-Neoantigen vaccine for Melanoma: Integrating Immunoinformatics and Biophysical Approaches

Saba Ismail¹, Khaled Barakat¹

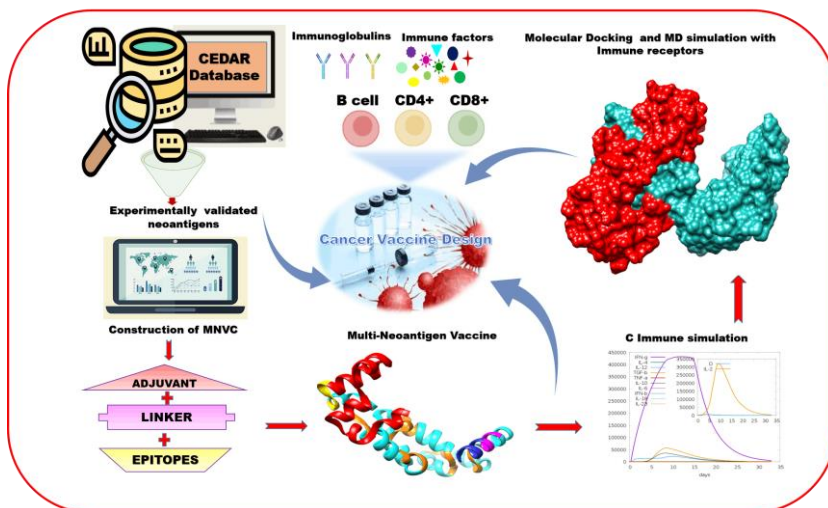
¹Faculty of pharmacy and pharmaceutical sciences, university of Alberta, Edmonton, Alberta, Canada.

Purpose: Cancer evolves through the accumulation of several genetic alterations. In this context, somatic mutations create tumor-specific neopeptides, termed as neoantigens. These neoantigens are recognized by T cells as non-self, rendering them prime candidates for cancer vaccine design. Such vaccines train the immune system to recognize and eliminate cancer cells effectively. Therefore, neoantigen-based vaccines can be a viable strategy for cancer immunotherapy. Their distinctive capacity to trigger a specific immune response against cancer cells highlights their importance as a promising cancer immunotherapy approach. The objective of the current study is to use various computer-aided-design tools to hypothesize multi-neoantigen based vaccine-construct (MNVC) to target melanoma. In building, MNVC we used experimentally verified neoantigens from the CEDAR database, ensuring the relevance of our approach.

Methods: A collection of 700 neoantigens underwent immunoinformatics analysis, resulting in shortlisting 08 neoantigens. These were linked together using GPGPG linkers to design a MNVC, subsequently conjugated to a β -defensin adjuvant through an EAAAK linker to enhance immune response. A designed vaccine construct was subjected to de-novo structure prediction using a scratch-predictor. Following that, molecular docking was conducted with immune-receptors using blind docking method by cluspro. Subsequently, MD simulation of complexes was carried to assess the construct's capacity to stimulate an immune response.

Results: Shortlisted neoantigens for MNVC cover 99.74% of the global population. The MNVC comprised of 167 amino acid, 18.1kda M.W and has a 0.8335 antigenic score. The MNVC was cloned and reverse-translated in *Escherichia coli* to optimize vaccine protein expression. Molecular docking showed binding affinity for MHC-I, MHCII, and TLR-4 with global energy scores of 1045.5, -1517.9, and -1020.1kcal/mol. A 100-ns MD simulation showed constant binding stability for complexes.

Conclusion: The proposed vaccine construct is highly antigenic, presents a robust binding affinity towards immune receptors, and could potentially exhibit efficacy as a treatment for Melanoma.



Chemical Synthesis Of Foxm1-Targeting Protacs Possessing A Folate Receptor Ligand

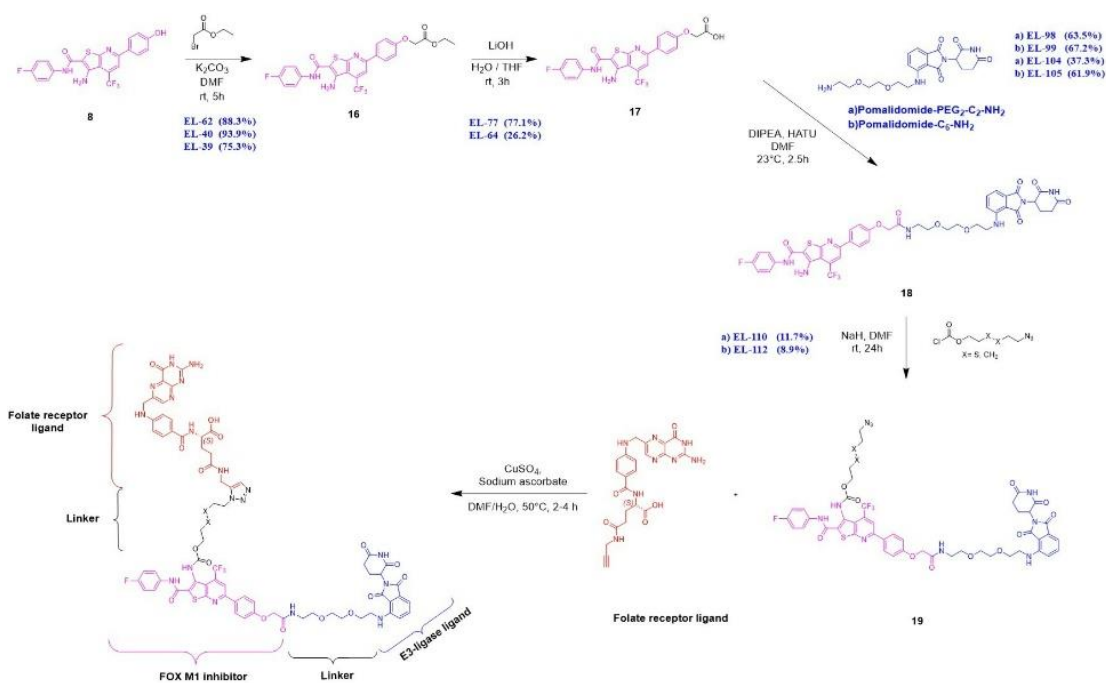
Erika Loreda Calderon¹, Antonio Vega¹, Bahar Mahani¹, Adam Karpf², Carlos Velazquez¹

¹University of Alberta, Edmonton, AB, ²University of Nebraska, Omaha, NE

Purpose. A series of four new PROTACs were designed to target the folic acid receptor protein expressed in cancer cell lines, and synthesized following reported procedures. The use of folate receptor ligands along with PROTACS has been shown to increase the selectivity of the drug toward malignant cells and it is a promising approach that is being pursued by our research group to target and potentially degrade the oncogenic FOXM1 transcription factor. In this regard, the folate receptor α (FOLR1) is perhaps one of the most well-defined targets for selective drug delivery to cancer cells, because it is highly expressed in many cancer types, including High Grade Serous Ovarian Cancer (HGSC), while normal cells have very low or no FOLR1 expression.¹⁻³ The FOXM1 transcription factor is one of many proteins that are abnormally and consistently upregulated in most human cancers, and it is involved in cancer initiation, cancer development, and drug resistance,⁴⁻⁷ which makes this hybrid approach a promising medicinal chemistry approach to develop new molecules for the treatment of ovarian cancer in susceptible individuals. The main goal of this project was to synthesize and evaluate four novel FOXM1-targeting PROTACS containing a) FOXM1 inhibitor (F7), b) linker, c) E3- ligase ligand (pomalidomide) and d) folate receptor ligand that will confer specificity toward HGSC ovarian cancer cells.

Methods. To synthesize four novel FOXM1-targeting PROTACS containing folate receptor ligand as the synthetic scheme describes.

Results and Conclusion. At this point of the project, we only have preliminary conclusions regarding the synthetic part of the project. The parts a) and d) of the PROTACS has been synthesized with good yields (except for intermediate 6). All the intermediates and final compounds were characterized by LCMS, ¹H and ¹³C NMR.



References

1. Scaranti, M., Cojocaru, E., et al. Nature reviews. Clinical oncology 17, 349-359 (2020).
2. Chen, H., Liu, J., et al. J Med Chem 64, 12273-12285 (2021).

Antisense Oligonucleotide-Loaded Liposomes for Potential Treatment of Bacterial Biofilms

Kaidy Orellana¹

¹University of Waterloo, Waterloo, ON

Purpose: Key pathogens in chronic wound infections include *Pseudomonas aeruginosa* (*P. aeruginosa*) and *Staphylococcus aureus* (*S. aureus*), which form biofilms on compromised skin barriers [1]. Targeting the synthesis of autoinducer factors (AIs) is a promising approach to disrupt biofilm production and reduce bacterial virulence [2]. This study aims to investigate the potential of nanocarriers in effectively delivering antisense oligonucleotides (ASOs) to silence genes involved in AI production, thereby reducing biofilm biomass.

Methods: Polymicrobial biofilms composed of *P. aeruginosa* (PAO1) and *S. aureus* (ATCC 25923) were grown in 24-well plates. Bacterial culture was standardized to concentrations of 1×10^4 to 1×10^7 CFU/mL, and biofilm biomass was quantified via a crystal violet (CV) assay after 0, 24 and 48-hour incubations. Liposomes were formulated using microfluidic pumps and a herringbone mix chip with the ionizable cationic lipid DC-cholesterol-HCl and the structural lipid DOPE. The encapsulation efficiency was quantified with a Ribogreen assay. Furthermore, the internalization of liposomes into bacteria was observed via microscopy using fluorescent lipid DiOC18(3) labelling.

Results: The CV assay revealed significant growth of the polymicrobial biofilm over 24 and 48-hour incubation periods, with no significant changes between the control and various bacterial concentrations at 0 hours. Liposomes formulated with a TFR of 3 mL/L and FRR of 3 had a mean size of 149.3 nm, PDI of 0.1398, and mean zeta potential of +41.28 mV. Liposomes loaded with 1.0 μ M of mock nucleic acid had a mean size of 151.0 nm, PDI of 0.1653, a mean zeta potential of +40.52 mV, and encapsulation efficiency of 78.36%.

Conclusion: The polymicrobial biofilm model showed increased biomass over time, and it provides a means of tracking changes in biofilm biomass after treatment with ASO-loaded liposomes. Overall, liposomes are adequate in size and have high encapsulation efficiency for the effective internalization and administration of ASOs.

References

Sci Rep 2022 12:1-14

Nat Chem Biol 2007 3: 541-548

Contrast agent-encapsulating hydrogel for real-time tracking and monitoring of controlled release

Natalie Guirguis¹, Wida Brumand², Yanis Zellagui³, Simon Matoori¹

¹Université de Montréal, Montreal, QC, ²Université de Genève, Geneva, Switzerland, ³Université de Haute-Alsace, Mulhouse, France

Purpose: Hydrogel-based biomaterials are widely established systems for tissue engineering and drug delivery applications. As their function generally depends on their localization, tracking the hydrogels' position or content release in the body is crucial. Incorporating contrast agents into hydrogels can potentially enable non-invasive in vivo tracking of hydrogels and monitoring of stimuli-responsive release through imaging. However, as hydrogels alone or loaded with hydrophilic contrast agents are not suited for imaging, we loaded hydrogels with a commercial ethiodized oil-based contrast agent. We hypothesized that immobilizing contrast agent emulsion droplets in hydrogels will render them visible on computed tomography (CT), and that ultrasound (US)-triggered release of the contrast agent can be monitored using CT.

Methods: We prepared calcium alginate hydrogels loaded with ethiodized oil emulsion droplets and imaged them in mice using micro-CT. An US pulse was applied to trigger contrast agent release.

Results: The CT signal intensities of contrast agent-loaded hydrogels increased in a contrast agent-dependent manner with high linearity ($R^2 = 0.995$). In mice, hydrogels with different contrast agent concentrations also displayed significant differences in signal intensity ($p < 0.01$). After applying US on the hydrogels in mice, a significant decrease in signal intensity was observed ($p < 0.05$), suggesting that the contrast agent had been released.

Conclusion: We loaded a hydrogel with a contrast agent and were capable of localizing the hydrogel and monitoring contrast agent release after an US pulse in mice, paving the way for personalized medicine with US-responsive hydrogels.

References: AAPS J 2023 25(5):79

Gene silencing and cellular uptake of novel conjugates of low molecular weight polyethyleneimine in cancer

Zoha Hajikhani^{1,2}, Amarnath Praphakar Rajendran³, Saba Abbasi Dezfoli¹, Hasan Uludag^{1,3,4}, Afsaneh Lavasanifar^{1,3}

¹Department of Pharmacy and pharmaceutical science, University of Alberta, Edmonton, AB, Canada., ²Department of Pharmaceutical biomaterials, Tehran university of medical sciences, Tehran, Iran., ³Department of Chemical and Materials Engineering, Faculty of Engineering, University of Alberta, Edmonton, AB, Canada, ⁴Department of biomedical engineering, Faculty of Medicine and Dentistry, University of Alberta, Edmonton, AB, Canada

Purpose: This study aimed to develop and characterize a novel siRNA delivery system using α -benzyl carboxylate- ϵ -caprolactone (BCL)-modified low molecular weight polyethyleneimine (PEI-BCL) to enhance siRNA transfection while minimizing cytotoxicity.

Methods: Success in the synthesis of PEI-BCL using various Ethyleneimine:BCL molar ratios (1:0.5, 1:1, 1:10, and 1:20), was assessed using NMR and IR. Polyplexes of PEI-BCL and siRNA were characterized for size, polydispersity, and ζ -potential. SiRNA binding, release, and hemocompatibility were tested. Transfection efficiency and cellular uptake were evaluated in three cancer cell lines.

Results: Spectroscopy studies confirmed polymerization of BCL on PEI when 1:10 and 1:20 BCL to EI ratios were used. Polyplexes displayed a compact size, ranging from 130-150 nm ($PDI \leq 0.2$). The ζ -potential of polyplexes in water measured around 43 ± 0.63 mV. Notably, 1:10 and 1:20 PEI:BCL ratios demonstrated superior transfection efficiency compared to PEI2k. Furthermore, they exhibited lower cytotoxicity than commonly used transfecting agents. The highest green fluorescent protein (GFP) silencing efficiency was observed with PEI-BCL 1:10 and 1:20, reaching 66% and 46% in MDA-MB-231 GFP+ cells and 40% and 43% in H1299 GFP+ cells, respectively. In H1975 GFP+ cells, 45% and 57% silencing were achieved, with no significant toxicity. The 1:10 and 1:20 PEI-BCL showed 88% and 81% cell uptake in MDA-MB231 after 24 h of treatment. These polymers exhibited 81% and 53% cell uptake in the H1299 cell line. The polyplexes made with 1:10 and 1:20 polymers were hemocompatible and showed no significant hemolysis at the concentration of 20 $\mu\text{g/mL}$. At neutral pH, the 1:20 and 1:10 polyplexes released 73% and 65% of siRNA, respectively. At acidic pH, they released 28% and 58%, respectively.

Conclusion: Our study introduces PEI-BCL as a new siRNA delivery system, with enhanced transfection efficiency, lower cytotoxicity, high cellular uptake, hemocompatibility, and pH-responsive siRNA release with potential in oncogene silencing in cancer.

References

- Xie, L. et al. (2016), ACS Applied Materials & Interfaces, 8(43), pp. 29261-29269.
Rajendran, A.P. et al. (2023) ,ACS Applied Bio Materials, 6(3), pp. 1105-1121.

Development of a new hybrid formulation of sustained release tablet: naproxen as a model drug

Tracy Fu¹

¹université de montréal

Purpose : This study aimed to develop a novel formulation of sustained-release tablets of naproxen utilizing a combination of lipophilic and hydrophilic excipients. The formulation process involved the preparation of individual tablets containing either Compritol or Geleol⁽¹⁾ in combination with either HPMC or Eudragit RL PO⁽²⁾, followed by the comprehensive characterization and evaluation of their physical and release properties.

Methods : The weight uniformity and tensile strength of the tablets were determined. Furthermore, the dissolution profiles of the tablets were investigated.

Results : HPMC tablets exhibited a mean weight of 303.7 ± 16.8 mg (n=10) and a tensile force of 1.75 ± 0.80 MPa (n=6). In contrast, Geleol tablets showed a similar mean weight but a tensile force of 1.00 ± 0.07 MPa (n=6). The hybrid tablets displayed a mean weight of 279.9 ± 13.5 mg (n=10) and a mean tensile force of 1.41 ± 0.30 MPa (n=10). All formulations displayed a sustained release profile, with the hybrid tablets releasing up to 106 ± 8 % (n=6) of naproxen in 12 h, whereas the HPMC-only tablets releasing up to 95 ± 1 % (n=3), and the Geleol-only tablets up to 57 ± 4 %. Although surprising, these results demonstrated the potential of the hybrid formulation to provide a prolonged release of naproxen compared to individual components. Other formulations are currently under study. Further investigations involving structural analysis (such as TGA and XRD) are ongoing to decipher these results.

Conclusion: This novel formulation could offer promises to enhance the therapeutic efficacy and patient compliance of naproxen therapy, presenting opportunities for further optimization and clinical evaluation.

References

- (1) Lipids Health Dis 2017 16:1-75
- (2) J Pharm Bioall Sci 2012 4:5-90

Reproducible Synthesis of PLGA Nanoparticles via Solvent Evaporation: A Methodological Blueprint for Precision Particle Engineering

Arash Amanlou¹, Azita Haddadi¹

¹Division of Pharmacy, College of Pharmacy and Nutrition, University of Saskatchewan, Saskatoon, SK, Canada

Purpose: The purpose of this study was to develop a method for the preparation of poly(lactic-co-glycolic acid) using the solvent evaporation technique, aiming for reproducible results, a low polydispersity index (PDI), tunable particle size, and zeta potential. This study strived to provide a clear and comprehensive methodology that can be readily adopted by other researchers and displayed some of the often neglected details that can lead to a significant impact.

Method: Variables that were investigated in this study were polyvinyl alcohol (two molecular weights and hydrolysis rates, varying concentrations, two solutions/buffers, concentration validation, preparation method), needle (different gauges and lengths), Injection rate (different injection rates), centrifugation (differential centrifugation, two-step centrifugation at different speeds and duration), wash cycles, sonication cycles (ice bath, generated energy, sample rotation), magnetic stirring bar (different lengths, and shapes), dynamic light scattering (considerations).

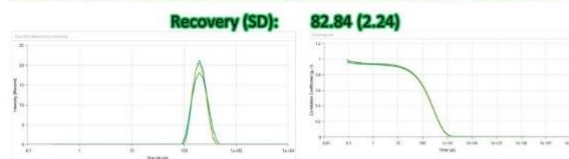
Results: This study explored the impact of variable adjustments on the physicochemical properties of PLGA nanoparticles. The reproducibility of findings was demonstrated across multiple experiments and replicates. Facile manipulation of variables yielded tunable particle size and zeta potential while achieving a more uniform nanoparticle distribution (low Polydispersity Index). These findings highlight the method's effectiveness and potential for precise nanoparticle synthesis.

Conclusion: A clear methodology and material section in a PLGA nanoparticle synthesis study will enhance the clarity and comprehensiveness and it will facilitate understanding and implementation of the method by other researchers. The

reproducibility of the study is evidenced by obtaining consistent results during the replicates and multiple experiments. Tunable particle size and a low polydispersity index are achieved by understanding the solvent evaporation method and emulsion preparation science.



Physicochemical Features	Nano Emulsion	Nanoparticles Resuspended in Water	Nanoparticles Resuspended in 10% Sucrose Solution	After Freeze-Drying
Z-Average (nm) (SD)	197 (5.256)	196.6 (6.473)	193.2 (2.576)	196.2 (2.968)
PDI (SD)	0.06224 (0.0268)	0.05124 (0.0128)	0.05229 (0.02222)	0.07478 (0.007981)
Zeta Potential (mV)	-14.34 (1.427)	-24.03 (3.391)	-28.01 (1.727)	-25.54 (3.859)



Needle Gauge	Gauge-21	Gauge-26	Gauge-30
Z-Average (nm)	197.6	193.2	189.5
PDI (SD)	0.07827	0.05229	0.08355

Centrifugation	2-Step Centrifugation	Differential Centrifugation
Z-Average (nm)	198.7	196.2
PDI	0.2307	0.07478

Generated Energy	1 seconds ON, 3 seconds OFF (1127 Joules)	2 seconds ON, 3 seconds OFF (1074 Joules)
Z-Average (nm)	196.3	193.2
PDI	0.1397	0.05229

Structure-Function Characterization of a New Generation of Nanodiamond Carriers

Iulia Spataru¹, Ildiko Badea¹, Saniya Alwani², Deborah Michel¹, Eiko Kawamura¹, Jian Wang³

¹University of Saskatchewan, ²Memorial University of Newfoundland, ³Canadian Light Source Inc.

Purpose: Nanodiamonds (NDs) are carbon particles of 20-40 nm, easily and inexpensively obtained by detonating carbon-containing explosives. Their small size, large surface area and chemical stability has led to their consideration as gene delivery agents. Their advantage compared to lipid- and polymer-based gene therapy agents is their lack of toxicity and immunogenicity. Genes causing cancer can be blocked by small interfering RNA (siRNA). NDs functionalized with amino acids, such as lysine and histidine, are of interest due their ability to bind and protect siRNA, creating diamoplexes, and deliver them inside cancer cells.

Methods: Four types of fNDs: lysine/lysyl-histidine-NDs (H50K50-NDs), where the attachment of the amino acids to the diamond core is done via 3 and 6 carbon linkers alternatively, were synthesized and characterized. For Scanning Transmission X-ray Microscopy (STXM) and Transmission Electron Microscopy (TEM) studies, cells treated with diamoplexes were embedded in low viscosity acrylic resin.¹ A Hitachi HT7700 Electron Microscope was used for TEM, and STXM studies were conducted at the Canadian Light Source.

Results: We identified specific signals for NDs (C1s region) and their localization in cells. Particle size of internalized diamond NPs range from 20-100 nm depending on degree of particle aggregation. STXM provided the confirmation that the sub-cellular fragments, seen on correlative TEM (*Figure 2*), contain the characteristic sp³ diamond core and helped prove that the fNDs can interact with target cells to achieve a therapeutic effect (*Figure 1*). Cellular uptake appears to be mainly via macropinocytosis, based on the freely circulating NDs within the cytosol and the absence of endosomal sequestration of NDs.²

Conclusion: The correlation of the TEM images, with the presence of the diamond peaks identified via STXM will aid to elucidate the cellular fate of a series of HK-NDs. (*Figure 1*)

Figure 1. STXM images to confirm the identity of internalized entities in HepG2 cells treated with H50K50-ND-based diamoplexes (A) Map identifying the region of interest (5 µm) within the cell (B) Average stack of X-ray micrographs scanned at photon energy ranging from 280 eV to 320 eV representing the region of interest with ND inclusions illustrated as the bright region. (C) STXM generated micro-spectroscopy showing X-ray absorption spectra. The red spectrum shows peaks corresponding to sp³ carbons thus confirming the presence of internalized NDs.

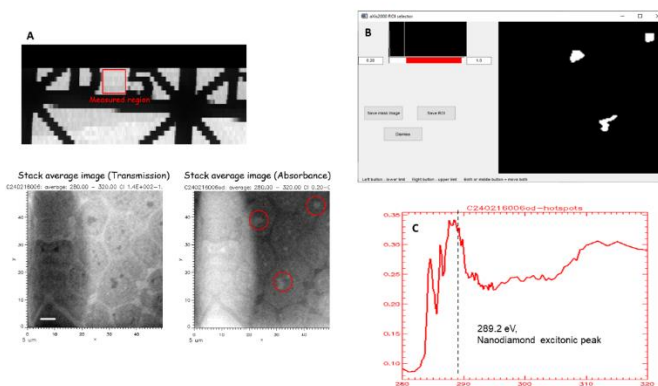
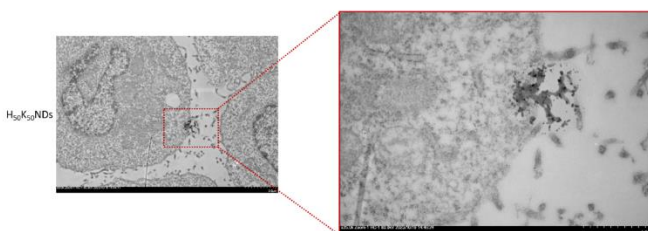


Figure 2. Cellular internalization of fNDs in HepG2 cells captured via TEM. Red boxes indicate the magnified regions on the micrograph. Unlike untreated cells, fND treated cells showed an active membrane internalizing the NDs.



References: 1. Diam and Rel Mat 2023. 137, 110071; 2. Diam and Rel Mat 2019. 98, 107477.

Niclosamide nanoemulsion: development, physicochemical characterization and *in vitro* anticancer activity

Nadia Bou Chacra¹, Eduardo Jose Barbosa¹

¹University of Sao Paulo

Colorectal cancer is characterized by the abnormal proliferation of colon and rectum cells. In advanced cases, chemotherapy plays an important role in the treatment, but the adverse effects of commonly used drugs bring unpleasant consequences for the patient. The promising anticancer activity of the anthelmintic niclosamide makes this drug substance a strong candidate for drug repositioning. This drug substance has shown promising anticancer activity by inhibiting oncogenic signaling pathways - such as Notch, mTOR, NF- κ B, STAT-3 and Wnt/ β -catenin - which, when unregulated, contribute to arise and progression of cancers, justifying the claim for drug repositioning^{1,2}. However, its low water solubility compromises its oral absorption and, consequently, its therapeutic activity. Incorporating niclosamide in nanoemulsion allows administrating it already dissolved in the lipidic system, which surpass the dissolution limiting step and improves the oral absorption. Hence, this study aimed at the development, physicochemical characterization, and *in vitro* anticancer activity of a niclosamide nanoemulsion, using HCT-116 as the cell model. During the nanoemulsion development, Miglyol® 812 proved to be a suitable liquid lipid for the system. Niclosamide nanoemulsion (~200 nm) with Miglyol® 812 and poloxamer 188 was stable for 56 days, with monomodal particle size distribution during the period. The cell viability assay with the human colorectal carcinoma cell line HCT-116 demonstrated that niclosamide cytotoxicity was both time and concentration dependent.

References

Cell Signal 2018 41:89-96

Eur J Pharm Biopharm 2019 141:58-69

Rapid, Low-Cost Detection of Zika virus and *Mycobacterium tuberculosis* Using Locally Manufactured Reagents

Ana Luisa Lot Divarzak¹, Severino Jefferson Ribeiro da Silva¹, Quinn Matthews¹, Keith Pardee¹

¹Department of Pharmaceutical Sciences, Leslie Dan Faculty of Pharmacy, University of Toronto, Toronto, ON M5S 3M2, Canada.

Purpose: In the past few decades, our global society experienced several public health emergencies caused by infectious agents, including Ebola virus, Zika virus, SARS-CoV-2, and *Mycobacterium tuberculosis*. Currently, molecular diagnostics are typically done by certified laboratories for the diagnosis of many infectious diseases, which requires technical expertise, specialized equipment, and extensive sample preparation that is incompatible with use in remote and low-resource settings. Cell-free, point-of-care diagnostic systems can increase accessibility and affordability by minimizing transportation costs with freeze-dried reagents, and decrease turnaround times by decentralizing diagnostic testing. We have developed a low-cost RT-LAMP assay using cell-free-based produced enzymes (Bst-LF and M-MLV) for the diagnosis of Zika virus RNA and *Mycobacterium tuberculosis* DNA.

Methods: Using real-time fluorescence and colorimetric readouts, we first optimized the performance of our in-house manufactured enzymes Bst-LF and M-MLV by monitoring the fluorescence signal obtained in response to addition of enzyme to positive controls containing the genetic material of interest (Zika virus RNA or *Mycobacterium tuberculosis* DNA). Once optimized, another fluorescence assay was used to determine the lowest concentration of genetic material for detection using our locally manufactured enzymes. Finally, we performed a real-life validation of our enzymes using positive controls with synthetic saliva.

Results: We demonstrated that our homemade enzymes had equivalent or superior performance compared to commercially available RT-LAMP enzymes, at a fraction of the cost (<1%).

Conclusion: The results demonstrated suggest that cell-free, locally manufactured reagents may be beneficial in increasing the accessibility of molecular tests, while preserving the sensitivity and specificity of the more expensive and less portable commercial counterparts. This can be a practical solution for expanding the distribution of molecular diagnostics, especially to establish effective disease control programs in low- and middle-income countries. This presentation is supported by the 2024 Canadian Society for pharmaceutical Sciences National Undergraduate Student Research Program Award.

Sensitization of cancer cells to platinum based chemotherapy by pyronaridine and its liposomal formulation, as novel ERCC1/XPF inhibitors, is cell dependent.

Ahmed Abdelfattah^{1,2}, Parnian Mehinrad¹, James Donnelly³, Michael Weinfeld^{4,5}, Frederick G West³, Afsaneh Lavasanifar^{1,6}

¹Faculty of Pharmacy and Pharmaceutical Sciences, University of Alberta, Edmonton, AB, Canada., ²Department of Industrial Pharmacy, Faculty of Pharmacy, Assiut University, Assiut, Egypt., ³Department of Chemistry, Faculty of Science, University of Alberta, Edmonton, AB, Canada., ⁴Department of Experimental Oncology, Cross Cancer Institute, Edmonton, AB, Canada., ⁵Department of Oncology, Faculty of Medicine and Dentistry, University of Alberta, Edmonton, AB, Canada., ⁶Department of Chemical Engineering, University of Alberta, Edmonton, AB, Canada.

Background and Purpose DNA repair pathways contribute significantly to cancer treatment resistance. ERCC1-XPF is a crucial DNA repair enzyme, the overexpression of which correlates with poor platinum treatment outcomes in many tumors (1). Our team has identified the anti-malarial drug pyronaridine (PYD) to be a potent ERCC1/XPF inhibitor (2). The purpose of this study was to investigate the synergistic activity of free versus liposomal PYD in combination with platinum chemotherapeutics in head & neck cancer (HNC) FaDu, non-small cell lung cancer (NSCLC) A549, H1299 cells, and colorectal cancer (CRC) HCT116, SW620 cells.

Methods Liposomes were prepared via ethanol injection method followed by PYD active loading. The cytotoxicity of PYD and liposomal PYD, in the presence or absence of platinum-based chemotherapeutics (cisplatin, carboplatin, or oxaliplatin) against five different cell lines was evaluated using MTT and colony formation assays. Combeneft was used to determine the synergistic versus additive effects of the combinations.

Results Combeneft analysis revealed synergy between cisplatin and PYD in HNC and NSCLC cell lines. The synergy was enhanced with liposomal PYD in FaDu and A549 cells. However, In H1299 synergy was observed in higher cisplatin concentrations and was lower with PYD liposomal formulation. HCT116 and SW620 cells exhibited synergy between PYD and carboplatin, which was further enhanced with liposomal PYD. Combining free or liposomal PYD with oxaliplatin resulted in modest synergistic activity in HCT116 cells. Nevertheless, synergy was not observed between PYD or its liposomal formulation with oxaliplatin in SW620 cells.

Conclusions Our findings show PYD and its liposomal formulation to sensitize cancer cells to platinum chemotherapeutics in a cell dependent manner emphasizing the need for tailored approaches in utilizing PYD-based cancer therapies.

References

1-J Clin Oncol. 2015;33(34):4007-4014.

2-Pharmaceutics 2022, 14(12):2795.

A comparison between different poly(ethylene oxide)-poly(ester) nanocarriers for the solubilization and delivery of S4, a novel competitive inhibitors of polynucleotide kinase/phosphatase (PNKP), for colorectal cancer therapy

Sara I. Abd-El Hafeez¹, Prashant Pandey², Cameron Murray³, James Donnelly⁴, Mark Glover³, Frederick West⁴, Kristi Baker⁵, Michael Weinfeld⁶, Afsaneh Lavasanifar⁷

¹Department of Pharmacy and pharmaceutical science, University of Alberta, Edmonton, AB. Department of Pharmaceutics, Assiut university, Assiut., ²Department of Pharmacy and pharmaceutical science, University of Alberta, Edmonton, AB., ³Department of Biochemistry, University of Alberta Edmonton, AB., ⁴Department of Chemistry, University of Alberta, Edmonton, AB., ⁵Department of Oncology, Cross Cancer Institute, University of Alberta, Edmonton, AB. Department of Medical Microbiology and Immunology, University of Alberta, Edmonton, AB., ⁶Department of Oncology, Cross Cancer Institute, University of Alberta, Edmonton, ⁷Department of Pharmacy and pharmaceutical science, University of Alberta, Edmonton, AB. Department of Chemical Engineering, University of Alberta, Edmonton, AB.

Purpose: Inhibitors of polynucleotide kinase/phosphatase (PNKP) can make cancer cells more sensitive to DNA damage by ionizing radiation or topoisomerase I inhibitors. The aim of this study was to develop nanocarriers of S4, a potent competitive inhibitor of PNKP ($IC_{50}=170$ nM), that can potentially redirect the encapsulated S4 towards colorectal cancer (CRC) and reduce its exposure to normal tissues.

Methods: Encapsulation of S4 was accomplished by dissolving S4 and either of poly(ethylene oxide)-poly(benzyl caprolactone) (PEO-PBCL), poly(ethylene oxide)-poly(caprolactone) (PEO-PCL) or poly(ethylene oxide)-poly(D, L-lactide) (PEO-PDLLA) in DMSO followed by dropwise addition to water and dialysis against water or phosphate buffer saline (PBS, pH 7.4). The prepared formulations were characterized for the level of encapsulated S4 using UV/Vis spectroscopy at 440 nm and average diameter using dynamic light scattering. Cytotoxicity of S4 as free or part of nanocarriers was measured in wild type HCT116 (WT HCT116) and its Phosphatase and tensin homolog (PTEN) knock-out (HCT116 PTEN^{-/-}) phenotype using MTT and colony forming assay.

Results: The average diameter of all formulations under study was < 150 nm. Highest encapsulation efficiency of 13.90 % and loading content of 3.9 % for S4 was achieved in PEO-PDLLA nanoparticles using S4/polymer 1:2.5 w/w ratio. Free S4 showed signs of aggregation in water but the aggregates of drug were not stable in PBS. After 8 hours, S4 released from PEO-PDLLA nanoparticles in PBS and water was 73.5 and 51.6%, respectively. Higher IC_{50} for S4 in WT HCT 116 ($IC_{50}=2.9$ μ M) compared to HCT116 PTEN^{-/-} cells (0.07 μ M) was observed indicating synthetic lethality[1]. Clonogenic survival assay showed HCT116 /PTEN^{-/-} to be more sensitive to S4 at 20 μ M, than WT HCT116 at same concentration.

Conclusions: Data confirms the anti-cancer activity of S4 in PTEN negative CRC and a good potential for PEO-PDLLA nanocarriers for S4 solubilization.

References

1. Sadat, S.M.A., et al., A synthetically lethal nanomedicine delivering novel inhibitors of polynucleotide kinase 3'-phosphatase (PNKP) for targeted therapy of PTEN-deficient colorectal cancer. *Journal of Controlled Release*, 2021. 334: p. 335-352.

Ion-sensitive in situ gel development with *Andrographis paniculata* extract loaded for preventing SARS-CoV-2 infection

Jeerakit Kerdhiri¹, Neti Waranuch¹, Siwaporn Boonyasuppayakorn², Parvapan Bhattarakosol², Tasana Pitaksuteepong¹, Raimar Löbenberg³

¹Naresuan University, ²Chulalongkorn University, ³university of alberta

Purpose: COVID-19, an emerging respiratory disease, significantly impacts human and animal health. This study aims to formulate an ion-sensitive nasal spray composed of hydroxypropyl methylcellulose (HPMC) blended with carrageenan containing *Andrographis paniculata* extract for its anti-SARS-CoV-2 properties.

Methods: The anti-SARS-CoV-2 activity of *Andrographis paniculata* extract was assessed on vero E6 cells using a TCID50 titration assay. The extract was incorporated into the developed nasal spray. Ion-gelation studies were conducted to examine the interaction between a simulated nasal electrolyte solution and the blended polymer in the nasal spray. The time taken to form a gel was compared between the base formula without blended polymers and the interaction with the simulated nasal electrolyte solution.

Results: The *Andrographis paniculata* extract exhibited over 90% inhibition of SARS-CoV-2 on vero E6 cells at a concentration of 10 μ g/ml. This extract was then loaded into the nasal spray formula for its anti-SARS-CoV-2 properties. The developed nasal spray demonstrated effective interaction with ions in the simulated nasal electrolyte solution (Ca^{2+} , Mg^{2+} , and Na^{+}). Upon application to a membrane absorbing the simulated nasal electrolyte solution and water, the tail length of the developed nasal spray was measured at 1.74 ± 0.07 cm and 3.87 ± 0.03 cm, respectively. Furthermore, it exhibited a shorter gel formation time compared to the base formula (3.37 ± 0.15 cm).

Conclusion: The polymeric system consisting of HPMC, and carrageenan exhibited gel formation through ion-responsive reactions with the electrolytes present in the mucus of nasal cavity. Additionally, *Andrographis paniculata* extract displayed promising potential as a natural active ingredient for anti-SARS-CoV-2 products.

Intranasal delivery of low-dose anti-CD124 antibody enhances treatment of chronic rhinosinusitis with nasal polyps

Jiamin Wu¹

¹University of British Columbia

Purpose: Frequent injections of anti-CD-124 monoclonal antibody (α CD124) over long periods of time are used to treat chronic rhinosinusitis with nasal polyps (CRSwNP). Intranasal administration of α CD124 is expected to provide advantages for localized delivery, improved efficacy, and enhanced medication adherence. However, delivery barriers such as the mucus and epithelium in the nasal tissue persist and impede penetration of α CD124.

Methods: We synthesized two novel protamine nanoconstructs: allyl glycidyl ether conjugated protamine (Nano-P) and polyamidoamine-linked protamine (Dendri-P). α CD124 was dissolved in an aqueous phase with Nano-P or Dendri-P, and the transcellular delivery efficiency were compared in different models, including 3D cell spheroids and animals. Medical application of Nano-P or Dendri-P for delivering α CD124 was demonstrated in mouse models of chronic rhinosinusitis with nasal polyposis (CRSwNP).

Results: Our findings indicated that Nano-P and Dendri-P enhanced α CD124 penetration through multiple epithelial layers compared to protamine in 3D model and mice. α CD124 was mixed with Nano-P or Dendri-P and then intranasally delivered for the treatment of severe CRSwNP in mice. Micro-CT and pathological changes in nasal turbinates showed that these two nano-formulations achieved ~50% and ~40% reductions in nasal polypoid lesions and eosinophil count, respectively. These effects were superior to those in the protamine formulation group and the high s.c. dose. Therapy with subcutaneous α CD124 achieved ~30% reductions in both nasal polypoid lesion and eosinophil count compared to the PBS-treated control. Both nano-formulations provided enhanced efficacy within 8 weeks in suppressing nasal and systemic Immunoglobulin E (IgE) and nasal type 2 inflammatory biomarkers, such as IL-13 and IL-25, compared to the protamine formulation and subcutaneous α CD124 given at a 12.5-fold higher dose. Intranasal delivery of protamine, Nano-P, or Dendri-P did not induce any measurable toxicities in mice.

Conclusion: The novel protamine nanoconstructs are effective and safe systems for non-invasive delivery of monoclonal antibodies.

Development of cationic mRNA-gemini lipid nanoparticles for neuroprotective treatment of the retina in glaucoma

Antoine Hakim¹

¹University of Waterloo

Purpose: Glaucoma is a complex group of eye disorders which has been traditionally connected to elevated intraocular eye pressure (IOP). Evidence from different studies indicates that IOP elevation damages retinal ganglion cells (RGCs) and the optic nerve by blocking the axonal transport of neurotrophic factors (NFs). The objective was to evaluate lipid nanoparticles (LNPs) engineered from dicationic gemini surfactants, (GS) and lipids as potential carriers for mRNA encoding NFs, with the goal to overcome the limitations of conventional IOP lowering glaucoma therapy and the side effects of viral gene delivery vectors.

Method: We formulated and physicochemically characterized two sets mRNA(GFP)-cationic LNPs constructed from GS and phospholipids with and without PEGylation (mPEG-DSPE, 0.5, 1, 2%). A non-PEGylated LNP1 (18-7NH-18) and a PEGylated LNP2 (18-7NH-18, mPEG-DSPE 0.5%) were selected and evaluated for transfection efficiency (TE) in potential retinal target cell lines, such as astrocytes (A7), Müller cells (rMC-1), and RGC-like cells (XFC-3), using flow cytometry and confocal microscopy.

Results: LNP1(18-7NH-18) had Z-average size of 89.6 ± 1.5 nm, PDI of 0.270 ± 0.000 , charge $+34.7 \pm 2.8$ mV and encapsulation efficiency (EE) of $75.6 \pm 6.4\%$. LNP2(18-7NH-18, mPEG-DSPE-0.5%) had Z-average size of 120.3 ± 1.3 nm, PDI of 0.31 ± 0.03 , charge $+39.8 \pm 3.5$ mV and EE of $67.7 \pm 0.9\%$. TE (n=4) was highest in rMC-1 cells for both LNPs, $45.6 \pm 4\%$ and $46.5 \pm 4.4\%$, followed by A7 cells $26.5 \pm 4.9\%$ and $38.2 \pm 3.7\%$, and XFC-3 cells $12.9 \pm 1.4\%$ and $11.7 \pm 0.5\%$, respectively. Cell viability assay showed over 95% viability for all cell lines when treated with the two types of LNPs. Comparatively, a commercial transfection agent, TransIT®-mRNA showed TE $49.2 \pm 6.1\%$ for rMC-1 cells, $55.5 \pm 4.9\%$ for A7 cells and $28.3 \pm 15.2\%$ for XFC-3 cells.

Conclusion: Both PEGylated (0.5%) and non-PEGylated LNPs showed similarly high TE in difficult-to-transfect retinal cells, as well as low toxicity. These results support further studies in *in vivo* animal models.

Hepatotoxicity Screening Array: Optimizing cytotoxicity indicators and assay conditions.

Kirtpal Singh¹, Arno G Siraki¹

¹Faculty of Pharmacy and Pharmaceutical Sciences, Katz Group-Rexall Centre for Pharmacy and Health Research, University of Alberta, Edmonton, Alberta, T6G 2E1 Canada.

Purpose: This study aims to utilize advanced methods and arrays to improve the screening process for detecting cytotoxicity of drugs in HepG2 cells and to establish a reliable concentration-dependent model for screening assays to assess potential hepatotoxicity.

Methods: HepG2 cells were treated with different concentrations of drugs that induce hepatotoxicity (diclofenac, troglitazone) and a known cytotoxic compound (menadione) over 24 hours under both serum and serum-free conditions. Concentration-response relationships were determined using cell-based assays, including WST-8, Neutral Red Uptake (NRU), and CellTiter-Glo® (ATP-assay).

Results: Diclofenac demonstrated less cytotoxicity when serum was present (CellTiter-Glo® $IC_{50} = 549.78 \pm 12.59$ μ M, WST-8 $IC_{50} = 519.26 \pm 18.61$ μ M, NRU $IC_{50} = 1687.23 \pm 46.31$ μ M), whereas more cytotoxicity was observed using serum-free conditions ($IC_{50} = 274.55 \pm 8.78$ μ M, $IC_{50} = 330.37 \pm 19.09$ μ M, $IC_{50} = 1505.41 \pm 22.34$ μ M). Troglitazone exhibited significant variations in cytotoxicity between serum-containing ($IC_{50} = 119.42 \pm 8.65$ μ M, $IC_{50} = 158.57 \pm 8.48$ μ M, $IC_{50} = 148.90 \pm 9.03$ μ M) and serum-free conditions ($IC_{50} = 47.44 \pm 7.40$ μ M, $IC_{50} = 115.12 \pm 7.59$ μ M, $IC_{50} = 32.62 \pm 5.84$ μ M) conditions. Menadione was the most cytotoxic compound used. However, serum-containing conditions ($IC_{50} = 3.14 \pm 0.891$ μ M, $IC_{50} = 11.27 \pm 1.41$ μ M, $IC_{50} = 30.75 \pm 6.06$ μ M) and serum-free ($IC_{50} = 1.79 \pm 0.53$ μ M, $IC_{50} = 8.46 \pm 2.0$ μ M, $IC_{50} = 11.12 \pm 2.28$ μ M) revealed a difference in cytotoxic potency.

Conclusion: Diclofenac and troglitazone revealed significant effects of protein binding, as did the cytotoxic control, menadione. Troglitazone has demonstrated reversible protein binding to serum albumin, and these effects appear to be revealed with these assays. These findings emphasize the role of serum in drug accessibility and the importance of screening with different endpoints for cytotoxicity. Further cytotoxicity endpoints are required for a holistic screening profile for drug cytotoxicity

Development of Cyclodextrin-based Nanoparticles for Intranasal Delivery of Anti-inflammatory Peptide for the Treatment of Neutrophilic Asthma

Yonglu Wang^{1,2}, Deborah Michel², Emma Finch², Noah Lim³, Michelle Vargas Fernandes², Alexandra Cullen², John Gordon⁴, Ildiko Badea²

¹College of Pharmacy, Nanjing Tech University, Nanjing, China, ²College of Pharmacy and Nutrition, University of Saskatchewan, Saskatoon, Canada, ³Medical Sciences, Western University, London, Canada, ⁴College of Medicine, University of Saskatchewan, Saskatoon, Canada

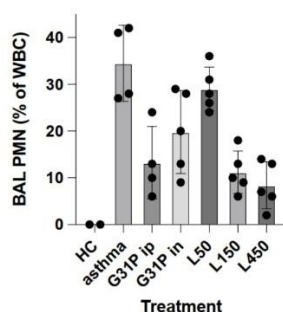
Purpose: Neutrophilic asthma is considered severe refractory asthma which does not respond well to conventional treatment such as steroid therapy. An anti-inflammatory peptide CXCL8 (3-72) K11R/G31P (G31P) reduces neutrophilic inflammation, and is highly

effective to treat neutrophilic asthma. However, injectable administration of G31P is not practical, thus an alternative, non-invasive intranasal delivery based on cationic gemini surfactant-conjugated β -cyclodextrin (G31P/CD-Gem) was developed.

Methods: An air-liquid interface in BEAS-2B cell model was established for safety and the trans-membrane delivery assessment of G31P/CD-Gem. Functional studies were conducted in ova-induced asthmatic murine model.

Results: Transepithelial electrical resistance results showed that G31P/CD-Gem had no toxic effect on membrane of BEAS-2B cells. Intranasal administration G31P/CD-Gem reduced percentage of polymorphonuclear cells significantly compared to untreated animals ($p < 0.05$), while no significant difference was measured from the intraperitoneal injection ($p > 0.05$).

Conclusion: These results indicate that the CD-Gem formulation is a feasible alternative for non-invasive delivery of G31P for the treatment of neutrophilic asthma.



References

J Leukocyte Biol 2005 78:1265-1272

Int. J. Pharm. 2012 81:548-556

⁶⁴Cu-labeled panitumumab for PET imaging of EGFR+ non-small cell lung cancer in subcutaneous versus metastatic models

Nasim Sarrami¹, Melinda Wuest², Igor Paiva¹, Samantha Leier², Afsaneh Lavasanifar¹, Frank Wuest²

¹Faculty of Pharmacy and Pharmaceutical Sciences, University of Alberta, Edmonton, Alberta, Canada, ²Department of Oncology, Cross Cancer Institute, University of Alberta, Edmonton, Alberta, T6G 1Z2 Canada

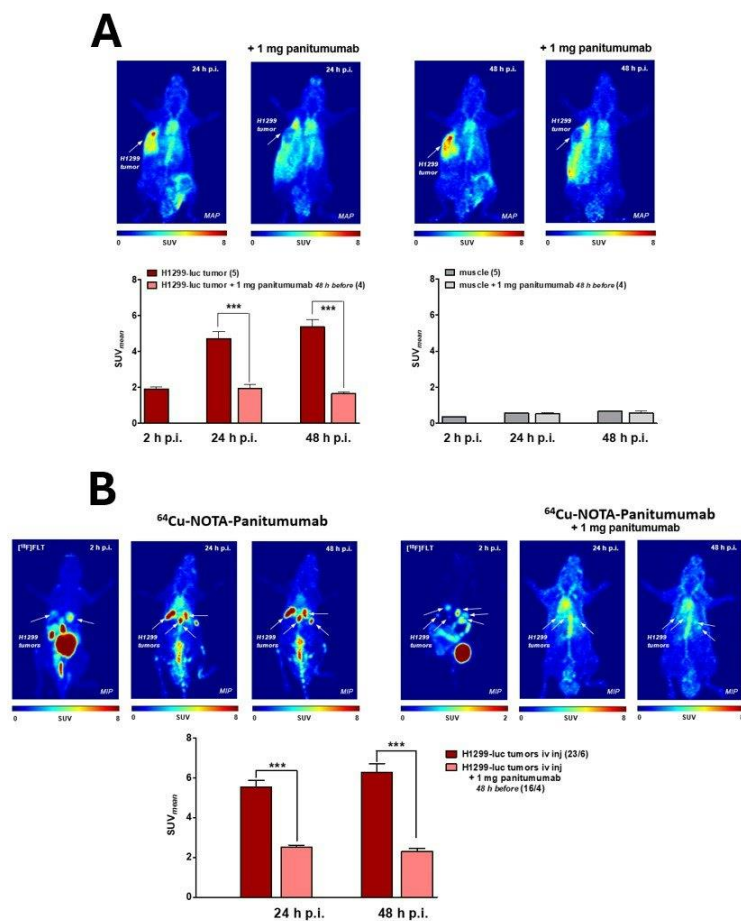
Purpose: We aim to develop ⁶⁴Cu labeled panitumumab and assess its potential for homing on epidermal growth factor receptor (EGFR)⁺ NSCLC *in vitro* and *in vivo* models.

Methods: 2-S-(4-Isothiocyanatobenzyl)-1,4,7-triazacyclononane-1,4,7-triacetic acid (NOTA-NCS) was attached to panitumumab. Radiolabeling with ⁶⁴Cu was performed at pH 5.5 at 37 °C for 1 hour. The incorporation efficiency of ⁶⁴Cu into NOTA-panitumumab was measured using radio-TLC. The cellular interaction of the developed EGFR-targeted PET probe was assessed using H1299 cells in the absence and presence of cold mAb measuring cell radioactivity. The homing of developed EGFR-targeted PET probes on EGFR+ H1299 subcutaneous versus metastatic mouse model was evaluated with and without cold panitumumab pre-treatment. To develop the subcutaneous (sc) model, NSG mice were injected with 3×10⁶ H1299 cells subcutaneously into the left shoulder. To develop the metastatic tumor model, 1×10⁶ H1299 cells were injected intravenously into NSG mice. Static PET imaging was performed at 2-, 24- and 48-hour post-injection of ⁶⁴Cu-labeled panitumumab via tail vein after fluorothymidine F-18 measurements confirmed tumor establishment in the metastatic model.

Results: Radiolabeling efficiency with ⁶⁴Cu was 93.8 ± 5.7 %. PET images of both mice models indicated a significant accumulation of ⁶⁴Cu-panitumumab in the tumors. The biodistribution studies for the sc model indicated tumor-to-blood (T/B) of 2.75 ± 0.41 versus 0.54 ± 0.02 and tumor-to-muscle (T/M) of 26.33 ± 3.90 versus 6.31 ± 0.71 for non-blocked and blocked groups respectively. For the metastatic model, liver tumors indicated a T/B of 5.97 ± 3.84 versus 0.66 ± 0.18 and T/M of 53.22 ± 35.18 versus 10.04 ± 7.46

and the lung tumors, T/B was 2.42 ± 0.99 versus 0.42 and T/M was 20.58 ± 13.35 versus 5.74 for non-blocked and blocked groups respectively.

Conclusions: ^{64}Cu -labeled panitumumab is a suitable immuno-PET probe for imaging ERFG+ tumors in both sc and metastatic settings



A) PET/CT scans via ^{64}Cu - Panitumumab radiotracer in H1299 subcutaneous tumor-bearing mice. B) PET/CT scans of mice bearing orthotopic metastatic NSCLC. Tumors are scanned via 18F-FLT and ^{64}Cu -Panitumumab as radiotracers. Both PET/CT scans with ^{64}Cu -panitumumab radiotracer were done 24 and 48- hours after injection of radiotracer

Developing aspirin-loaded polymeric microneedles with novel baseplate for HIV prevention

Alistair K.C. Chan¹, Ryan Nodder¹, Emmanuel A. Ho, Ph.D.¹

¹University of Waterloo School of Pharmacy, Kitchener, ON

Purpose: Preventing HIV infection is important, lest infected individuals develop AIDS. Current preventions include the use of condoms or pre-exposure prophylaxis, which are not readily available and stigmatised. Dissolving microneedle (MN) patches are pain-free, easy to self-apply, gender-neutral, and can deliver drugs for prolongedly, hence enhancing patient compliance[1].

As such, we developed a dissolving, MN patch composed of PLGA with a novel baseplate for the sustained delivery of acetylsalicylic acid (ASA) to the systemic T cells as a novel strategy to prevent HIV. Since activated T-cells, the primary HIV target cells, are 1000x more susceptible to HIV infection their counterparts in an immune quiescence state(IQ), this strategy reduces susceptible HIV target cells, whereby delivery of ASA to such cells would induce a state of IQ[2].

We postulate that the MN patch is mechanically strong enough to penetrate the stratum corneum, release ASA sustainedly subcutaneously such that ASA can induce IQ in systemic T Cells.

Methods: To fabricate MNs, rhodamine123(RhB), model fluorophore for ASA, and PLGA that had been casted into a MN mould were dried at room temperature. Afterwards, self-adhesive baseplates were attached to the patch to enhance mechanical strength and drug loading. The mechanical strength of such MNs was validated with insertion analysis[1]. To determine *in vitro* the release kinetics of the patch, aliquots of the RhB-loaded MNs that had been incubated in PBS and collected at the appropriate time points were assayed for the concentrations of RhB with a microplate reader.

Results: PLGA MNs were not only able to penetrate the first 2 layers of the folded Parafilm M sheet in insertion analysis but also able to release its payload sustainedly for over a week.

Conclusion: This is a proof-of-concept demonstrating our MNs possess adequate mechanical strength and release kinetics for subsequent transdermal delivery of ASA.

References

- [1] Nano-Micro Lett. 13 (2021) 93.
- [2] Retrovirology 10 (2013) 141.

Assessment of Melatonin Content and Dissolution Variability in Over-the-Counter Natural Health Products

Shengnan Zhao¹, Neal M. Davies¹, Raimar Loebenberg¹

¹University of Alberta

Purpose: Melatonin is used for the treatment of insomnia, adjustment of sleep cycles, and other sleep disorders. Natural Health Products (NHPs) containing melatonin are regulated as over-the-counter (OTC) medications, and are readily available on the market in Canada. This study aims to evaluate and compare the actual melatonin content and dissolution of commercial melatonin NHPs.

Method: A survey of the Health Canada Licensed NHP database was conducted to identify melatonin products with an NHP number and their dosage forms. Fifteen melatonin NHP products were randomly selected for content and dissolution analysis using the methods outlined in the US Pharmacopeia (USP) monograph for melatonin tablets, with necessary adjustments for other dosage forms.

Results: The Licensed Natural Health Product (NHP) database indicates the presence of 620 products where melatonin is the only active ingredient. Among the tested products, the melatonin content ranged from 93.6% to 132.0%, with all but one product adhering to the NHP quality requirement of 80% to 120%. Nonetheless, when evaluated against the US Pharmacopeia (USP) monograph 90% to 110%, 7 products were deemed non-compliant. In performance testing, it was found that one immediate-release tablet failed to reach a dissolution rate of NLT 75% within 30 minutes, and two controlled-release tablets did not achieve the required dissolution rate of NLT 80% within 8 hours.

Conclusion: Six out of fifteen products exhibited moderate deviations from the melatonin content declared on the label, with deviations being over 10% but less than 20%, and all deviations were higher than the labeled amount. Additionally, one product significantly exceeded the labeled melatonin content by more than 30%. Three tablet products demonstrated lower than expected dissolution rates. The variability in melatonin efficacy in feedback from patients could potentially be attributed to the dissolution of the products, rather than insufficient quantities of melatonin.

Engineering dual drug-loaded Hollow Gold Nanoparticles for targeted therapy of Glioblastoma

Tabassum Khan¹, Mansi Damani², Munira Momin², Raghumani S Ningthoujham³

¹Department of Pharmaceutical Chemistry, SVKM's Dr. Bhanuben Nanavati College of Pharmacy, Mumbai, Maharashtra, India,

²Department of Pharmaceutics, SVKM's Dr. Bhanuben Nanavati College of Pharmacy, Mumbai, Maharashtra, India, ³Chemistry Division, Bhabha Atomic Research Centre, Trombay, Mumbai - 400085, Maharashtra, India

Purpose: Temozolomide (TMZ) is the standard FDA-approved drug for Glioblastoma (GBM) chemotherapy but with long-term exposure to the drug, the glioblastoma-initiating cells (GICs) develop resistance to the action of TMZ. The use of metallic nanoparticles like hollow gold nanoparticles (HAuNPs) has been explored for photothermal treatment of cancer cells because they demonstrate strong surface plasmon absorption and photothermal coupling in the near-infrared (NIR) spectrum. Resveratrol (RES), a phytoconstituent can induce GICs to the activity of TMZ-induced apoptosis. Our study aims to develop 808 nm NIR laser-induced photothermal therapy using TMZ-RES loaded HAuNPs for the management of GBM.

Methods: HAuNPs were formulated with slight modifications in sacrificial galvanic replacement of cobalt core and coated with modified PEG and glutathione (GSH) for targeting. Particle size was determined using HR-TEM and zeta-analyser. The amount of drug released from HAuNPs was determined using a modified Franz diffusion apparatus and dialysis bag method in PBS pH 7.4. The cytotoxicity potential of GSH-PEG-HAuNPs was determined on a panel of GBM cells (C6, U87, and LN229). The *in vivo* efficacy and biodistribution studies of HAuNPs were studied using an orthotopic rat model.

Results: The developed HAuNPs showed a hydrodynamic particle size of 83.03nm after PEGylation; HR-TEM imaging confirmed the hollowness of the core and drug entrapment of 50.97% and 41.94% of TMZ and RES. The particles showed a good photothermal effect and complete release of both drugs when irradiated with a power of 3.2watts/cm.sq. MTT assay confirmed the enhanced cytotoxic potential of TR-PEG-HAuNPs against free drugs. The efficacy studies revealed that tumor inhibition was highest when formulation TMZ RES was administered with NIR laser.

Conclusion: The synthesized GSH-PEG-TR HAuNPs have the potential to target brain delivery of the drugs and exert cytotoxic action on the GBM cancer cells; thus, mitigating the disadvantages of the conventional drug therapy.

Enhanced Enrichment Methods for Extracellular Vesicles from Human Mast Cells (LAD2) for Targeted Drug Delivery

Feng Wang¹

Purpose: Extracellular vesicles (EVs) are naturally released vesicles from cells that shuttle nucleic acids, proteins, lipids and metabolites between cells, making them excellent therapeutic carriers for target drug delivery. However, isolation and enrichment of EVs are challenging due to the heterogenous mixture in the cell medium. Herein, we aim to find an optimized method to isolate and enrich the EVs from human mast cells (LAD2) cultured in a complex protein-enriched serum-free media.

Methods: Five different methods were utilized to enrich EVs: ultracentrifugation (UF), polymer precipitation (PP), immunoaffinity (IA), anion exchange chromatography (AEC) and tangential flow filtration (TFF). Cryogenic transmission electron microscopy (Cryo-TEM), dynamic light scattering (DLS) and western immunoblot analysis were used to characterize the EVs and their subpopulations.

Results: Each enrichment method produced EVs with slightly different characteristics on size, PDI and Zeta potential (by UF: 83.69nm with PDI at 0.40 and the highest Zeta potential at -30.74 mV; by IA had the lowest zeta potential at -13.38 mV but the highest PDI at 0.68; by PP were the smallest in diameter at 55.06nm; by AEC were 86.7 nm and by TFF were 75.61nm with the lowest PDI at 0.29.) Cryo-TEM analysis of EVs enriched by UC revealed EVs ranging from 20 nm to 400 nm in diameter, with heterogenous shapes and various internal densities. CD9 was detected by western blot in EVs purified by UF, PP and IA, but could not be detected from EVs enriched by AEC and TFF due their dilution and the protein contaminants in the media.

Conclusions: The method of EV enrichment has a large influence on the size, charge and purity of the resulting EVs. Thus far, UF appears to be the most efficient way to isolate EVs from LAD2 for target drug delivery, although there may be bias for specific subpopulations.

Predictive *in silico* Pharmaceutical Modeling of Cannflavin Metabolism, Physicochemical, Pharmacokinetic, and Pharmacological Effects

Conor O'Croinin¹, Andres Garcia Guerra¹, Malaz Yousef¹, Michael R. Doschak¹, Raimar Löbenberg¹, Neal Davies¹

¹University of Alberta

Purpose: Prenylated flavonoids called cannflavins are bioactive compounds with therapeutic potential. Cannflavin A, B, C, and caflanone are all flavonoids determined in the *Cannabis sativa* and *Mimulus biglelovii* plants and can be extracted to be investigated for their pharmacological activities. Past research has demonstrated antiviral, anticancer, and anti-inflammatory properties of these compounds, but more research is needed to understand the full potential of these poorly characterized flavonoids.

Methods: *In silico* modeling was used to further our understanding of cannflavin A, B, C, and caflanone. Predictive pharmaceutical modeling was performed using ADMET Predictor™ 11.0 (Simulations Plus, Lancaster, CA, USA) to obtain predicted metabolism, transporter, physicochemical, and pharmacokinetic properties of the cannflavins.

Results: The four cannflavins are predicted to inhibit many of the cytochrome P450 (CYP) isoforms and are substrates for CYP1A2 and CYP2C9. They are predicted to be readily glucuronidated in the body by various UDP glucuronosyltransferase isoforms. All four cannflavins show potential inhibition of breast cancer resistance protein, which may aid in chemotherapeutic treatment. The compounds are also predicted to have anti-retroviral properties based on the inhibition of HIV-1 integrase. Topical and oral delivery of cannflavins show promise as routes of administration due to high skin and jejunal permeability values.

Conclusion: Predictive pharmaceutical modeling of the four cannabis-derived flavonoids has yielded promising results that can be used to guide future developmental research into their use. The *in silico* modeling tools have provided foundational knowledge about their metabolism, activity, physicochemical properties, and pharmacokinetics. These data justify further investigation and development of cannflavin products using *in vitro* and *in vivo* models.

Development of Novel Cellulose-based Soy Biopolymer for Sustainable 3D Printing and Drug Delivery

Ryan Nodder¹, Emmanuel Ho¹

¹University of Waterloo

Purpose: The excessive global consumption and improper disposal of plastics has led to dramatic environmental consequences that continue to harm our planet, highlighting the need for the development of sustainable materials and processes. Most materials currently used in 3D printing are thermoplastics with minimal degradability and made from non-renewable resources, proving unsustainable to support the anticipated expansion of the 3D printing industry in years to come. In this study, the first ever paper-based soy biopolymer feedstock for 3D printing applications is developed. With paper accounting for one third of Canada's waste, this provides both a solution to the growing problem of environmental pollution and global warming worldwide, as well as the need for sustainable materials and processes in 3D printing. The biomaterial developed can also be used for various drug delivery applications as a biodegradable drug delivery system.

Methodology: A formulation of soy protein, paper and additives has been developed to produce a biopolymer paste to be used for extrusion 3D printing. This bioplastic is composed entirely of generally regarded as safe (GRAS) components to provide an alternative, environmentally friendly, and non-toxic material for 3D printing. This novel paper-feedstock material can be 3D printed using a syringe-based extrusion mechanism to create a wide variety of 3D structures. Mechanical properties, biodegradability, cytotoxicity, water uptake and additional characterizations were performed to help evaluate the applications of this novel material.

Results: Characterizations of this material reveal rapid biodegradation in soil, as well as tunable mechanical strength suitable for a wide range of real-world applications.

Conclusion: The cellulose-based soy bioplastic introduced in this work helps to highlight a solution to global issues in both the recycling of paper waste and provides a sustainable pathway for the ever-expanding applications of 3D printing, as well as the potential for use in biodegradable drug delivery systems.

Development of chow formulations for olaparib and lunresertib to maintain sustained exposure in mice

Marie-Eve Leclaire¹, Shou Yun Yin¹, Janek Szychowski², Sara Fournier¹, Gino B. Ferraro¹, Bitra Lotfollahzadeh Barzili¹, Rosie Kryczka¹, Anne Roulston¹, C. Gary Marshall¹, Robert Papp¹

¹Repare Therapeutics, ²adMare BioInnovations

Purpose: Formulated chow is an alternative to oral gavage that provides the advantage of stable exposure of the drug of interest. The resultant uniform PK profile is often useful to establish a PK/PD relationship driver or to sufficiently sustain blood levels to conduct proof-of-concept studies in mice. The aim of this study was to develop lab-scale chow formulations of olaparib (PARP inhibitor) and lunresertib (PKMYT1 inhibitor), to assess their homogeneity and to evaluate their PK profile in mice.

Methods: Chow formulation conditions were first optimized. Compounds were fully dissolved in solvent and then blended with a granular rodent diet using a stand mixer. The resulting material was vacuum-dried overnight and presence of residual solvent was evaluated by gas chromatography. Drug extraction conditions were optimized and compounds levels were quantified by UPLC-MS/MS to determine accuracy and uniformity of the blend. The chow was stored at room temperature and content analysis was re-assayed after 3 months. Chow formulations were provided *ad libitum* to CD1 mice and blood levels were measured by UPLC-MS/MS at multiple timepoints.

Results: The optimal solvent for olaparib was 2:1 dichloromethane/methanol with a maximum solubility of 60 mg/mL and for lunresertib, acetone provided a maximum solubility of 4 mg/mL. The optimal extraction solvent for olaparib was 1:2:2 water/acetonitrile/methanol and 1:9 acidified water/acetonitrile for lunresertib. Accurate and homogeneous chow formulations were obtained after 2 hours of blending, achieving drug content between 85%-115% of targeted dose and a coefficient of variation <15%. Olaparib and lunresertib chow formulations achieved sustained blood levels over 24 hours.

Conclusion : Olaparib and lunresertib chow formulations were successfully developed and optimized. The drug content of the resulting blends was accurate, uniform and stable under storage. Chow formulations of both compounds maintained consistent blood levels over time in mice.

Formulation of prenylated hemp polyphenols for improved bioavailability

Kelly Boddington
Canurta, Guelph, Ontario, Canada

Purpose. Cannflavins are prenylated polyphenols found in the *Cannabis sativa* plant which show appealing anti-inflammatory and neuroprotective effects. However, due to their limited water solubility and anticipated metabolism by the liver, these compounds

require advanced formulation to be effective as drugs.

Methods. The anti-inflammatory and neuroprotective effects of cannflavins A and B were investigated in *in vitro* assays and in zebrafish and nematode models. Subsequently, the oral bioavailability of unformulated cannflavins and their ability to cross the blood-brain barrier were tested. Due to the low bioavailability of cannflavins, several different formulation projects were initiated, each with its own specific goal. A natural health product formulated for lymphatic absorption is being launched. This project will be followed by further investigation into optimizing formulation for oral bioavailability in a botanical drug. Additionally, collaboration is underway to develop transdermal and buccal strips, and efforts are being made to develop solid lipid nanoparticles for delivery across the blood-brain barrier.

Results. Cannflavins show a dual anti-inflammatory effect with the inhibition of mPGES and 5-LO in cell-based models. Moreover, they display improvement of motility in a zebrafish model that mimics ALS motor neuron defect as well as in *C. elegans* models for ALS and frontotemporal dementia. During formulation development, it was found that incorporating cannflavins with an oily vehicle solubilizer significantly improves dissolution in simulated gastric and intestinal fluids, as well as lymphatic absorption in an *in vitro* model. Formulation of cannflavins in transdermal and buccal strips increases penetration in *in vitro* and *ex vivo* porcine models. Solid lipid nanoparticles can be successfully formed to encapsulate cannflavins.

Conclusion. Our formulation development efforts have unveiled promising strategies for enhancing the solubility, absorption, and delivery of cannflavins to secure their therapeutic potential, which underscores the commitment at Canurta Therapeutics to advancing botanical drugs with targeted formulation approaches.

A sodium butyrate nano-emulsion modifies glycosaminoglycan synthesis in human mast cells paving the way for endogenous production of anticoagulants

Syed Benazir Alam¹, Marianna Kulka^{1,2}

¹Nanotechnology Research Centre, national research Council Canada, Edmonton, AB, ²Medical Microbiology and Immunology, University of Alberta, Edmonton, AB

Purpose: Glycosaminoglycans (GAGs) such as heparin are used as anticoagulants and is given to patients undergoing different treatments where blood clotting is a serious risk. Understanding and controlling GAG production is an important precursor to developing more targeted anticoagulant treatments. Sodium butyrate (NaBu), a short chain fatty acid, is a histone deacetylase inhibitor that modulates expression of about 7-10% of the genes in transformed cells. Previous work from our lab suggests that NaBu causes ultrastructural changes in secretory granules of the transformed human mast cell (HMC-1) subline 2 (HMC-1.2)¹. In the present study we investigated the effect of NaBu on GAGs which are a major component of HMC-1 granules.

Methods: Fluorescence from berberine (BBR) that stains GAGs and other cell permeant dyes was measured using flow cytometry. HMC-1.2 cells were treated with 1 mM NaBu/PBS for 24, 48 and 72 hr followed by total RNA extraction and cDNA synthesis. mRNA expression of genes was evaluated by reverse transcriptase quantitative polymerase chain reaction (RT-qPCR) using *GAPDH* as endogenous control. NaBu cholesteryl solid lipid nano-emulsion (NaBu NE) was synthesized using warm microemulsion method².

Results: When HMC-1.2 were treated with 1 mM NaBu, a significant increase in BBR fluorescence was observed. However, an increase in fluorescence was not found when NaBu treated HMC-1.2 were stained with other cell permeant dyes such as calcein, Nile red and near IR live dead stain. By RT-qPCR genes such as *GLCE*, *NDST1*, *NDST2*, *HS6ST1* and *GALT1*, involved in the synthesis/elongation/maturation of sulphated GAGs such as heparin sulphate and heparan sulphate, were significantly upregulated after NaBu treatment. Furthermore, NaBu NE showed greater potency than NaBu in increasing GAGs.

Conclusion: NaBu modifies GAG synthesis by human mast cells suggesting that NaBu could be used to develop more targeted anticoagulant treatments that may directly stimulate the production of endogenous GAGs.

References

1. Front Allergy, 2023 4
2. Br J Pharmacol 2: 233-244

Enhancing Neuronal Reprogramming: Gemini Lipid-Based Lipid Nanoparticles for Targeted Nucleic Acid Delivery to Astrocytes

Jonathan Rekve

University of Saskatchewan

Purpose: Neuronal reprogramming and lipid nanoparticles (LNPs) represent innovative approaches for treating incurable neurological diseases and delivering gene therapies, respectively. Reprogramming astrocytes into induced neurons (iNeurons) offers a promising method to replenish lost neuronal populations and counteract neurodegeneration. Additionally, utilizing gemini lipids in LNPs has shown significant promise in enhancing the delivery of nucleic acid payloads to specific cell types, such as astrocytes, which are vital for brain health and disease pathology.

Methods: Our study synergizes direct neuronal reprogramming with advanced LNP formulations, emphasizing the use of gemini lipids and 1,2-dioleoyl-sn-glycero-3-phosphoethanolamine (DOPE) for targeted astrocyte delivery. A cornerstone of our analysis was the application of Small Angle X-ray Scattering (SAXS), providing essential insights into the nanostructural organization and lipid molecular arrangement of the LNPs, which are crucial for enhancing cellular targeting and nucleic acid release.

Results: SAXS investigations revealed that the inclusion of DOPE in gemini lipid-based LNPs leads to the formation of a hexagonal phase, resulting in an 8-fold increase in nucleic acid delivery efficiency while maintaining minimal toxicity. This hexagonal configuration signifies a more orderly and stable structure, optimizing the encapsulation, protection, and subsequent release of nucleic acids into targeted cells.

Conclusion: The hexagonal phase structure within DOPE-incorporated LNPs is pivotal for their enhanced delivery capabilities. These structural insights are critical for optimizing nanoparticle design to improve interactions with astrocytes, thereby increasing delivery success rates. Our research advocates for a hybrid approach that combines cellular reprogramming with nanotechnological delivery enhancements, opening new avenues for treating neurodegenerative diseases and brain injuries. Ongoing refinement of these techniques has the potential to introduce novel therapeutic modalities in neurology.

Development of a polymersome blood ammonia assay coupled with a portable near-infrared fluorometer

Marie-Lynn AL-HAWAT¹, Justine CARON¹, Sarah DJEBBAR¹, Simon MATOORI¹

¹Faculté de Pharmacie, Université de Montréal

PURPOSE: Ammonia is an endogenous metabolite that has crucial roles in pH homeostasis and protein metabolism. Moreover, it is a key biomarker in inborn and acquired liver disease. At high levels, ammonia exerts neurotoxic effects. As clinical point-of-care blood ammonia assays are lacking, we developed a polymersome formulation for point-of-care blood ammonia sensing combined with a portable fluorometer.

METHODS: To prepare the polymersomes, polymers were dissolved in dichloromethane, followed by addition into an isotonic citric acid solution containing a pH-sensitive near-infrared (NIR) fluorescent dye : IRDYE 680RD. After sonication, emulsification and solvent evaporation, purification was achieved using columns, replacing the external phase with an isotonic sodium chloride-containing phosphate buffer. Mouse blood was obtained from cardiac puncture. And the polymersomes solution and mouse blood were spiked with ammonium chloride standards from 0 to 0.5 mM. As typically used in capillary blood assays, merely a small

volume of whole blood (3 μ L) was needed.

RESULTS: Initially, the fluorescence of PS-b-PEG polymersomes was assessed using a plate reader, covering a clinically relevant range of ammonia at concentrations up to 500 μ M. A highly linear response ($R^2 = 0.9948$) was observed over time with a concentration-dependent increase. Then, the fluorescence was tested with a portable fluorometer, revealing a concentration-dependent increase in both ammonia-spiked buffer and blood.

CONCLUSION: The portable fluorometer effectively detected a pH-dependent fluorescence increase of the pH-sensitive NIR dye. Combined with the polymersome formulation and the NIR-dye, this assay required merely three microliters of blood, offering promising potential for point-of-care blood ammonia diagnostics. These encouraging results underscore the need for further development and clinical translation of this innovative approach to blood ammonia testing.

Nanostructured formulation for optimized antifungal drug delivery of fluconazole and baru nuts and chia seeds extracts as stabilizer

Camila G. Dias¹, Julia C. Coco², Raimar Loebenberg¹, Priscila G. Mazzola²

¹University of Alberta, ²State University of Campinas - UNICAMP

Purpose: The aim was to design a multifunctional formulation as an alternative to current fungal topical treatments that are long and inconvenient to patients. Thus, liposomes, baru nuts and chia seed extracts were combined in a formulation that may enhance the stability and permeation of fluconazole, a drug with low permeability.

Methods: Baru nuts and chia seeds were cold pressed, and the residue was macerated with ethanol 70% (v/v) for 3 days under agitation. The extracts were incorporated into liposomes produced by self assembly, and their physicochemical stability was evaluated by dynamic light scattering, while morphology was examined via electron cryomicroscopy. Encapsulation efficiency and the release profile of fluconazole were evaluated by HPLC.

Results: Baru and chia extracts presented satisfactory phenolic content (27 and 3 mg GAE/g) and antioxidant activity (DPPH IC₅₀ of 1.4 and 21 mg/mL; FRAP EC₅₀ of 2.6 and 26 mg/mL) respectively. Liposomes were produced with soy lecithin and water by direct sonication. Liposomes presented sizes around 170 nm, zeta potential of -41 mV, were monodisperse (PDI of 0.28), spheric, and unilamellar. The extracts improved the physicochemical stability of liposomes for 15 days. Fluconazole encapsulation efficiency (38%) and release (46% after 72 h) were not modified by the presence of extracts.

Conclusion: Baru and chia extracts presented antioxidant activity, and enhanced the stability of liposomes without affecting the encapsulation or release of fluconazole. Further studies will assess the optimization of stability past 15 days, skin permeation, and the antifungal activity of the formulations, seeking a potential synergy between the extract and the drug.

Harnessing Dermal Fibroblast-Derived Exosomes as Modulator for Extracellular Matrix Remodelling in Wound Healing

Jin Wang¹, Emmanuel Ho^{1,2}

¹School of Pharmacy, University of Waterloo, ²Waterloo Institute for Nanotechnology

Introduction: Cutaneous wound healing involves organized biological and molecular events of cell migration, proliferation, and extracellular matrix (ECM) disposition. Dermal fibroblasts balance the degradation and synthesis of ECM¹, which is crucial for preventing chronic wound formation or fibrotic healing². Despite their importance, exosomes derived from dermal fibroblasts have been rarely studied in wound healing. As nanosized extracellular vesicles, exosomes composed of lipid bilayer membrane with nucleic acids and proteins, are active therapeutics for promoting healing and addressing skin disorders^{3,4}. Exosomes are also drug delivery carriers as they communicate between cells and transport cellular contents across barriers².

Methods: Firstly, exosomes were first purified from dermal fibroblasts. The role of exosomes as carriers was explored by encapsulating Pirfenidone, an anti-inflammatory and anti-fibrotic compound. Exosomes and PFD-exosomes were characterized by NanoSight and transmission electron microscopy. In vitro cytotoxicity of exosomes and PFD-exosomes was assessed using the MTS assay. Exosomes and PFD-exosomes were studied for their ability to induce fibroblast migration in vitro by scratch assay. The expression of target genes COL1A1, COL3A1, MMP-1 and TIMP-1 were analyzed by quantitative real-time PCR. TIMP-1, MMP-1, collagen-I and collagen-III expression were quantified using ELISA assays.

Results: Dermal fibroblasts serve as the source for isolating and characterizing exosomes, which demonstrate excellent biocompatibility in vitro. Both exosomes and PFD-exosomes promote fibroblast proliferation and migration, which are essential tissue remodeling functions. Treatment with exosomes significantly up-regulate the expression of collagen (type I and III) in dermal fibroblasts by 2-fold and 10-fold, respectively, in vitro. Comparatively, PFD-exosomes markedly decreased collagenase MMP-1 expression by half while demonstrating a 1.4-fold increase in TIMP-1 expression, an inhibitor of MMP-1.

Conclusion: Exosomes and PFD-exosomes show different beneficial effects on ECM remodeling. Our findings highlight the significance of dermal fibroblast-derived exosomes as therapeutic agents and drug transporters, indicating potential complementary therapeutic for promoting wound healing.

References

1. Tomasek JJ, Gabbiani G, Hinz B, Chaponnier C, Brown RA. Myofibroblasts and mechano-regulation of connective tissue remodelling. *Nat Rev Mol Cell Biol.* 2002;3(5):349-363. doi:10.1038/nrm809
2. Canady J, Karrer S, Fleck M, Bosserhoff AK. Fibrosing connective tissue disorders of the skin: molecular similarities and distinctions. *J Dermatol Sci.* 2013;70(3):151-158. doi:10.1016/j.jdermsci.2013.03.005
3. Zhao B, Zhang Y, Han S, et al. Exosomes derived from human amniotic epithelial cells accelerate wound healing and inhibit scar formation. *J Mol Histol.* 2017;48(2):121-132. doi:10.1007/s10735-017-9711-x
4. Zhao D, Yu Z, Li Y, Wang Y, Li Q, Han D. GelMA combined with sustained release of HUVECs derived exosomes for promoting cutaneous wound healing and facilitating skin regeneration. *J Mol Hist.* 2020;51(3):251-263. doi:10.1007/s10735-020-09877-6

Assessing Food and Excipients Impact on Intestinal Lymphatic Drug Uptake: Insights from an Innovative In-vitro Model

Malaz Yousef^{1,2}, Conor O’Croinin¹, Nadia Bou-Chacra², Neal M. Davies¹, Raimar Löbenberg¹

¹Faculty of Pharmacy and Pharmaceutical Sciences, University of Alberta, Edmonton, Alberta, Canada, T6G 2E1, ²Faculty of Pharmaceutical Sciences, University of Sao Paulo, Sao Paulo, Brazil, 05508-000

Purpose. Chylomicrons are lipid particles formed in enterocytes upon lipids ingestion, to primarily facilitate their transport. Additionally, they help xenobiotics -especially those with high lipophilicity (log P >5)- traverse the intestinal lymphatic system and enter the general circulation(1). Our aim was to investigate how foods and excipients enhance lymphatic uptake via chylomicrons, employing our established *in-vitro* model.

Methods. Rifampicin (1 mg/mL) was introduced into the donor compartment of Franz cells while the receiver compartment was filled with Intralipid® (artificial chylomicrons) or a mixture with another agent, and maintained at 37.0 ± 0.5 °C. Various oils (olive, sesame, peanut, coconut) were explored at a 2% concentration. Compartments were separated by a PVDF membrane. Samples were regularly extracted and analyzed via HPLC to assess drug uptake(2). Morphological characterization of Intralipid® using TEM was conducted to understand oil placement. Additionally, oleoyl-polyxyl-6 glycerides are often used in formulations and have been examined.

Results. Coconut oil displayed high early-stage release effects on rifampicin, while olive oil consistently boosted uptake, yielding a 3.5-fold increase. Sesame oil initially mirrored olive oil behaviour but eventually matched the release profile of peanut oil, yielding a 1.5-fold increase in uptake. All oils improved uptake by emulsifying into Intralipid®, creating a carrier area, as indicated by TEM results. The superior performance of coconut oil was attributed to its enhanced emulsification. Also, formulations with oleoyl-polyxyl-6 glycerides demonstrated increased lymphatic uptake in the model.

Conclusion. Unlike medium-chain-rich coconut oil, the behavior of other oils containing long-chain fatty acids (LCFs) closely resembled their *in-vivo* performance. The medium chain fatty acids (MCF) are reportedly transported through the intestinal lymphatics, unlike LCFs. Furthermore, the examination of the effect of oleoyl-polyxyl-6 glycerides on intestinal lymphatic uptake underscored the practical utility and applicability of this model in formulation development and regulatory assessments for products targeting the lymphatic system.

References: 1. J Pharm Pharm Sci 2021 24: 533-547; 2. Pharmaceutics 2023 15(11): 2532

Microfluidic development of a pneumolysin-responsive liposomal platform for selective treatment of *Streptococcus pneumoniae*

Ethan Watt¹, Ilinca Andriescu¹, Emmanuel Ho^{1,2}

¹School of Pharmacy, University of Waterloo, Kitchener, ON, ²Waterloo Institute of Nanotechnology, Waterloo, ON

Purpose: Pathogenesis of *Streptococcus pneumoniae* is largely associated with production of the virulence factor pneumolysin (PLY), which recognizes and binds to cholesterol domains within cellular membranes to cause lysis.¹ As liposomes naturally mimic membrane composition, it suggests that PLY can be exploited to similarly induce responsive release of encapsulated therapeutic in the proximity of pneumococcal infections. Consequently, the aim of this study was to optimize liposomal synthesis via microfluidic methods and then examine the interplay between cholesterol content and PLY-induced drug release.

Methods: An in-house microfluidic system was optimized for the fabrication of liposomes through the use of a three-level, three-factor Box Behnken surface response design. Encapsulation and subsequent release of the antimicrobial peptide nisin was evaluated through CBQCA assay fluorescence measurements upon incubation with recombinant serotype 2 PLY. Hemolytic and sequestration assays were conducted with both 23-F *S. pneumoniae* culture and purified PLY with human erythrocytes and liposomes. Antibacterial activity was quantified through minimum inhibitory concentration (MIC) assays of both free nisin and liposomal suspension through 24 hour incubation with *S. pneumoniae*.

Results: The Box Behnken design output an optimized solution at a desirability factor of 0.99, with agreeance values >80% for all response variables. It was found that cholesterol-rich formulations led to full sequestration of PLY hemolytic activity (<10%) at a dosage of 10 µM and full nisin release after 30 min, while those at low cholesterol showed little change in hemolytic rates (>80%) and negligible therapeutic leakage. Cholesterol-rich formulations also displayed a comparative MIC to free nisin in solution (3 µg/mL), while liposomes containing low cholesterol content had a ~3-fold reduction in effectiveness.

Conclusion: Cholesterol content had a pivotal role in PLY binding, with only cholesterol-rich formulations capable of therapeutic release through toxin-induced liposomal rupture, leading to potent bactericidal effect and simultaneous neutralization of PLY's hemolytic capabilities.

References

1. PNAS 2019 116: 13352-13357

Use of the anti-LRP1 5A6 antibody as a transport vector across the blood-brain barrier

Anne-Frédérique Beaudry¹, Frédéric Calon^{1,2}, Vincent Émond²

¹Université Laval, Québec, ²Centre de recherche du CHU de Québec-Université Laval

Purpose: The blood-brain barrier (BBB) poses a significant obstacle to the passage of drugs into the central nervous system (CNS). This can greatly hinder the therapeutic use of monoclonal antibodies, especially for Alzheimer's and Parkinson's diseases, two neurodegenerative conditions with increasing prevalence in Canada. However, a promising strategy to enhance drug transport to the brain is the targeting of native receptor-mediated transport systems (RMT) that utilize vesicular traffic to transport endogenous ligands across the BBB endothelium. The purpose of the present work was to determine whether the anti-LRP1 5A6 antibody, LRP1 being a receptor of the LDL receptor family found in the brain endothelial cells, could be used to facilitate drug access to the CNS using RMT.

Methods: We employed immunofluorescence to assess the internalization of the anti-LRP1 5A6 antibody in cell lines in vitro and in vivo in the BBB endothelium. Mice were injected with fluorochrome-labeled 5A6 antibody (~8 mg/kg) and, after one hour, their brains were retrieved and sectioned using a cryostat. Finally, brain samples were analyzed under the microscope to conclude in which cell types the antibody internalized.

Results: The 5A6 antibody internalized in the N2A (neuroblastoma) and bEnd5 (brain endothelioma) cells. After i.v. injection in the mouse, the apparent 5A6 signal in the brain endothelium was limited to a region between the hippocampus and the midbrain. However, upon further analysis, the 5A6 signal colocalized with a marker of erythrocytes. These results suggest that the signal limited to particular brain microvessels was caused by residual 5A6, which the perfusion failed to clear from the circulation, rather than a true internalization in endothelial cells.

Conclusion: To conclude, the findings do not support the use of anti-LRP1 5A6 as an effective vector for targeting BBB endothelial cells. This abstract is presented within the context of the student undergraduate award.

References

J Neuro 2017 61: 2-10

Annu Rev Pharmacol Toxicol 2015 55: 613-631

in vitro Characterization and Preclinical In vivo Evaluation of Bone-Seeking Gd2O3 Nanoparticles as Medical Imaging Contrast Agents

Adibehalsadat Ghazanfari¹

¹University of Alberta

Purpose: Ultrasmall nanoparticles of heavy metal oxides, particularly Gadolinium oxide nanoparticles (GdNPs), show promise for X-ray imaging due to their strong X-ray attenuation. This study enhances biocompatibility and specificity by attaching bone-targeting bisphosphonates (BP) to GdNPs, creating markers for bone turnover monitoring. Citric acid-coated GdNPs linked with BP demonstrate excellent colloidal stability, offering a non-ionizing alternative for medical imaging, replacing conventional 99mTechnetium medronate. This approach utilizes bisphosphonates for bone targeting and replaces the radioactive element with GdNPs, enabling detection via Computed Tomography (CT) or Magnetic Resonance Imaging (MRI).

Methods: A one-pot polyol method synthesized Citric acid-Gadolinium oxide nanoparticles (CA-GdNPs) conjugated with Bisphosphonate (BP). Analytical techniques including X-ray diffraction, thermogravimetric analysis, Fourier Transform Infrared Spectroscopy, Transmission Electron Microscopy, and Dynamic Light Scattering were used to investigate the formation process. X-

ray attenuation power was assessed by atomic concentration. GdNPs-Bisphosphonate affinity towards bone was determined by examining binding to HA microparticles in different dispersants. Longitudinal water-proton relaxivity (r_1) values were measured to evaluate MRI contrast agent efficacy. Cytotoxicity was assessed in vitro, and in vivo CT images were obtained post-intravenous injection of suspension samples.

Results: Our study found that Gadolinium oxide nanoparticles have an average size of 3.6 nm, suitable for diverse biomedical uses. These nanoparticles have cubic crystal structures and are coated with approximately 34.75 wt% surface coating. Importantly, in vitro cytotoxicity tests showed their non-toxic nature in cell cultures. Additionally, the sample solution displayed a sevenfold higher longitudinal water proton relaxivity (r_1) than commercial Gd-chelates (OMNI scan) solutions. Finally, we demonstrated the effectiveness of nanoparticle suspension samples as a bone-seeking CT contrast agent through in vivo imaging, using both micro-CT and MRI scanners.

Conclusion: Bisphosphonate conjugated Gadolinium oxide nanoparticles show potential as new-generation CT and MRI contrast agents for non-invasive imaging of bone turnover without the need for radionuclides.

References: ACS Appl Mater Interfaces 2013 5: 5219–5226

The Selectivity Potential of PSMA-Targeting Aptamers

Nicole Robinson^{1,2}, Atsuhiko Yoshizawa^{2,3}, Laetitia Garnier^{2,3}, Ivan Yu^{1,2}, Kun Liu⁴, Dogancan Ozturan^{1,2}, Sougata Dey⁴, Mitali Pandey², Igor Moskalev², David Perrin⁴, Nathan Lack^{1,2,5,6}, Michael Cox^{2,3}, Larry Goldenberg²

¹Faculty of Medicine, Experimental Medicine Graduate Program, University of British Columbia, ²Vancouver Prostate Centre, ³Department of Urologic Sciences, University of British Columbia, ⁴Department of Chemistry, University of British Columbia, ⁵Koç University Research Center for Translational Medicine (KUTTAM), ⁶Koç University School of Medicine

Purpose: This project seeks to develop an aptamer to target Prostate Specific Membrane Antigen (PSMA) in the treatment of advanced prostate cancer (PCa). Small molecule based, PSMA targeting therapy has been seen to modestly extend patient survival, but with dose-limiting off-target damage to the salivary glands, kidneys and other organs which also produce PSMA[1-3]. We have evaluated modified aptamers produced by our industry partner Somalogic as an alternative targeting approach with many potential benefits of modification capacity, conjugation and selectivity.

Methods: Bio-layer interferometry and flow cytometry competition and binding assays using PSMA expressing cells and CRISPR modified PSMA negative cells were employed to evaluate and characterize the binding of these aptamers in vitro. Lead candidates were evaluated through in vivo imaging of PSMA-expressing and PSMA-negative xenografts in athymic nu/j mice. IVIS fluorescence imaging was performed after injection of a fluorescently conjugated aptamer with controls established using the clinically approved small molecule and non-targeted DNA.

Results: We have established a relative rank order of the SOMAmers based on binding saturation and affinity kinetics, and characterized which aptamers competed with PSMA probes on known binding sites. In vivo, aptamer biodistribution resembled that of the clinically approved small molecule ligand. This included preferential accumulation in PSMA-expressing xenografts over PSMA-negative xenografts, but also accumulation in the liver, kidney, and salivary glands. However, this accumulation was also seen when using non-targeted DNA, suggesting that PSMA targeting may not be the sole reason for aptamer signal at those sites.

Conclusions: This study provides initial evidence that modified DNA aptamers have the potential to target PSMA with a similar quality of a clinically approved small molecule. They also suggest salivary accumulation of aptamers independent of targeting. If this PSMA independent salivary accumulation can be evaluated and overcome, aptamers may offer a novel targeting approach to PCa theranostics.

References

1. Lancet 2021 397:797-804.
2. N Engl J Med 2021 385.12: 1091-1103

Development and Characterization of Novel Pharmaceutical Formulations of Prenylated Flavonoids

Conor O'Croinin¹, Tyson S. Le¹, Vorawut Wongumpornpinit¹, Michael R. Doschak¹, Raimar Löbenberg¹, Neal Davies¹

¹University of Alberta

Purpose: Prenylated flavonoids are found in a variety of plants. They possess pharmacological activity including antiviral, anti-inflammatory, and anticancer properties. Due to these benefits and unique pharmaceutical properties the development of formulations for the delivery of this compound is necessary. *In vitro* and *ex vivo* laboratory models of formulation performance analysis were developed in order to quantify the dissolution and permeation and uptake across biological membranes.

Methods: Transdermal patches and oral dissolving film formulations were developed, characterized, and formulated using various polymers, plasticizers, and film forming agents. Excipient concentrations were altered based on the consistency and texture of the formulations until uniform formulations were obtained. The optimized novel formulations were subsequently analyzed for the release of the active pharmaceutical ingredient across membranes. Franz diffusion cells were used to mimic penetrance across dermal or buccal membranes using synthetic hydrophobic membranes and fresh *ex vivo* porcine membranes. Samples were collected and quantified using liquid chromatography-mass spectrometry.

Results: Transdermal patches and oral dissolving film formulations were both successfully created using a cannabis derived polyphenol extract as the active pharmaceutical ingredient. Doses of 4-5 ug for the transdermal patches and 10-15 ug for the oral dissolving films were obtained for the active pharmaceutical ingredient. Both formulations showed ability to cross the synthetic hydrophobic membranes as a model of penetrance and release using the Franz diffusion cells. The use of fresh isolated *ex vivo* porcine membranes also revealed penetrance although over time although reduced compared to the synthetic membranes.

Conclusion: The successful development of these prototype formulations demonstrates that transdermal patches and oral dissolving film are promising candidates for the delivery of prenylated flavonoids into the body. The ability to formulate and characterize the formulations for effectiveness was proven for subsequent clinical studies.

Debating on hydrated versus dehydrated imaging of drug delivery nanocarriers in transmission electron microscopy

HUI QIAN¹

¹Quantum and Nanotechnology Research Center, National Research Council Canada, Edmonton, Alberta, Canada

Purpose: The increasing complexity of drug delivery systems, aimed at precision medicine, demands advanced characterization to thoroughly comprehend the formulations throughout production, storage, and application. Beyond the need for access to cutting-edge infrastructure and expertise, the pharmaceutical community faces the challenge of developing robust, high-throughput analytical methods. Transmission Electron Microscopy (TEM) has been utilized as a sophisticated, complementary technique for the morphological and structural characterization of drug delivery nanocarriers for several decades. However, the decision between dehydrated and hydrated imaging of nanocarriers often impedes the accuracy of characterization, in addition to the challenge of developing new approaches in TEM.

Method: Inorganic/organic hybrid nanoparticles, virus-like particles, liposomes, nanostructured lipid nanoparticles, and extracellular vesicles were chosen as typical types of nanocarriers to illustrate the advantages and disadvantages of both hydrated and dehydrated imaging. These nanocarriers were prepared using negative staining, plunge freezing, or immunolabeling methods for TEM imaging.

Results: The intact structure of drug delivery nanocarriers is well-preserved in native buffer via cryofixation and visualized using cryo-TEM. Quantitative size distribution analysis of nanocarriers is achieved through customized automated data processing of cryo-TEM micrographs. The biomarker/payload in lipid nanoparticles is identified and localized by immuno-TEM. For dehydrated specimen, the overall morphology of nanocarriers with enhanced contrast is revealed. However, the intact structure and shape of nanoparticles are disrupted.

Conclusion: The selection of techniques to be used in TEM depends on the questions to be answered and the resources available. Cryo-TEM, while producing high-quality results, requires specialized facilities and expertise, and is time-consuming. On the other hand, conventional imaging, which requires less specialized facilities and expertise, provides quick feedback and is less costly.

Vitreous pharmacokinetics of anti-VEGF mAb following the intravitreal injection of thermosensitive sol-gel containing drug nanoparticles

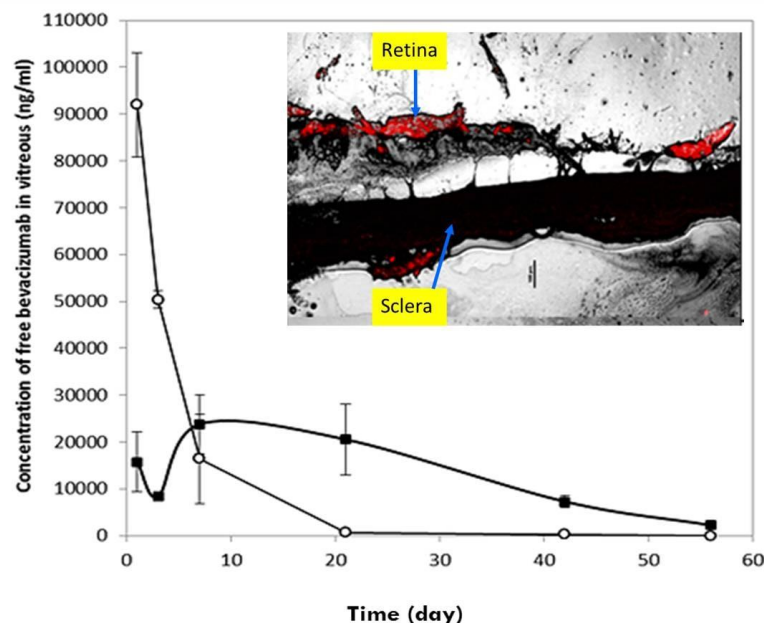
Reyhaneh Varshochian¹, Mohammad Riazi Esfahani², Rassoul Dinarvand³

¹Department of Pharmaceutics and Pharmaceutical Nanotechnology, School of Pharmacy, Shahid Beheshti University of Sciences, Tehran, Iran., ²Gavin Herbert Eye Institute, Department of Ophthalmology, University of California Irvine, Irvine, CA 92697, USA, ³Nanotechnology Research Centre, Faculty of Pharmacy, Tehran University of Medical Sciences, Tehran, Iran

Purpose: The intravitreal injection of anti-vascular endothelial growth factor (VEGF) drugs such as bevacizumab is currently the method of choice in age-related macular degeneration (AMD) treatment. However, the major restriction is the requirement of repetitive intraocular injections due to the short half-life of these drugs in vitreous which can lead to serious adverse effects. To address this problem a new sustained release formulation was prepared and its vitreous pharmacokinetics were evaluated.

Methods: The chitosan nanoparticles containing bevacizumab (anti-VEGF mAb) were prepared and embedded in thermoresponsive PLGA-PEG-PLGA copolymer sol-gel obtained through the ring-opening polymerization. The final formulation was characterized and the in-vitro drug release was evaluated. During the in-vivo investigations, following the single dose intravitreal injection of the formulation in rabbits, the vitreous concentration of bevacizumab was assayed in defined time intervals using ELISA method and the intraocular pharmacokinetic parameters were determined.

Results: According to the results the prepared formulation showed an appropriate sol-gel transition behavior in temperature change from 25 to 37°C and was able to extend the drug release time. The pharmacokinetic results showed that the bevacizumab vitreous concentration remained above 500 ng/ml (the minimum concentration required for the complete inhibition of VEGF function) more than 8 weeks in our formulation group, while, it fell below this value in less than 6 weeks in the control group treated with the free drug. According to the non-compartmental analysis, four times greater mean residence time (MRT) and halved clearance of bevacizumab was observed in rabbits treated with our formulation in comparison to the control rabbits which resulted in 14 days mean vitreous half-life of the drug in our formulation group compared to that of the control group, 3.5 days. **Conclusion:** Consequently, our results indicated the promising potentials of the designed formulation as a novel sustained release retinal drug delivery system.



References

1. Medicina. 2023; 59(5): 920.
2. ACS Polym. 2023, 3, 1, 118-131.

Preliminary biodistribution evaluation of radiolabeled bone targeting Gadolinium oxide nanoparticles

Ruikun Tang¹, Adibehalsadat Ghazanfari¹, Tsolmonbaatar Khurelbaatar², Daniel Romanyk², Neal Davies¹, Michael Doschak¹

¹Faculty of Pharmacy and Pharmaceutical Sciences, University of Alberta, Edmonton, Alberta, ²Department of Mechanical Engineering, Faculty of Engineering, University of Alberta, Edmonton, Alberta

Purpose: Developing non-ionizing alternatives to the technetium bone-scan for accurately diagnosing tibial bone stress syndromes (shin splints) would be of enormous utility for diagnosis of bone pathology in juvenile patients. Previous research in our lab has developed several variants of bone-targeting metal oxide contrast agents for Magnetic Resonance Imaging (MRI) and/or micro-Computed Tomography (micro-CT), by coupling bone-targeting drugs to paramagnetic metal oxide nanoparticles. In this study, we attempted several chemical strategies to radiolabel our bone-seeking Gadolinium oxide nanoparticle contrast agents to facilitate the detection of dynamic bone activity in juvenile rats with active growth plates for biodistribution evaluation.

Methods: We synthesized bisphosphonate conjugated citric acid gadolinium oxide nanoparticles (BP-CA-GdOx) and non-targeting control CA-GdOx nanoparticles using a one-pot polyol method. In-vivo assessments of tissue localization after intravenous injection of these bone-targeting contrast agents were conducted in rats using micro-CT and MRI. Additionally, we utilized Electron Probe Microanalysis (EPMA) and undecalcified histology with fluorescent calcein green and xylenol orange double labeling to gather dynamic bone turnover information in the tibia of normal rats. Iodine-125 labeled nanoparticles were used to confirm and validate the biodistribution of these nanoparticles after intravenous injection in rats.

Results: BP-CA-GdOx nanoparticles and control nanoparticles were synthesized, characterized and bone affinity confirmed using hydroxyapatite binding assays. Preclinical in-vivo micro-CT imaging measured increased uptake of BP-CA-GdOx nanoparticles at newly mineralizing bone in growth plates of juvenile rats, with spatial localization confirmed by EPMA and fluorescence microscopy. Iodine-125 labeled nanoparticles confirmed uptake of nanoparticles at growth plates of juvenile rats.

Conclusion: The enhanced mineral uptake of BP-CA-GdOx nanoparticles offers the opportunity to acquire clinically valuable dynamic bone activity data, surpassing the static geometry provided by X-ray imaging. Consequently, BP-CA-GdOx nanoparticles serve as non-ionizing contrast agents for detection of dynamic bone activity, bypassing the need for juvenile patient exposure to radionuclide tracers.

References

Official Journal of the Canadian Academy of Sport Medicine, 1996, 6(2), 85-89

Osteoarth & Cartilage, 2012, 20(7), 694-702.

ACS Appl Mat & Interfaces, 2013,5(11), 5219-26.

Fluorescent pH-sensing bandage for point-of-care wound diagnostics

Katia Cherifi¹, Marie-Lynn Al-Hawat¹

¹Faculté de Pharmacie, Université de Montréal, Canada

Diabetic foot ulcers (DFU) are a serious and prevalent complication of diabetes. Current diagnostic options are limited to macroscopic wound analysis such as wound size, depth, and infection. Molecular diagnostics promise to improve DFU diagnosis, staging, and assessment of treatment response. Here, we developed a rapid and easy-to-use fluorescent pH-sensing bandage for wound diagnostics. In a fluorescent dye screen, we identified pyranine as the lead compound due to its suitable pH-sensing properties in the clinically relevant pH range of 6.0 and 9.0. To minimize the release of this dye into the wound bed, we screened a library of ionic microparticles and found a strong adhesion of the anionic dye to a cationic polymeric microparticle. These dye-loaded microparticles showed a strong fluorescence response in the clinically relevant pH range of 6.0 and 9.0 and a dye release below 1% after one day in biological media. The dye-loaded microparticles were subsequently encapsulated in a calcium alginate hydrogel to minimize the interaction of the microparticles with the wound tissue. This pH-sensing diagnostic wound dressing was tested on full thickness dorsal wounds of mice, and a linear fluorescence response ($R^2 = 0.9909$) to clinically relevant pH values was observed. These findings encourage further development of this pH-sensing system for molecular diagnostics in DFU. This system was also lately adapted for colorimetric analysis with the use of a smartphone camera, which could allow for better accessibility to the general public.

References: (1) Advanced Functional Materials. 2023, 33: 2215116; (2) ACS Measurement Science. 2022, 2(5): 377-384; (3) ACS Sens. 2021, 6(6): 2366-2377 ; (4) Sci. Transl. Med. 2021, 13(585): eabe4839; (5) Diabetes. Metab. Res. Rev. 2020, 36 Suppl 1: e3266; (6) Adv. Sci. 2022, 9(22): 2201254

Enhancing siRNA Therapy in Acute Lymphoblastic Leukemia through Lipopolymer-Based Delivery Systems

Mohammad Nasrullah¹, Remant KC², Hasan Uludag^{1, 2, 3}

¹Faculty of Pharmacy & Pharmaceutical Sciences, University of Alberta, Edmonton, Alberta, ²Department of Chemical and Materials Engineering, Faculty of Engineering, University of Alberta, Edmonton, Alberta, Canada, ³Department of Biomedical Engineering, Faculty of Medicine & Dentistry, University of Alberta, Edmonton, Alberta, Canada

Purpose: The therapeutic promise of short-interfering RNAs (siRNAs) in addressing genetic diseases is immense but is currently hindered by delivery challenges, notably their ability to traverse the cell membranes due to their negative charge and large size. This issue is particularly pronounced in lymphocytes, where the minimal surface area of cell and limited cytoplasm complicate it more.

Method: To overcome these hurdles, we engineered advanced lipopolymer-based delivery system incorporating lipid-conjugated polyethyleneimine (PEI). By modifying low molecular weight PEI (1.2 kDa) with aliphatic lipids, we formulated a platform of lipopolymer that yields nanocomplexes with siRNA, to facilitate efficient siRNA uptake into lymphocytes. This method utilizes the positive charge of PEI to bind with the negatively charged siRNA, enhancing cellular uptake through lipid-mediated mechanisms. We

tested the delivery system's efficacy in targeting the oncogenes *STAT5A* and *MLL-AF4* in acute lymphoblastic leukemia (ALL) cell lines RS4;11 and SUP: B15 through *in vitro* and *in vivo* experiments.

Results: The application of our lipopolymer complexed with *STAT5A* siRNA led to successful siRNA delivery, apoptosis induction, and significant gene silencing into both ALL cell lines. This resulted in decreased colony formation *in vitro* and significantly reduced tumor growth *in vivo*. Further testing with *MLL-AF4* siRNA/lipopolymer complexes demonstrated substantial leukemia burden reduction and improved survival rates in an RS4;11 xenograft model.

Conclusion: Our investigation presents a proof-of-concept for a lipopolymer-based siRNA delivery system, proposing a potential therapeutic approach for ALL.

Transplacental Delivery of Targeted Lipid Nanoparticles: A New Route for Fetal Gene Therapies

Amr Abostait^{1, 2, 3}, Zeqing Bao⁴, Yuichiro Miyake³, Wai Hei Tse³, Christine Allen⁴, Richard Keijzer³, Hagar Labouta^{1, 2, 3, 4}

¹Unity Health Toronto, Toronto, Canada, ²College of Pharmacy, University of Manitoba, Winnipeg, Canada, ³Children's Hospital Research Institute of Manitoba, Winnipeg, Canada, ⁴Leslie Dan Faculty of Pharmacy, University of Toronto, Toronto, Canada

Purpose: Congenital disorders, such as congenital diaphragmatic hernia (CDH), are a considerable challenge in maternal-fetal health [1]. Gene therapies are a promising modality in restoring normal development, however, there's a need for safe and efficient gene delivery vehicles to fetal organs during pregnancy. Lipid nanoparticles (LNPs) has become the gold standard for RNA delivery, especially, after the renowned success of mRNA vaccines developed by Pfizer and Moderna. [2]. However, LNPs interactions with the placental barrier and fetal organs are still understudied.

We aim to study the design features affecting LNPs transport across the placental barrier. In addition, we aim to study the effect that LNPs could have on fetal organ development, especially the fetal lung.

Methods: Using microfluidic chips, we synthesized a library of 53 different LNPs formulations, and characterized them for 19 design features; this includes features in LNPs formulation components, and the placental model used. Besides, diverse LNPs formulations were studied in a tracheal occlusion rat lung model.

Results: Hundreds of in-vitro transport data points were collected and modeled using the machine learning algorithm XGBoost. The model identified the top features driving placental transport, such as zeta potential and PEGylated lipid end functional group. In addition, fetal lungs showed normal airway development in histological staining and no effect on the Apoptosis and Proliferation markers after 24 H exposure to LNPs. Also, dynamic flow induced different cell morphology and affected receptor expression resulting in differences in nanoparticle uptake.

Conclusion: Utilizing machine learning has improved our understanding of the mechanisms and key determinants of the transplacental transfer of LNPs under physiologically relevant conditions, which will enable the design of fetal therapies that are safe to use in pregnancy.

References

- [1] Annals of Surgery 269(5):p 979-987, May 2019.
- [2] Int J Mol Sci. 2023 Jan; 24(1): 787.

Microbubble assisted drug delivery for glioblastoma

Isabella C Zittlau¹

¹University of Saskatchewan, Saskatoon, SK

Glioblastoma is the most common and malignant brain tumour in adults; moreover, the blood-brain barrier (BBB) is a significant obstacle in the effective delivery of anti-cancer therapies. Microbubble (MB) is a colloidal particle that consists of a gas core surrounded by a protective shell composed of biocompatible materials, used as contrast agents and, when combined with low-intensity focused ultrasound, is a promising technique to cross physiological barriers.

Gemini lipid is a new class of surfactants, presenting a unique structure and properties compared to conventional surfactants. Besides a lower critical micellization concentration, it is also a versatile non-viral gene delivery system that, if incorporated into MB could bring beneficial advantages to the formulation. Throughout mechanical vibrations, High-intensity focused ultrasound (HIFU) forms an ultrasound wave which propagates across tissues, causing alternating cycles of increased and reduced pressure. MBs loaded with drug or gene therapy vectors, if applied with HIFU, can be used to deliver and release the transport of substances into tissues of hard access.

The microbubbles' formulation combined with Gemini Lipid has been tested at various charge and molar ratios of the constitutive elements, in addition to component concentration exploration. Also, size measurement, zeta potential, and stability, the same as conjugation and lipid arrangement are being evaluated by small-angle X-ray scattering.

This project focuses on synthesizing MB combined with Gemini Lipids to increase chemotherapeutic cross BBB into glioblastoma, maintaining low toxicity and reducing side effects. Moreover, the ability of MBs to disrupt biological barriers and permeate the BBB, evaluating the delivery efficiency and toxicity in vitro astrocytes, will be tested through a small animal HIFU system.

References: Badea I Gene Ther 2012 19(10), 978-987; Badea I J Gene Med 2005 7(9), 1200-1214; Chowdhury SM J Control Release 2020 326:75-90; Guzman ML Blood 2005 105(11), 4163-4169; Parmar R Chemical Engineering and Processing 2013 64, 79-97; Roovers S Microb Fund to Clinical Translation 2019 35(31):10173-10191; Singh J Nanomedicine 2015 10(3):405-17; Sirsi S Bubble Sci Eng Technol 2009 1(1-2):3-17; Stride E Ultrasound Med Biol. 2020 46(6):1326-1343; Sun C World J of Pharmacy and pharmaceutical sci 2017 1290-1314; Tinkov S J Pharm Sci 2009 98(6):1935-61; Ton N Mol Imaging Biol 2022 24(4):590-599

Modeling Intestinal Lymphatic Uptake of Halofantrine Postprandially: Advancements and Implications in Physiologically Based Pharmacokinetic Modeling

Malaz Yousef^{1, 2}, Nadia Bou-Chacra², Neal M. Davies¹, Raimar Löbenberg¹

¹Faculty of Pharmacy and Pharmaceutical Sciences, University of Alberta, Edmonton, Alberta, Canada, T6G 2E1, ²Faculty of Pharmaceutical Sciences, University of Sao Paulo, Sao Paulo, Brazil, 05508-000

Purpose: Despite the significance and unique attributes of the intestinal lymphatic pathway for xenobiotic absorption, *in-silico* modelling of this route remains unexplored. This work aimed to develop a physiologically based pharmacokinetic model (PBPK) to reflect the lymphatic uptake of halofantrine after a fatty meal.

Methods: Modelling of absorption, distribution, metabolism, and elimination of halofantrine in both fasting and fed states was constructed using GastroPlus™ 9.8.3 (Simulation Plus, Inc., Lancaster, US), based on data reported by Milton et al (1). Model parameters were obtained through ADMET Predictor® 10.4 (Simulations Plus, Lancaster, CA, USA) or from reported *in-vitro* values.

Results: The pharmacokinetic models revealed a considerable decrease in the first-pass effect of halofantrine in the fed state (9.9 %) compared to the fasting state (77.2 %). The fasting state was appropriately represented by a two-compartment pharmacokinetic model,

while the fed state necessitated a three-compartment model. In the PBPK modelling, adjustments in CYP 3A4 kinetics sufficed for the fasting state. However, for the fed state, adjustments were necessary for both metabolism kinetics to account for reduced loss during the first-pass and for altering the pKa of halofantrine to 5.6 (from 8.2). These changes reflected molecular alterations of halofantrine in the intestine and more accurately replicated postprandial conditions.

Conclusion: This study emphasizes the need for further exploration and direct modelling options for intestinal lymphatic uptake through PBPK models, underscoring its underexplored nature in simulation algorithms. Theoretical considerations about food impact on drug absorption pathways, particularly for high extraction ratio (E) drugs like halofantrine, suggest ways to adjust existing predictive models. However, this might not be feasible for other medium or low E lymphotropics. Additionally, the importance of incorporating representative physicochemical factors for drugs, particularly when considering postprandial conditions or lipid formulations is evident. The findings contribute to advancing predictive regulatory and developmental considerations in drug development.

References

1. Br J Clin Pharmacol 1989 28(1): 71-77

Influence of diet-induced obesity on the expression of rat hepatic enzymes involved in arachidonic acid metabolism

Amel Hamza¹, Ayman O.S. El-Kadi ¹, Dion Brocks¹

¹University of Alberta, Edmonton, AB

Purpose: Obesity, which can be considered to be a low grade chronic inflammatory condition, can alter the regulation of metabolizing enzymes. This includes cytochrome P450 (CYP450) enzymes which are involved in xeno- and endobiotic catalysis. One such endobiotic is arachidonic acid which may be catalyzed by a number of CYP isoforms. Other involved enzymes are 5-LOX, 12-LOX, and COX2. Here we sought to explore the effects of experimental obesity on enzymes expression.

Methods: Four-week-old Sprague-Dawley rats (n=5/sex/diet) were fed either standard (13.4% kcal as fat) or high fat (45% kcal as fat) for 14 weeks. Rats were euthanized and livers processed. The mRNA (real-time PCR) and microsomal protein (Western blot) levels of several hydroxylases (CYP1B1, 4A1, 4F, and 2E1), epoxygenases (CYP2C3 and 2J), 5-LOX, 12-LOX, and COX2 were measured. Student's t-test was used to determine significance (p<0.05).

Results: Protein: Obesity was associated with significant decreases in male rats of exhibited 36 and 34% in CYP4A1 and 2C23, respectively. 12-LOX displayed a significant obesity-related increase of 114%. However, no changes were observed in CYP1B1, 4F1, or 2J. There were obesity-related reductions in the levels of all analyzed enzymes in the female rats, with the exception of CYP2J. CYP1B1, 4A1, 4F1, 2C23 each decreased by 47, 71, 57, and 43%, respectively. Additionally, COX2, 5-LOX, and 12-LOX decreased by 62 and 43%, respectively, in the obese rats. **mRNA:** Obese male rats displayed a 491% increase in cyp1b1 mRNA without significant alterations in other examined genes. In contrast, female rats showed a decrease in the expression of genes cyp4a1, cyp2c6, and cyp2e1 by 65.1, 52.4, and 64.9%, respectively.

Conclusion: Obesity caused mostly significant decreases in expression of a number of the enzymes at the protein level. Some sex-specific differences were noted. Translational measures did not fully concur with transcriptional measures.

Exploring the analgesic and anti-inflammatory activity of novel kinase inhibitors targeting TrkA, JAK2 and Src

Conall McCutcheon¹, Petar Iliev¹, Brent D. G. Page¹

¹Faculty of Pharmaceutical Sciences, University of British Columbia, Vancouver, BC

Purpose: As opioid-related mortality continues to escalate, novel non-opioid treatment options for pain management are necessary as part of comprehensive strategies to combat the opioid epidemic. In pursuit of this goal, our team has identified chemically novel small molecule kinase inhibitors that are potent against TrkA, Src, and Jak2, which are intricately linked to pain and inflammatory signaling cascades.^{1,2} This study seeks to evaluate and optimize the pharmacokinetic properties of our lead inhibitors for later *in vivo* studies in inflammatory pain models.

Methods: Lead compound BP8 is a potent inhibitor of TrkA, Src, and Jak2 ($K_d = 36, 640, \text{ and } 1100$, respectively), demonstrating TrkA binding in cell models. Structure-activity relationship studies have produced new analogues with higher affinities for TrkA while preserving the kinase activity profile of BP8. Ongoing efforts are focused on characterizing the pharmacokinetic properties of both BP8 and newly synthesized derivatives. *In vitro* pharmacokinetic profiling experiments include: intrinsic clearance and metabolite identification studies in liver microsomes; equilibrium dialysis to evaluate plasma protein binding; membrane permeability using the Caco-2 permeability assay.

Results: Initial tests demonstrated BP8 had moderate metabolic stability in mouse liver microsomes, with a half life of 39 minutes. BP8 exhibited high plasma protein binding (unbound fraction = 0.4%) and low membrane permeability. A series of novel analogues have subsequently been produced and will be assessed for their *in vitro* pharmacokinetic properties.

Conclusion: A promising series of kinase inhibitors has been identified with nanomolar affinity for TrkA, Src, and Jak2. Within this lead series, optimization of the pharmacokinetic properties will enable future *in vivo* efficacy studies.

References

1. Pain Pract 2016 16: 175-182
2. Aging Dis 2024 15: 186-200

An immortalized renal proximal tubule epithelial cellular model for investigating the pharmacokinetic interactions of mycophenolic acid

Jinal Adhiya¹, Ala'a R. Al-Dajani¹, Tony K. L. Kiang¹

¹Faculty of Pharmacy and Pharmaceutical Sciences, University of Alberta, Edmonton, AB

Purpose: Mycophenolic acid (MPA) is an immunosuppressant commonly used to prevent allograft rejection in kidney transplant patients. MPA undergoes extensive pre-systemic metabolism in the intestines and liver to generate MPA-glucuronide (MPAG). Renal proximal tubule epithelial cells are responsible for the excretion of MPAG and the further metabolism of MPA; hence, contributing to the pharmacokinetic variabilities of MPA. This research aims to develop a mechanistic renal *in vitro* model to investigate the pharmacokinetic interactions involving MPA.

Methods: Human renal conditionally immortalized proximal tubule epithelial cells (ciPTEC) overexpressing organic anion transporter 3 (OAT3) were seeded in 24-well plates (155,800 cells per well). To determine the effects of MPA on OAT3-mediated substrate uptake, cells were exposed to fluorescein (1-15 μM ; OAT3 probe) with known OAT3 inhibitors (e.g., probenecid 90 μM or diclofenac 390 μM) or MPA (4 $\mu\text{g/mL}$, physiological concentration). To determine the effects of metabolism modulators on the renal intrinsic clearance of MPA, the kinetics of MPAG formation in ciPTEC cells exposed to MPA (0.4 or 4 $\mu\text{g/mL}$) were characterized. Fluorescein uptake was determined by fluorescence microplate reader (excitation 485nm/emission 535nm) and MPAG formation was quantified by a liquid chromatography-tandem mass spectrometry assay developed in our lab.

Results: Fluorescein uptake into ciPTEC OAT3 cells was concentration-dependent (3 μ M over 10 min represented the initial velocity condition). Probenecid, diclofenac, and MPA reduced fluorescein (3 μ M) uptake by $41.1 \pm 7.7\%$ ($p < 0.0001$), $42.8 \pm 1.2\%$ ($p < 0.0001$), and $31.2 \pm 5\%$ ($p < 0.005$) respectively. ciPTEC cells exposed to 0.4 μ g/mL or 4 μ g/mL of MPA generated 146.98 ± 48.78 and 790.75 ± 56.48 ng/mL/million cells of MPAG in the culture supernatant over 72 hours, respectively. MPAG formation was linear for both MPA concentrations from 0-72 hours of incubation.

Conclusion: We have developed an in vitro renal model suitable for characterizing the pharmacokinetic interactions involving MPA with respect to renal uptake and intrinsic clearance.

Assessment of Potency of Topical Corticosteroids using the Vasoconstrictor Assay (VCA)

Seeparani Rath¹, Isadore Kanfer¹

¹University of Toronto

Purpose. Potency of topical corticosteroids (TCs) is important because the clinical choice of a TC depends on various factors which are considered by dermatologists when prescribing such products to achieve optimum safety and efficacy. Potencies of TCs have usually been classified based on clinical or vasoconstrictor assay (VCA) data. However, several discrepancies exist in the potency classifications leading to ambiguity. We propose classification of TC active pharmaceutical ingredients (APIs) based on their inherent potencies using VCA.

Method. Standardized solutions (0.0025M) of TCs in a common vehicle were used and skin blanching in human participants measured with a chromameter. Eight TC APIs were assessed for their relative potencies in two sets of clinical studies - Part A involved 4 APIs, Part B involved 6 APIs. Two APIs were common between the studies. The E_{\max} model was used to fit VCA data following application of the respective TCs, and the parameters, E_{\max} and ED_{50} , were derived. The E_{\max} values were used as a metric to assess the potencies of the TCs and rank them.

Results. Part A of the table shows that the inherent potency of mometasone furoate was greater than fluocinolone acetonide which was similar to clobetasol propionate. Halcinonide had the lowest potency. Whereas Part B depicts that inherent potencies of fluticasone propionate, mometasone furoate, and hydrocortisone butyrate were similar. There were no significant differences between hydrocortisone butyrate and clobetasol propionate, while there was a significant difference between clobetasol propionate, fluticasone propionate, and mometasone furoate. The potency of hydrocortisone butyrate appears to overlap two potency classes and the potencies of betamethasone valerate and methylprednisolone aceponate were similar but lower than the other APIs.

Conclusion. Inherent potency assessment of TCs provides information that will be useful when choosing a suitable candidate for incorporation into an appropriate TC product for a specific clinical indication.

Table 1. Summary of population model results

Study	Topical Corticosteroids	E_{\max}	AIC
Part A			
1	Clobetasol propionate	-75.44 ± 12.89	3.93
1	Halcinonide	-60.31 ± 3.75	3.84
2	Clobetasol propionate	-60.05 ± 13.31	3.79
2	Fluocinolone acetonide	-62.84 ± 5.98	3.64
3	Clobetasol propionate	-58.79 ± 15.65	3.57
3	Mometasone furoate	-94.45 ± 0.21	3.73
Part B			
1	Clobetasol propionate	-46.42 ± 15.45	3.92
1	Mometasone furoate	-55.27 ± 8.19	3.83
2	Methylprednisolone aceponate	-37.49 ± 14.79	3.84
2	Betamethasone valerate	-38.01 ± 17.90	3.8
3	Fluticasone propionate	-55.50 ± 19.27	4.07
3	Hydrocortisone butyrate	-48.82 ± 21.90	4.06

References: Zvidzayi M Pharmaceutics 2021; Tapfumaneyi P Mol. Pharm 2023

Activation of Toll-like Receptor (TLR)-7 is associated with Dysregulation of P-glycoprotein (Pgp) and Cyp3A Enzymes in a Pregnant Rodent Model of Viral Infection.

Mario Riera Romo¹, Eliza McColl², Micheline Piquette Miller¹

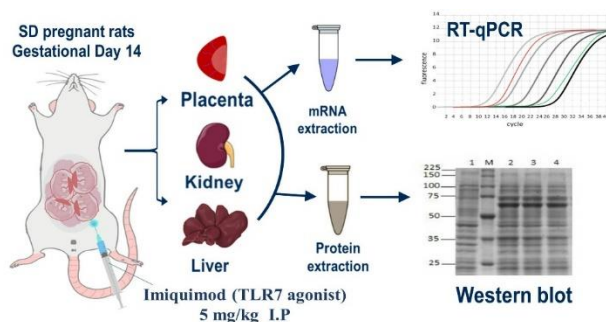
¹Leslie Dan Faculty of Pharmacy (LDFP), University of Toronto, ²Baylor College of Medicine, Houston, Texas, United States

Purpose: Our previous work in preclinical models has shown that immune activation during pregnancy alters the expression and activity of several placental transporters and can therefore impact fetal exposure to their substrates ^{1,2}. Single-stranded RNA viruses like SARS-CoV-2 stimulate immune responses through activation of TLR-7; thereby inducing production of interferons and inflammatory mediators ³. As this could impact fetal drug disposition, our goal was to examine the impact of TLR7 activation on the expression of drug transporter and metabolizing enzymes in pregnant rats.

Methods: Pregnant SD rats were administered a single dose of the selective TLR-7 agonist, imiquimod (IMQ, 5 mg/kg, IP) or vehicle (control) on gestational day 14 and sacrificed at 6 hr (n=4/group) or 48 hr (n=8/group). Tissues were analyzed by qRT-PCR and western blotting.

Results: IMQ treatment was associated with pronounced increases in placental and hepatic transcript levels of interferon regulatory factor (IRF)-7, IL-6 and TNF- α and IFN- α target genes ($p < 0.05$), demonstrating IMQ-mediated activation of TLR-7 and associated inflammation. Levels of the genes which encode Pgp (Mdr1b and Mdr1a) were significantly decreased in the placenta, livers and kidneys of the IMQ group. Corresponding decreases in protein expression of Pgp were seen in placenta. IMQ treatment was also associated with significantly decreased CYP3A2 and CYP3A9 mRNA in liver, while CYP3A2 mRNA was increased in placenta.

Conclusions: TLR7 activation stimulated the maternal immune system resulting in stimulation of IL-6, TNF- α and type I Interferon pathways in maternal and fetal tissues. IMQ activation of TLR-7 also resulted in decreased placental, hepatic and renal expression of P-glycoprotein as well as dysregulated expression of Cyp3A2 and Cyp3A9 enzymes in placenta and liver. Overall, this demonstrates that viral infections with SARS-CoV could alter the clearance and distribution of Pgp and Cyp3A substrates, thereby impacting fetal exposure. Further investigation is warranted.



References

1. Petrovic, V., et al. (2010) J Drug M Disposition 38(10): p. 1760-1766.
2. Karimian Pour, N., et al. (2019) J Pharmaceutics 11(12): p. 624.
3. Marcken M., et al. (2019) Sci. Signal. 12:605, eaaw1347.

Potential selective endogenous probes for characterizing the kinetics of five major sulfotransferases in humans

Ali Shalaby¹, Ayman O. S. El-Kadi¹, Tony K. L. Kiang¹

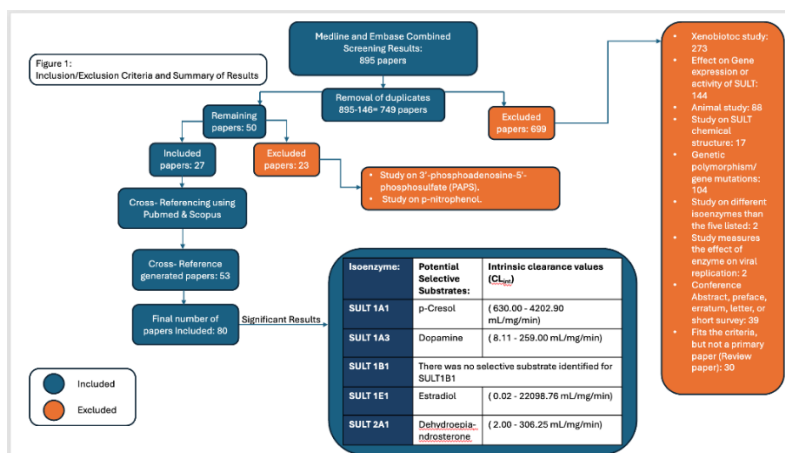
¹Faculty of Pharmacy and Pharmaceutical Sciences, University of Alberta, Edmonton, AB

Purpose: The sulfotransferase (SULT) enzyme family mediates the conjugation of a variety of xenobiotics, including endogenous compounds. Sulfonation can result in bioactivation or detoxification, and plays an important role in maintaining normal physiological functions. The objective of this research was to identify endogenous SULT substrates which may serve as selective markers for the five major human isoenzymes (SULT1A1, SULT1A3, SULT1B1, SULT1E1, and SULT2A1) using literature data.

Methods: A comprehensive literature search was conducted in Medline and Embase using the following search terms: SULT1A1, SULT1A3, SULT1B1, SULT1E1, SULT2A1, metabolism, and sulfonation. Articles were limited to those published in English before March 2024, and only human data and endogenous (i.e., natural) xenobiotics were included (Figure 1). Detailed exclusion criteria are explained in Figure 1. The identified papers were further subjected to manual bibliography screening and citation analysis (using the “cited by” function) in Pubmed and Scopus. Relative selectivity of a substrate was determined qualitatively based on intrinsic clearance values (CL_{int} ; i.e., higher values indicating higher affinity and higher capacity) toward a specific recombinant-expressed enzyme.

Results: Our search resulted in 80 papers (from an initial 895 papers). The probe substrates with the highest CL_{int} values in individually-expressed isozymes were: *p*-cresol (630.00 - 4202.90 mL/mg/min) for SULT1A1, dopamine (8.11 - 259.00 mL/mg/min) for SULT1A3, estradiol (0.02 - 22098.76 mL/mg/min) for SULT1E1, and dehydroepiandrosterone (2.00 - 306.25 mL/mg/min) for SULT2A1; with much lower activities of the same substrates in other isozymes. There was no selective substrate identified for SULT1B1.

Conclusion: We have identified potentially selective probe substrates for the major human sulfotransferase enzymes. Additional analyses on data derived from cytosolic preparations and reaction phenotyping experiments are ongoing. This study was funded by a New Frontiers in Research Fund grant.



Modelling of the Full Geometry of Cav1.2 and Predicting its Interactions with Ire1alpha

Azeez Adeniyi¹, Khaled Barakat¹

¹University of Alberta

Purpose. Cav1.2 is an L-type calcium channel that is encoded by the gene CACNA1C and has a broad tissue expression [1]. Opening of Cav1.2 channels enables the influx of Ca^{2+} and initiates intracellular Ca^{2+} -mediated signalling of which alterations are associated with neuropsychiatric diseases. The interest of this research is to model the full geometry of cav1.2 which is very significant to

understanding the mechanism of the opening and closing of the Ca^{2+} ion gate. The second interest is to predict the interaction of Cav1.2 with Ire1 Alpha (ire1alpha) which was known to downregulate cav1.2 [2].

Methods. Starting from crystal geometry, Cav1.2 missing regions were first predicted using Swissmodel combined with AlphaFold and Robetta server. The docking of ire1alpha to Cav1.2 was done using both MOE and Haddock server [3]. The final four models were selected based on their MM-PBSA predicted energies following MD simulations on the Cav1.2- Ire1alpha complexes immersed in a lipid membrane.

Results. The modelled full cav1.2 successfully predicted the secondary structure of the missing loop in the cryo-EM structure as shown in Figure 1 a. The geometry of the full Cav1.2 with the four homologous repeat units and the six transmembrane helices are shown in Figure 1 b. The best interaction of ire1alpha with Cav1.2 was selected based on MM-PBSA analysis of the MD trajectory. The best interaction energy obtained for Cav1.2-ire1alpha was -78.615 ± 16.660 kcal/mol for the system in the water while the membrane system gave -85.785 ± 11.822 kcal/mol.

Conclusion. The full Cav1.2 model in this study is relevant to understanding the opening and closing gate mechanism and the effect of mutations. We also show the first-ever predicted interaction between Cav1.2 and ire1alpha, which can be very useful in mitigating some of the associated dysfunction of Cav1.2.

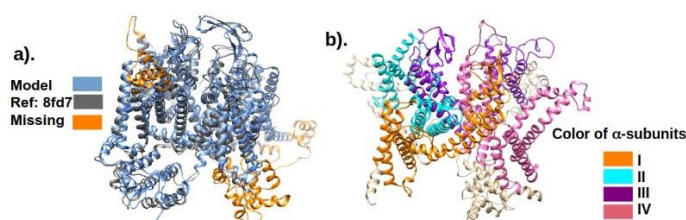


Figure 1: (a) Predicted model aligned with experimental 8fd7 pdb (b) Full cav1.2 model showing the four α -subunits with the six transmembrane helices of each.

References

1. Marcantoni A, Calorio C, Hidisoglu E, et al (2020) Cav1.2 channelopathies causing autism: new hallmarks on Timothy syndrome. *Pflugers Arch Eur J Physiol* 472:775-789. <https://doi.org/10.1007/s00424-020-02430-0>
2. Safiarian MS, Ugboya A, Khan I, et al (2023) New Insights into the Phototoxicity of Anthracene-Based Chromophores: The Chloride Salt Effect†. *Chem Res Toxicol* 36:1002-1020. <https://doi.org/10.1021/acs.chemrestox.2c00235>
3. Van Zundert GCP, Rodrigues J, Trellet M, et al (2016) The HADDOCK2. 2 web server: user-friendly integrative modeling of biomolecular complexes. *J Mol Biol* 428:720-725

Vancomycin Dosing Optimization in Neurocritical Care Population With Augmented Renal Clearance: A Monte Carlo Simulation

Asma Aboelezz¹, Maged Kharouba¹, Novel Solomon Tesfamariam², Sherif Hanafy Mahmoud¹

¹Faculty of Pharmacy and Pharmaceutical Science, University of Alberta, Edmonton, Alberta, Canada, ²Department of Pharmacy, Uppsala University, Uppsala, Sweden

Purpose: Vancomycin is a widely used antimicrobial to treat hospital acquired infections, especially methicillin resistant staphylococcus aureus among critically ill patients. As vancomycin is mainly eliminated through the kidney, the renal function plays a crucial role in the dosing of vancomycin. Augmented Renal Clearance (ARC) is a common condition among neurocritical ill patients. The aim of this study is to determine vancomycin pharmacokinetics alterations and optimize the dosing of vancomycin in neurocritical ill patients.

Methods: A prospective observational study of neurocritical ill patients received vancomycin at the University of Alberta Hospital. Population pharmacokinetics modeling of vancomycin was conducted using MonolixSuite to suggest vancomycin dosing especially in

ARC patients. Monte Carlo simulations were performed to predict the percentage of patients reaching the target trough concentrations following different doses.

Results: A total of 33 patients with 96 observations were included in this study. The population clearance was 0.07 L/kg.hr, and the volume of distribution was 1.169 L. The model which best fitted the population was one compartment model and logarithmic creatinine clearance (CrCl) was added as covariate on vancomycin clearance. Simulated 4 different dosing regimens of 15 mg/kg or 20 mg/kg every 8 or 12 hours were used to predict trough concentrations between 10 and 20 mg/L. In ARC patients, a simulated dose of 15 mg/kg every 8 hours resulted in 63.9% patients reaching target trough of 10mg/L and 78% having their trough below 20 mg/L. On the other hand, the 20 mg/kg every 8 hours resulted in 75% of trough concentrations ≥ 10 mg/L, but higher percentage of patients 39% achieving trough ≥ 20 mg/L.

Conclusion: Vancomycin clearance is affected by changes in CrCl, therefore, dosing optimization in such population is required to improve the outcomes. Patients with ARC may require higher vancomycin doses to reach the target concentrations.

Establishing a Direct Interaction Between the 19,20-EDP Analog SA-22 and SIRT3: Impact on Cardiac Mitochondrial Homeostasis

Joshua W Kranrod^{1,2}, Robert Valencia³, Ahmed M Darwesh¹, Marawan Ahmed¹, Mobina Heidari¹, Adeniyi Michael Adebesein⁴, Sailu Munnuri^{4,5}, Khaled Barakat^{1,6}, John R Falck⁴, John M Seubert^{1,2,3}

¹Faculty of Pharmacy and Pharmaceutical Sciences, University of Alberta, Edmonton, AB, ²Cardiovascular Research Institute, University of Alberta, Edmonton, AB, ³Department of Pharmacology, Faculty of Medicine and Dentistry, University of Alberta, Edmonton, AB, ⁴Division of Chemistry, Departments of Biochemistry and Pharmacology, University of Texas Southwestern Medical Center, Dallas, TX, ⁵TCG GreenChem, Inc. Process R&D Center at Princeton South, Ewing, NJ, ⁶Li Ka Shing Institute of Virology, University of Alberta, Edmonton, AB

Purpose: Despite extensive study, the structural, metabolic, and mechanistic heterogeneity amongst polyunsaturated fatty acids (PUFA) has confounded identification of their molecular targets and roles in cardiovascular diseases. Previously our group demonstrated that the cardioprotective properties of both 19,20-epoxydocosapentaenoic acid (EDP), a CYP450-derived metabolite of docosahexaenoic acid (DHA), and a synthetic structural analog SA-22, were SIRT3-dependent¹. Thus, we investigated potential functional interactions between SA-22, SIRT3, and their impact on mitochondrial homeostasis in the context of hypoxic myocardial injury.

Methods: *in silico* analysis of NAD⁺/SA-22/hSIRT3 complexes employed the Schrodinger Suite and AMBER18. SA-22 ligand binding was validated via SYPRO Orange thermal shift assay. SIRT3 catalytic activity was measured using an acetylated HDAC fluorogenic substrate assay. Point mutagenesis experiments confirmed the involvement of residue SER149. H9c2 cells were used as an *in vitro* model of hypoxia/reoxygenation (HR) injury. Cells were deprived of oxygen for 24 hours followed by a 6-hour reoxygenation period wherein cells were treated with either vehicle, 19,20-EDP (1 μ M), or SA-22 (1 μ M), either with the pan-sirtuin inhibitor nicotinamide (NAM) (30 μ M), or the SIRT3-selective inhibitor 3-(1H-1,2,3-triazol-4-yl)-pyridine (3-TYP) (50 μ M). Mitophagy was assessed via immunoblotting and the pH-dependent fluorescent mitophagy reporter protein (mito-Keima). Mitochondrial respiration was measured using high-resolution respirometry (Oroboros-O2K).

Results: SA-22 stabilized highly conserved residues adjacent to the nicotinamide-binding C-pocket and improved their binding affinities to NAD⁺ *in silico*. Addition of SA-22 altered SYPRO Orange fluorescence and improved catalytic activity *in vitro* but was abrogated by SER149 substitution, indicating that SA-22 is a positive allosteric modulator of SIRT3. Lastly, SA-22 protected cardiac cells against HR-induced changes in mitophagy and mitochondrial respiration in a SIRT3-dependent manner. **Conclusion:** SA-22 directly binds and enhances the activity of SIRT3, preserving cardiac mitochondrial homeostasis despite myocardial hypoxia-reoxygenation injury.

References

1. J Cardiovasc Pharmacol 2024 83: 105-115

Prevalence and risk factors of Augmented Renal Clearance in Neurocritical Care Population: Preliminary results from the Neuro-ARC Study

Maged Kharouba¹, Demetrios J. Kutsogiannis², Aaron M. Cook³, Melissa L. Bastin³, Yan Yuan⁴, Sherif H. Mahmoud¹

¹1. Faculty of Pharmacy and Pharmaceutical Sciences, University of Alberta, Edmonton, AB, Canada, ²2. Division of Critical Care Medicine, Faculty of Medicine and Dentistry, University of Alberta, Edmonton, AB, Canada, ³3. College of Pharmacy, University of Kentucky, Lexington, KY, USA, ⁴4. School of Public Health, University of Alberta, Edmonton, AB, Canada

Purpose. Complications occur frequently following a stroke, traumatic brain injury (TBI), and status epilepticus (SE), significantly impacting overall prognosis. Most drugs managing those complications are renally eliminated with their doses adjusted in renal dysfunction. Conversely, minimal consideration is given to patients exhibiting augmented renal clearance (ARC). ARC is observed in critically ill patients and can lead to medications underdosing, resulting in therapy failures. Most ARC research has not focused on neurocritical care population. Therefore, the primary objective is to assess the prevalence and identify risk factors associated with ARC in neurocritical care patients.

Methods. A prospective multicenter observational study was conducted for patients admitted to the participating neuroscience ICUs for acute neurological illnesses. 8-h urine collection method was used to measure participants' CrCl daily for 10 days. Patients with urinary CrCl >130 mL/min/1.73m² were categorized as the ARC group. Participants' data were gathered and summarized to assess the prevalence and potential covariates associated with ARC.

Results. To date, 136 patients were enrolled [34% subarachnoid hemorrhage (SAH), 26% TBI, 19% intracerebral hemorrhage (ICH), 15% ischemic stroke (IS), and 6% SE]. A total of 111 participants (82%) experienced ARC for at least 1 day, with 30.1% having ARC 100% of the time. ARC was most prevalent in TBI patients (94.3%) followed by SAH (87%), ICH (80.8%), IS (65%) then SE (50%). Generally, compared to non-ARC group, ARC group were younger (52±15 vs. 66±12 years, p-value=0.0001), has more males than females [75(87.2%) vs. 14(28%), p-value=0.038], and has lower admission serum creatinine (73.6±19.6 vs. 92.4±37.6, p-value=0.0006).

Conclusion. ARC is notably more prevalent in neurocritical population compared to the reported prevalence in mixed ICUs (82% vs. 36%). Consequently, it is crucial for clinicians to remain vigilant in identifying and monitoring ARC within these populations to enable timely dosage optimization.

References; J Pharmaceutics. 2017 Sep 16;9(3):36; Euro J Drug Met-PKS. 2022 Sep;47(5):607-20.

Repurposing the Parkinson drug benztropine for host-directed therapy of tuberculosis

Henok Asfaw Sahile¹, Matthew Christofferson¹, Joseph Chao¹, Yossef Av-Gay¹

¹Department of Microbiology and Immunology, Life Science Institute, University of British Columbia

Purpose. Tuberculosis (TB), caused by *Mycobacterium tuberculosis* (*Mtb*), is the leading cause of death among infectious disease. New effective drugs that are less vulnerable to development of drug resistance are much needed. Host directed therapy (HDT) is a promising avenue to develop novel TB drugs. The aim of this study is to identify new HDT for TB.

Methods. The approach involves screening of a library containing different FDA approved drugs against intracellular *Mtb* in THP-1 derived macrophage infection model. The compound that showed only intracellular activity - no direct in broth antibacterial activity - was selected and mode of action study was conducted using pharmacological and genetic tools. The *in vivo* activity of the most active hit was also tested using a TB mouse model.

Results. The screening identified five new hits active against intracellular *Mtb*. Among these, the Parkinson's drug benztropine exhibited a dose dependent growth inhibition against intracellular *Mtb* with no direct antibacterial activity when grown in broth media. A combination of pharmacological and genetic approaches was used to determine benztropine mode of action revealing that

benztropine exerts its intracellular anti-*Mtb* activity through the host macrophage histamine receptor 1 (H1). Moreover, benztropine was found to be active against *Mtb* in human monocyte derived macrophages (hMDMs) obtained from three different donors. The efficacy and tolerability of benztropine was also assessed in murine macrophage cells (Raw 264.7 cells). *In vivo* infection study showed that benztropine is effective in blocking *Mtb* infection in the lungs of treated mice.

Conclusion. Altogether, our findings suggest the potential of benztropine to be repurposed for TB and may also pave the way for development of a new host-directed anti-TB drug class that targets H1 receptors in infected macrophages.

TECNIQ Aquarius: A Real-Time Clinical Pharmaco-BCI Analysis Software Module for Optimizing Clinical Ketamine and Esketamine Dosing and Psychedelic Pharmaceutical Research and Development

Yahuai Sun^{1, 2}, Tony Sun¹, Shahzaib Ahmed³, Hiritikk Kumar¹, Raymart Bless C. Datuin^{2, 3}, John-Paul R. Cooper¹, Danna Hristova¹, Aqib Muhamad Amran¹, Abdullah Sherwani³, Uzair Tariq³, Sunny Kim², Param Bhardwaj², Kevin W. Morin^{2, 4}

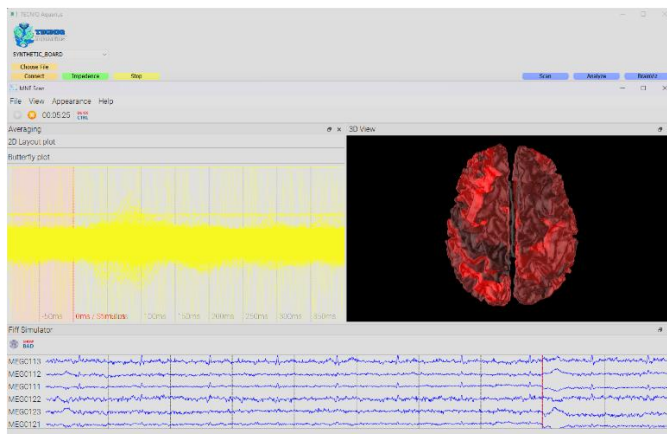
¹Faculty of Science, University of Alberta, Edmonton, AB, ²Sunmor Research Inc., Edmonton, AB, ³Faculty of Engineering, University of Alberta, Edmonton, AB, ⁴Department of Psychiatry, Faculty of Medicine and Dentistry, University of Alberta, Edmonton, AB

Purpose. Psychedelics are promising treatments for psychiatric disorders. However, concerns regarding pharmacokinetics, pharmacodynamic effects and the importance of optimizing doses have emerged. Advances in Brain-Computer-Interfaces and related software present novel solutions to address these issues with clinical and research applications. Transcriptomic Entropy Contrast Network Imaging and Quantification (TECNIQ®-Aquarius) is a proprietary real-time data processing and visualization software module for physicians and researchers. TECNIQ® software may be useful in interventional psychiatry, as a precision medicine tool to optimize oral or intranasal ketamine dosages for improved treatment outcomes. The module is engineered as a Class-II Software as a Medical Device (SaMD) that functions seamlessly with Health Canada approved Class-II medical device acquisition systems such as ANT-Neuro and NATUS devices. TECNIQ® may function as a standalone hardware control and acquisition software, allowing flexibility in various clinical and research settings.

Methods. TECNIQ®-Aquarius is a Windows-based software application written in Python under a streamlined user-interface. Open-source software written in C++ was integrated into the app through a Python wrapper to expand functions. Software development and documentation followed Health Canada Class-II SaMD guidelines according to IEC 62304, IEC 82304-1, ISO 14971 and ISO 13485 standards.

Results. We tested TECNIQ® software through several use cases, using sub-modules such as custom Time-Series, Spectrogram, Powerbin, Power-Spectral-Density and Lempel-Ziv complexity plots alongside open-source based MNE-CPP and BrainBay functions. Further clinical validation is required. Figure 1 shows a screenshot of the real-time source-localization function with sample data.

Conclusion. The TECNIQ®-Aquarius module is suitable for a wide-range of applications as a real-time analysis tool for clinical and research purposes. Through integration of custom code, open-source software, and industry standard acquisition hardware, TECNIQ® can assist physicians to deliver personalized care. Implementation with machine learning is easily accessible and can further guide treatments and support pharmaceutical innovations like nanoparticle-drug delivery systems.



Efficacy of Crocin from Saffron in Alleviating Diabetic Neuropathy: A Randomized, Double-Blind, Placebo-Controlled Clinical Trial

Ehsan Motaghi Dastenaee

Objectives: The main goal of this study was to assess the effectiveness of crocin, an ingredient of saffron, in treating diabetic neuropathy, providing initial findings in this area.

Methods: A total of 221 eligible participants with symptomatic CIPN ranging from mild to severe were enrolled between December 2018 and March 2020. They were randomly assigned to one of two groups: one receiving a 15 mg crocin tablet twice daily (total daily dose of 30 mg) and the other a placebo tablet for 8 weeks. A crossover design was used with a 2-week washout period. Patient progress was assessed weekly over the 8-week period.

Findings: There was a significant decrease in sensory, motor, and neuropathic pain grades in the crocin group compared to the placebo group ($P < 0.05$). Mild side effects were observed, with no statistically significant differences in adverse events between the two groups ($P > 0.05$).

Conclusions: Crocin appears to effectively alleviate symptoms of diabetic neuropathy in diabetic patients neuropathic pain. Nevertheless, further research is necessary to explore the potential neuropharmacological benefits of crocin and its lower risk of adverse effects compared to conventional medications like antidepressants, lamotrigine, and gabapentin.

Table 2

Secondary outcome analysis results for the crossover study in both groups. Digits in the parentheses were expressed as percentage. C/P; the group that received crocin in the first 8-week period and placebo in the second 8-week period. P/C; the group that received therapy in the reverse order. *P* values relate to comparisons between the 2 groups at the corresponding time point. * Higher scores indicate greater severity of symptoms. † Higher scores indicate fewer symptoms or improvement. NRS; numerical rating scale. NCIC-CTC; National Cancer Institute of Canada Common Toxicity Criteria. ENS; Eastern Cooperative Oncology Group Neuropathy Scale. WHO; World Health Organization. BPI; Brief Pain Inventory. SDS; Symptom Distress Scale. SGIC; Subjective Global Impression of Change. QOL; Quality of life. NPS; Neuropathy Pain Scale.

	Baseline	<i>P</i>	End of 8 weeks	<i>P</i>	End of 18 weeks	<i>P</i>
Number per group		-		-		-
C/P	89		73		66	
P/C	88		82		71	
NRS average pain*		0.5		0.002		0.002
C/P	4.3		2.1		4.5	
P/C	4.7		4.6		2	
NCIC-CTC scale*		0.7		0.005		0.005
C/P	2.5		1.6		2.4	
P/C	2.4		2.4		1.5	
ENS average pain*		0.7		0.007		0.007
C/P	1.8		1.3		1.7	
P/C	1.9		1.7		1.2	
Mean WHO neuropathy score*		0.7		0.003		0.002
C/P	2.1		0.9		2	
P/C	2		1.7		0.8	
BPI average score*		0.6		0.009		0.005
C/P	3.4		2.7		3.1	
P/C	3.2		3.1		2.2	
McGill pain rating index*		0.8		0.005		0.003
C/P	25.3		14.6		23.9	
P/C	24.1		22.9		13.8	
Mean total SDS score*		0.8		0.009		0.008
C/P	69.2		59.4		67.7	
P/C	67.4		66.6		56.9	
SGIC scale†		-		0.000		0.000
C/P	-		0.9		0.3	
P/C	-		0.3		1.1	
QOL scale‡		0.1		0.009		0.008
C/P	61.3		75.5		63.2	
P/C	66.2		67.4		77.3	
Mean NPS*		0.7		0.005		0.002
C/P	3.2		2.1		3	
P/C	3.1		3		1.9	

The Implementation of a Pharmacist-led Testing Service for HIV and Hepatitis C in Rural NL Correctional Facilities

Michael Coombs¹, Deborah Kelly¹

¹Memorial University, St. John's, NL

Purpose: Human Immunodeficiency Virus (HIV) and hepatitis C (HCV) are sexually transmitted and bloodborne infections that disproportionately affect people who are incarcerated. Testing for these infections in correctional facilities is a key component to effective detection and treatment. Point-of-care (POC) testing in correctional facilities aims to overcome barriers relative to traditional venipuncture. This pilot study aims to assess the feasibility and acceptability of a pharmacist-led testing service for HIV and HCV in rural correctional facilities in Newfoundland and Labrador (NL).

Methods: This pilot study followed a prospective, interventional cohort study design. Testing visits were conducted at three adult correctional facilities across rural NL. Participants were offered a choice of HIV and/or HCV POC tests. Testing pharmacists provided pre-test counselling, collected blood samples, administered the POC tests, and provided post-test counselling including interpretation of test results and information about preventative measures. Participants with reactive screening results referred to correctional health

staff for confirmatory testing and care. Participants completed pre-test and post-test surveys to collect information on demographics, risk behaviours, experiences, and acceptability. Descriptive statistics were used to analyze quantitative results.

Results: 75 participants of 103 total incarcerated individuals volunteered to receive HCV and/or HIV testing. A total of 74 tests were administered, including 58 HCV tests and 73 HIV tests. Proportions of reactive screening results were 6/58 for HCV and 0/73 for HIV and were offered confirmatory testing. Additionally, five individuals fell within the window period for the tests based on last possible exposure. Eleven confirmatory tests were completed and four new HCV infections were confirmed. Most participants who volunteered for testing had never been tested before (46%), have used substances (59%) and felt comfortable with pharmacist testing (100%)

Conclusions: HIV and HCV POC testing by pharmacists may be a feasible and acceptable alternative to traditional venipuncture within correctional facilities.

Efficacy of Ammaruekawadi Remedy on Treating Cough Symptoms in Post-COVID-19 Patients: A Preliminary Study

Thitharee Jacktornsuan¹, Arunporn Itharat², Neal M. Davies³, Santhad Chomphuphong¹

¹Department of Modernized Thai Traditional Medicine, Ratchaburi Hospital, Ratchaburi, Thailand, ²Center of Excellence on Applied Thai Traditional Medicine Research, Faculty of Medicine, Thammasat University, Pathum Thani, Thailand, ³Faculty of Pharmacy and Pharmaceutical Sciences University of Alberta, Edmonton, Alberta Canada

Purpose: Coronavirus disease 2019 (COVID-19) is caused by the novel coronavirus SARS-CoV-2, a member of the family Coronaviridae. Common clinical manifestations include fever, cough, sore throat, dyspnea, myalgia, and fatigue. Recent studies have identified persistent symptoms in patients even after recovery. At the Modernized Thai Traditional Medical clinic, Ratchaburi Hospital, Thailand, it was observed that 75% of post-COVID-19 patients experienced recurrent cough, significantly affecting their work capacity, incurring medical expenses, and causing social withdrawal due to the fear of spreading COVID-19. Ammaruekawadi Remedy, a traditional Thai medicine listed in the National List of Essential Medicine (NLEM), uses licorice root as a primary ingredient. This study aims to evaluate the efficacy of Ammaruekawadi remedy in alleviating cough symptoms in post-COVID-19 patients.

Methods: A retrospective cross-sectional study was conducted with 40 patients over the age of 20 who were administered 1,500 mg of Ammaruekawadi remedy daily for two weeks between October 2023 and December 2023. The Leicester Cough Questionnaire (LCQ) was the primary tool for assessing cough symptoms. Statistical analyses compared LCQ scores before and after treatment.

Results: The study found a significant reduction in cough symptoms among post-COVID-19 patients treated with Ammaruekawadi remedy. The LCQ scores showed marked improvement, indicating relief from cough symptoms.

Conclusion: This preliminary study concludes that Ammaruekawadi remedy effectively alleviates cough symptoms in post-COVID-19 patients. These findings suggest that Ammaruekawadi remedy offers beneficial post-COVID-19 care. Further studies with larger sample sizes and randomized controlled trials are recommended.

Knowledge and Perceptions of Pharmacogenomics among Pharmacists in Manitoba, Alberta, Canada

Abdullah Al Maruf^{1,2}, Meagan Shields², Amber Fryza¹, Amanda Wondrasek¹, Christine Leong¹, Kaarina Kowalec¹, Chad Bousman²

¹University of Manitoba, ²University of Calgary

Purpose: Pharmacogenomics (PGx)-informed prescribing can potentially improve drug effectiveness and prevent adverse drug reactions. Despite the potential benefit of using PGx testing to inform prescribing, widespread adoption of this strategy has not yet

occurred in the Canadian healthcare system, including pharmacy practice. This study aimed to describe knowledge of and perceptions toward PGx-supported prescribing in clinical practice among pharmacists in Manitoba.

Methods: A cross-sectional study design with convenience sampling was employed. Pharmacists practicing in Manitoba were invited to complete a 40-item, web-based survey to assess their knowledge, perception, and attitudes toward PGx.

Results: Of 74 participants, one-third had some education or training in PGx, and 12.2% had used PGx test results in their practice. Participants' self-rated knowledge of PGx testing and common PGx resources, e.g., the Pharmacogenomics Knowledgebase (PharmGKB) and the Clinical Pharmacogenetics Implementation Consortium (CPIC), was low. Most pharmacists surveyed believe that PGx can improve medication efficacy (82.4%) or prevent adverse drug reactions (81.1%). Practitioner knowledge was selected as the most significant barrier to PGx implementation. Most (91%) desired more education on PGx.

Conclusion: Manitoba pharmacists report positive perceptions towards PGx. However, they are currently underprepared to implement PGx into practice, as evidenced by low self-rated knowledge of PGx and limited awareness of common PGx resources.

***Pseudomonas aeruginosa* Susceptibility Trends for Piperacillin-Tazobactam, Ciprofloxacin, and Ceftazidime in Canada**

Doha Anwar¹, Nathan Beahm¹

¹Faculty of Pharmacy and Pharmaceutical Sciences, University of Alberta, Edmonton, AB, Canada

Purpose: Considering the variety of resistance mechanisms that *Pseudomonas aeruginosa* possesses against antimicrobials and the growing concern of increasing resistance rates, analyzing the most recent susceptibility trends of this pathogen is imperative. The objective was to determine the susceptibility trends of *P. aeruginosa* for piperacillin-tazobactam, ciprofloxacin, and ceftazidime across Canada (British Columbia [BC], Alberta [AB], Saskatchewan [SK], Manitoba [MB], Ontario [ON], Nova Scotia [NS], and Prince Edward Island [PEI]) between 2017 to 2021.

Methods: Data were obtained retrospectively from antibiograms provided by local resources, including health authority or laboratory websites, apps, or by directly contacting the microbiology facility (e.g., DynaLife, LifeLabs, or Shared Health). Regions with susceptibilities of at least 90% were highlighted and clinical significance was defined as a change in susceptibility of at least 10% over the included years. Rural versus urban susceptibilities were also compared.

Results: Data were collected and analyzed from a total of 726 antibiograms. Piperacillin-tazobactam and ceftazidime susceptibility rates remained above 90% for the majority of regions across all study years. Ciprofloxacin susceptibility rates generally remained below 90% -- but above 80% -- for almost every province every year with the only exception of Saskatchewan at 78.8% in 2020. Clinically significant differences were observed for piperacillin-tazobactam (BC: 2017-2018, -10.1%; 2018-2019, +10.2%; 2019-2020, -11.0%) and ciprofloxacin (SK: 2020-2021, +10.2%), with none observed for ceftazidime. In general, rural susceptibilities tended to be higher than urban, with a few exceptions.

Conclusion: For the years 2017 to 2021, clinical isolates of *P. aeruginosa* presented with high levels of piperacillin-tazobactam and ceftazidime susceptibility. Ciprofloxacin susceptibility rates were generally lower than 90%, but remained relatively stable. Both increasing and decreasing trends in susceptibility rates were seen for all 3 agents, with the largest variation being with piperacillin-tazobactam; but clinically significant differences were infrequent.

Acknowledgement: Recipient of the CSPA Undergraduate Student Research Award.

Examining hypoglycemia risk with systemic fluoroquinolone use: a meta-analysis

Irene Guo¹, Mira Máximos¹, John-Michael Gamble¹

¹University of Waterloo School of Pharmacy, Kitchener, ON

Purpose: Hypoglycemia associated with fluoroquinolone (FQ) use has been discussed in several case reports, yet there is currently no comprehensive meta-analysis investigating this relationship. Our objective was to bridge this gap in research by conducting a meta-analysis that synthesizes existing studies to quantify the relationship between FQs and the risk of hypoglycemia.

Methods: A literature search was conducted using PubMed (Medline), Cochrane Library, and Ovid Embase databases to identify primary studies that reported hypoglycemia events in FQ users. Each study was independently screened by two reviewers (IG, JG, or MM), with discrepancies resolved through consensus. A random effects model was used to calculate a summary odds ratio from pooled dichotomous outcomes. Studies with multiple comparators were stratified under cephalosporin, macrolide, or other antimicrobial comparator subcategories. All analyses were conducted using R statistical software (version 3.4.1).

Results: Twenty studies were included in the meta-analysis. The results showed a significantly elevated risk of hypoglycemia associated with FQ use compared to non-FQ antimicrobials (18 studies, OR 2.07 (95% CI 1.79-2.39), $p < 0.01$, $I^2 = 48\%$). Ciprofloxacin (5 studies, OR 1.54 (95% CI 1.29-1.84), $p = 0.01$, $I^2 = 54\%$), gatifloxacin (8 studies, OR 3.28 (95% CI 2.24-4.80), $p = 0.06$, $I^2 = 44\%$), and levofloxacin (5 studies, OR 2.61 (95% CI 2.31-2.94), $p = 0.37$, $I^2 = 7\%$) individually exhibited a significantly higher risk of hypoglycemia compared to non-FQ antimicrobial comparators. However, moxifloxacin did not show a significantly elevated risk of hypoglycemia (4 studies, OR 1.42 (95% CI 0.95-2.13), $p = 0.01$, $I^2 = 55\%$). Additionally, no significant difference for hypoglycemia risk between FQ users with or without diabetes were observed (6 studies, $p > 0.1$ for subgroup difference).

Conclusion: The results of this meta-analysis showed a significant association between FQs and an increased risk of hypoglycemia, irrespective of diabetes status, although there appears to be individual differences within this class of antibiotics.

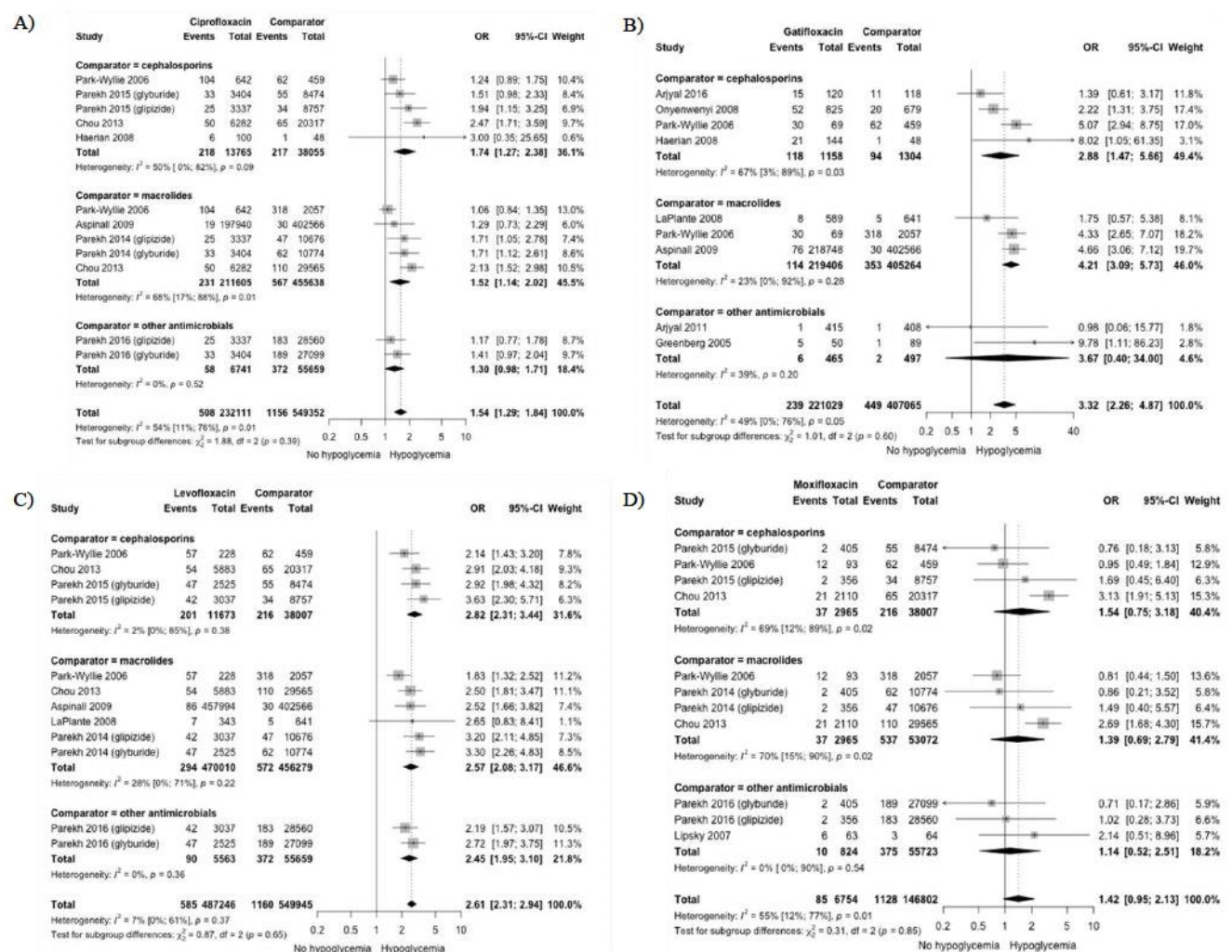


Figure 1: Forest plots of hypoglycemia risk associated with A) ciprofloxacin, B) gatifloxacin, C) levofloxacin, and D) moxifloxacin.

Prescription Patterns and Economic Analysis of Anticancer Medications for Breast Cancer Patients: Insights from a Three-Year Study at an Oncology Unit in the Sultanate of Oman

Abdullah Al Lawati¹, Nasser Al Wahaibi¹, Hanan Al Lawati², Yousuf Al Suleimani³

¹College of Medicine and Health Sciences, Sultan Qaboos University, Oman, ²Pharmacy Program, Department of Pharmaceutics, Oman College of Health Sciences, Oman, ³Department of Pharmacology and Clinical Pharmacy, College of Medicine and Health Sciences, Sultan Qaboos University, Oman

Purpose: Breast cancer remains a significant global health challenge, ranking as the fifth leading cause of cancer-related deaths among women worldwide in 2018 [1]. In Oman, it accounts for a substantial portion of female cancer cases, constituting 32% and representing the nation's second most common cause of death [2]. Given its gravity, understanding prescription patterns and treatment costs within Oman is crucial. This study aims to analyze such patterns and expenditures, offering insights into global comparative studies while potentially identifying areas for intervention to enhance treatment quality.

Methods: This retrospective cross-sectional study focuses on the prescription patterns of anticancer drugs among breast cancer patients at Sultan Qaboos University Hospital in Oman over three years, from January 2018 to January 2021. The sample comprises female patients aged 18 or older who underwent at least one treatment for breast cancer during this period.

Results: Findings reveal that the majority of patients received an average of 4.73 anticancer drugs, with the Anthracycline, Cyclophosphamide, and Docetaxel (AC-D) regimen being the most common, administered to 33.5% of patients. Cyclophosphamide emerged as the most frequently prescribed drug, followed by Doxorubicin and Docetaxel. Total drug expenditure on anticancer therapy during this period amounted to approximately 1.655 million Omani Riyals (~5,800,000 CA\$), with targeted therapy representing the majority (75%) of spending, while chemotherapy and hormonal therapy accounted for 20% and 5%, respectively.

Conclusion: Comparative analysis suggests that our prescription patterns align with previous international studies, though differences may stem from varied drug prescription guidelines across settings. These findings underscore the importance of optimizing drug utilization to enhance resource efficiency and healthcare delivery, thus ensuring better treatment outcomes for breast cancer patients in Oman and beyond.

References

1. Mod Pahol 2018 31:1770
2. Oman Med J 2014 29:408-413

Glycolysis in CD8⁺ T cells regulates the onset of abacavir-induced skin toxicity in HLA-B*57:01 transgenic mice

Takeshi Susukida¹, Yuchen Sun², Shigeki Aoki³, Kousei Ito³, Yoshihiro Hayakawa¹

¹Laboratory of Cancer Biology and Immunology, Section of Host Defenses, Graduate School of Medicine and Pharmaceutical Sciences, University of Toyama, Japan, ²Division of Medicinal Safety Science, National Institute of Health Sciences, Japan,

³Laboratory of Biopharmaceutics, Graduate School of Pharmaceutical Sciences, Chiba University, Japan

Purpose. Idiosyncratic drug-induced autoimmune toxicity (IDT) associated with specific human leukocyte antigen (HLA) allotype does not occur in all subjects of a given HLA model population, suggesting the difficulties to predict the IDT risk without considering additional factors. We have generated a unique transgenic mouse line carrying HLA-B*57:01 (B*57:01-Tg) and successfully reproduced abacavir (ABC)-induced skin toxicity in B*57:01-Tg mice. On the other hand, we recently conducted serum metabolomics analysis and revealed that the glycolysis was the most significantly upregulated pathway in ABC-treated B*57:01-Tg mice. Here, we examined whether intracellular glycolysis level change in CD8⁺ T cells contributes to the susceptibility to ABC-induced IDT in the B*57:01-Tg mouse model.

Results and Discussion. Our RNA-sequencing (RNA-seq) data analysis using isolated CD8⁺ T cells demonstrated that the expression levels of several glycolytic enzymes including Hk2 were significantly upregulated in ABC-treated B*57:01-Tg mice, compared with that in the vehicle-treated group. In line with this observation, glycolytic rate in CD8⁺ T cells was also significantly increased by ABC treatment in B*57:01-Tg mice, resulting in increase of pyruvate production. Treatment of a hexokinase (HK) inhibitor, 2-Deoxy-D-glucose, attenuated an increase of IFN- γ -secreting CD44^{high}CD62L^{low}CD8⁺ T cells (effector CD8⁺ T cells) in B*57:01-Tg mice, thereby abrogating plasma thymus and activation-regulated chemokine (TARC) level elevation and CD8⁺ T cell dermal infiltration. Under calorie restricted condition by diet change, ABC treatment also failed to activate CD8⁺ T cells and induce ABC-induced skin toxicity in B*57:01-Tg mice, where intracellular glycolysis rate and pyruvate production of CD8⁺ T cells were suppressed. These results suggested that glycolysis in CD8⁺ T cells might play a major role in the onset of ABC-induced IDT in B*57:01-Tg mice.

Conclusion. Individual differences in the energy metabolism status may affect the susceptibility to HLA-mediated IDT in humans.

Investigating the mechanism of myeloperoxidase-mediated toxicity of the industrial contaminant, 6-PPD, in vitro

Steven Lockhart¹, Arno Siraki²

¹Grad Research Asst Fellowship, Faculty of Pharmacy & Pharmaceutical Sciences, ²Faculty of Pharmacy & Pharmaceutical Sciences

Purpose A product of the industrial contaminant, 6-PPD (N-[1,3-Dimethylbutyl]-N'-phenyl-p-phenylenediamine), has been recently reported as highly toxic to coho salmon and potentially toxic to other aquatic organisms. The potential toxicity of 6-PPD in humans, however remains unknown. The enzyme myeloperoxidase (MPO) in neutrophils, is known to produce free radicals and oxidized metabolites from xenobiotics therefore its role in 6-PPD-mediated toxicity was investigated.

Methods UV- visible spectroscopy and liquid chromatography-mass spectrometry (LC/MS) were performed to investigate the MPO mediated oxidation of 6-PPD and identify possible metabolites in the absence/presence of glutathione (GSH). 6-PPD's cytotoxicity, effect on mitochondrial membrane potential (MMP), and GSH depleting ability in the HL-60 cell line, a MPO-rich human leukemia cell line, were assessed. Electron paramagnetic resonance (EPR) and DMPO spin-trap was applied to capture the possible radical products in the presence of GSH.

Results UV-Vis analysis of MPO-catalyzed oxidation of 6-PPD demonstrated changes in 6-PPD spectrum, whereas GSH addition altered the spectrum indicating possible GSH conjugation. LC/MS showed the formation of multiple products, including GSH-6-PPD conjugates, and a GSH-4-hydroxydiphenylamine conjugate (a known 6-PPD degradant) which could potentially induce cytotoxicity. 6-PPD demonstrates a positive concentration dependent relationship with cytotoxicity whereas [GSH] was decreased by 6-PPD in HL-60 cells. With increasing [6-PPD], MMP decreased which suggest cellular mitochondrial depolarization occurred. EPR spin-trapping demonstrated a concentration-dependent relationship between 6-PPD and GS radical signal intensity in the presence of H₂O₂. Spin-trapping of mitochondrial radical also shows a positive relationship with [6-PPD].

Conclusion 6-PPD's oxidation can induce radical formation and GSH conjugation in the presence of MPO. Furthermore, 6-PPD induces toxicity, disrupts MMP and depletes GSH in HL-60 cells. Our results suggest that MPO could be an activator of 6-PPD's toxicity in humans. A potential relationship between 6-PPD's oxidative metabolites and toxicity mechanism requires deeper investigation to determine its toxicity in mammals, including humans.

Cannabistilbene-1 protects against angiotensin II-induced cellular hypertrophy through the induction of Cytochrome P450 1A1 enzyme and its arachidonic acid metabolite 19(S)-HETE

Ahmad H. Alammari¹, Conor O'Croinin¹, Neal M. Davies¹, Ayman O. S. El-Kadi¹

¹Faculty of Pharmacy and Pharmaceutical Sciences, University of Alberta, Edmonton, Alberta, Canada

Purpose: This study aimed to elucidate the effects of cannabistilbene-1 on angiotensin II (Ang II)-induced cardiac hypertrophy and its potential role in modulating cytochrome P450 1A1 (CYP1A1) and arachidonic acid (AA) metabolites.

Methods: Adult human ventricular cardiomyocytes cell line (AC16) were cultured and exposed to 100 ng/ml cannabistilbene-1 in the presence and absence of 10 μ M Ang II. The assessment of mRNA expression pertaining to cardiac hypertrophic markers and CYPs was conducted using real-time polymerase chain reaction (PCR) while the quantification of CYPs protein levels was carried out by Western blot analysis. Cell surface area was analyzed using fluorescently labeled reagent and AA metabolites were quantified using LC-MS/MS.

Results: Ang II induced hypertrophic markers and increased cell surface area, while cannabistilbene-1 mitigated these effects. Gene and protein expressions analysis revealed that cannabistilbene-1 upregulated CYP1A1 leading to increased enzymatic activity of CYP1A1 assessed by 7-ethoxyresorufin O-deethylase (EROD). Moreover, cannabistilbene-1 inhibited the protein expression of CYP1B1. Also, our results demonstrated that Ang II increased midchain(R/S)-HETEs concentrations, which were attenuated by cannabistilbene-1. Notably, cannabistilbene-1 selectively elevated 19(S)-HETE concentration. On the other hand, cannabistilbene-1 reversed the decline of 19(S)-HETE caused by Ang II, suggesting its protective role.

Conclusion: This study provides novel insights into the potential of cannabistilbene-1 in modulating arachidonic acid metabolites and attenuating Ang II-induced cardiac hypertrophy and highlight its importance as potential therapeutic agents for cardiac hypertrophy.

Support: Cannabistilbene-1 was provided by Canurta Canada. This work was supported by a grant from the Canadian Institutes of Health Research [Grant 106665] to A.O.S.E. A.H.A. is the recipient of Saudi Arabian government scholarship directed by Qassim University. C.O. is the recipient of Natural Sciences and Engineering Research Council of Canada, Canada Graduate Scholarship and is a MITACS Intern.

sEH Deletion or Inhibition Elicits Cardioprotective Response and Senescence in Aged Female Mice Exposed to LPS

Ala' Youssef¹, Deanna Sosnowski¹, Renald James Legaspi², Jacob Korodimas³, Katharine Magor², John Seubert¹

¹Faculty of Pharmacy and Pharmaceutical Sciences, University of Alberta, Edmonton, Alberta, Canada, ²Department of Biological Sciences, Faculty of Science, University of Alberta, Edmonton, Alberta, Canada, ³Department of Pharmacology, Faculty of Medicine and Dentistry, University of Alberta, Edmonton, Alberta, Canada

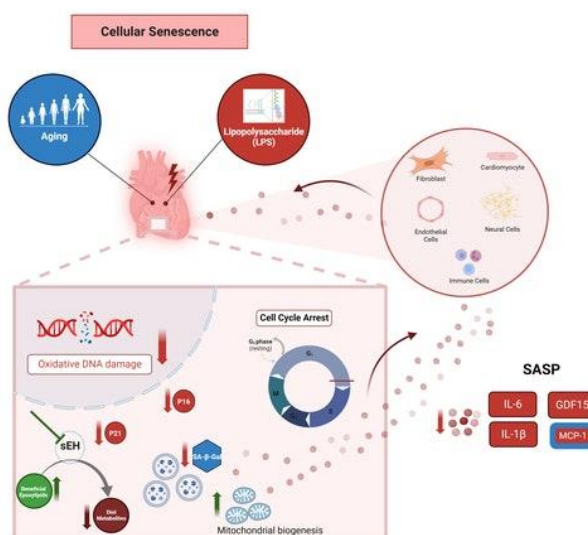
Purpose: Deterioration of physiological systems, like the cardiovascular system, occurs progressively with age impacting an individual's health and increasing susceptibility to injury and disease. Cellular senescence has an underlying role in age-related alterations and can be triggered by natural aging or prematurely by stressors such as the bacterial toxin, lipopolysaccharide (LPS). The metabolism of polyunsaturated fatty acids (PUFAs) by CYP450 enzymes produces numerous bioactive lipid mediators that can be further metabolized by soluble epoxide hydrolase (sEH) into diol metabolites, often with reduced biological effects. Previous research has demonstrated genetic deletion of sEH is cardioprotective and limits LPS-induced inflammation in young male mice. However, the cardioprotective effect of sEH deletion/inhibition in young and aged female mice has not been investigated.

Methods: Young (2-5 months) and aged (18-25 months) female wild type (WT), sEH null, and trans-4-[4-(3-adamantan-1-yl-ureido)-cyclohexyloxy]-benzoic acid (tAUCB) treated mice were administered either saline (control), 1 mg/kg or 10 mg/kg LPS via i.p. injection. Echocardiography was used to assess cardiac function at baseline and 24 hours after injections

Results: Age-related cardiac differences in female mice were observed, where young mice demonstrated resistance to LPS injury, and genetic deletion or pharmacological inhibition of sEH attenuated LPS-induced cardiac dysfunction in aged female mice. Bulk RNA-sequencing analyses revealed transcriptomics differences in aged female hearts. Confirmatory analysis demonstrated changes to inflammatory and senescence gene markers such as IL-6, Mcp1, IL-1 β , Nlrp3, p21, p16, and SA- β -gal were attenuated in the hearts of aged female mice where sEH was deleted.

Conclusion: Collectively, these findings highlight the role of sEH in modulating the aging process of the heart, whereby targeting sEH is cardioprotective.

Graphical Abstract



Treatment with a glucagon-like peptide-1 agonist reduces formation of toxic islet amyloid polypeptide oligomers and improves beta-cell survival in human islets during pre-transplant culture.

Janessa Sawatzky¹, Lucy Marzban¹

¹University of Manitoba, Winnipeg, MB

Purpose: Type 1 diabetes (T1D) is characterized by immune destruction of pancreatic islet beta cells, which leads to hyperglycemia. Human islet transplantation has provided a feasible approach for treatment of T1D but is currently limited by low number of donors and loss of islets during pre-transplant culture and post-transplantation. Aggregation of the beta-cell hormone, human islet amyloid polypeptide (hIAPP), contributes to beta-cell death in type 2 diabetes (T2D). Human IAPP aggregates also form in cultured and transplanted islets and contribute to islet graft failure. Importantly, small hIAPP aggregates (oligomers) that form at early stages of amyloid formation are the major toxic form. In this study, we examined if short-term treatment with Exenatide, a glucagon-like peptide-1 (GLP-1) analogue, can reduce formation of beta-cell toxic hIAPP oligomers in human islets.

Methods: Isolated human islets from cadaveric donors (n=4 donors) were cultured with or without exenatide (10 nM; 7 days; 37°C). Islets were fixed in 4% paraformaldehyde and paraffin-embedded islet sections were used for assessment of hIAPP oligomers and beta-cell apoptosis by quantitative insulin/A11 (oligomer) and insulin/TUNEL immunolabelling, respectively.

Results: Pre-culture human islets contained very low or no detectable hIAPP oligomers. Culture of human islets resulted in progressive hIAPP aggregation (oligomer formation), which was associated with increased number of TUNEL-positive beta cells in cultured human islets. Exenatide treatment effectively reduced the formation of hIAPP oligomers during 7-day culture, which was associated with a lower number of apoptotic beta-cells in treated islets as compared to non-treated cultured islets.

Conclusion: These findings suggest that treatment with exenatide reduces formation of hIAPP oligomers and enhances beta-cell survival in human islets. Treatment with GLP-1 agonists may protect islets from toxic hIAPP oligomers during pre-transplant culture thereby increasing islet yield for clinical islet transplantation and improving islet survival post-transplantation.

Cytochrome P450 1B1 Mediates the Cardiotoxic Effect of (R) and (S)11- hydroxyeicosatetraenoics (HETEs)

Sara A. Helal¹, Ahmed A. El-Sherbeni², Ayman O.S. El-Kadi¹

¹1. Faculty of Pharmacy and Pharmaceutical Sciences, University of Alberta, Edmonton, AB, Canada, ²2. Department of Clinical Pharmacy, Faculty of Pharmacy, Tanta University, Tanta, Egypt

Purpose: R/S enantiomers of 11-hydroxyeicosatetraenoic acid (11-HETE) are formed from arachidonic acid enzymatically and non-enzymatically [1]. 11-HETE is predominately formed by cytochrome P450 1B1 (CYP1B1). CYP1B1's role in the development of cardiovascular diseases is well established [2]. This study aimed to assess the cardiac hypertrophic effect of 11-HETE enantiomers and their association with CYP1B1 levels.

Methods: Human fetal ventricular cardiomyocyte, RL-14 cells were treated with 20 µM (R) or (S) 11-HETE for 24 h; cardiac hypertrophic markers and cell size were determined using real-time polymerase chain reaction (RT-PCR) and phase-contrast imaging. The mRNA and protein levels of selected CYPs were determined using RT-PCR and Western blot. Additionally, we examined the effect of (R) and (S) 11-HETE on CYP1B1 catalytic activity using human recombinant CYP1B1 and human liver microsomes.

Results: Both (R) and (S) 11-HETE increased cellular hypertrophic markers and cell surface area in RL-14 cells. 11(S)-HETE significantly upregulated the mRNA of CYP1B1, CYP1A1, CYP4A11, and CYP4F2 by 142%, 109%, 90%, and 257%, respectively, while the 11(R)-HETE upregulated them by 116%, 112%, 70%, and 167%, respectively. 11(S) HETE upregulated the protein expression of CYP1B1, CYP1A1, CYP4A11, and CYP4F2 by 186%, 129%, 152%, and 153%, respectively while 11(R)-HETE didn't affect the protein level to the same degree. Both (R) and (S) 11-HETE significantly increased the catalytic activity of CYP1B1 in human liver microsomes and recombinant human CYP1B1, suggesting allosteric activation in an enantioselective manner.

Conclusion: Our study provides the first evidence that 11-HETE can induce cardiac hypertrophy in RL-14 cells through the induction of CYP1B1 activity. The S-enantiomer allosterically activates the CYP1B1 at nM range in human recombinant CYP1B1 and heart microsomes.

This work was supported by a grant from the Canadian Institutes of Health Research [CIHR PS 168846] to A.O.S.E-K. S.A.H. is the recipient of Egyptian Government Scholarship.

References

1. Biochemistry 1997 36(7): 836-845.
2. Pharmacol Ther 2017 178:18-30.

in vitro Characterization of 3D-Bioprinted Hydrogel Constructs Over Time

Farinaz Ketabat¹, Reza Gharraei¹, Alex Guinle², Nicole Sylvain³, Michael E.Kelly³, Xiongbiao (Daniel) Chen¹, Ildiko Badea⁴

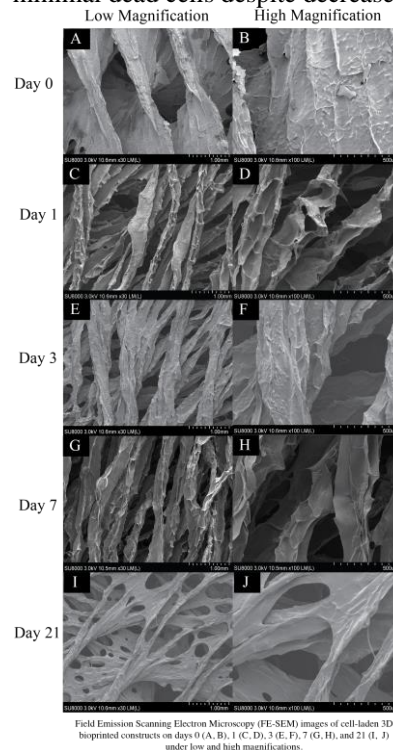
¹Division of Biomedical Engineering, University of Saskatchewan, SK, Canada, ²Institut Catholique des Arts et Metiers (ICAM)-Site de Bretagne, Vannes, France, ³Department of Surgery, College of Medicine, University of Saskatchewan, Saskatoon, Canada, ⁴College of Pharmacy and Nutrition, University of Saskatchewan, Saskatoon, Canada

Purpose: Incorporating advanced additive manufacturing, especially three-dimensional bioprinting, is crucial for engineered cardiac tissue development. The versatility of 3D printing allows building of top-down or bottom-up structures in the presence or absence of living cells in the bioink. However, developing a method to optimize printing parameters to accommodate the presence of the cells in the bioink is challenging. This study utilizes rheology and cell viability assessments to optimize the bioprinting of cell-laden constructs with printing parameters and bioink concentrations maintaining the properties of cell-free scaffolds, allowing a meaningful comparison between top-down and bottom-up approaches.

Methods: Rheological behavior of the bioink, an alginate/gelatin hydrogel with or without human umbilical vein endothelial cells (HUVECs), was studied. Computational fluid dynamics (CFD) and cell viability assays determined an adapted bioprinting pressure, followed by 3D (bio)printing of cell-free scaffolds and cell-laden constructs in an angular pattern mimicking heart fiber orientation. Over a 21-day period, the cell viability of cell-laden constructs as well as the physical and morphological properties of both cell-free and cell-laden constructs were examined.

Results: Under optimal printing conditions, both constructs exhibited viscoelastic behavior, and cell-laden constructs demonstrated elasticity at lower frequencies. Furthermore, cell-laden constructs displayed a lower elastic modulus overall than cell-free counterparts over 21 days. They also exhibited lower swelling and higher remaining mass percentage. Cells showed good viability post-bioprinting, consistently maintained for the initial week, persisting up to 21 days with

minimal dead cells despite decreased total cell count.



Conclusion: Successful optimization of 3D printing parameters for bioprinting living cells resulted in constructs with high stability for up to 21 days. These findings demonstrate that the physical and mechanical properties of the bioink are appropriate for advancing this technology to cardiac tissue engineering.

Arsenic trioxide (ATO) upregulates NAD(P)H: quinone oxidoreductase 1 (NQO1) expression in vivo and in vitro

Sara Elmahrouk¹, Mahmoud El-Ghiaty¹, Mohammed Alqahtani¹, Ayman El-Kadi¹

¹Faculty of Pharmacy and Pharmaceutical Sciences, University of Alberta, Edmonton, AB, Canada

Purpose: Arsenic trioxide (ATO) is a potent arsenical compound that has proven effective in treating acute promyelocytic leukemia. Despite its therapeutic efficacy, the treatment's benefits are often overshadowed by significant adverse effects, the underlying mechanisms of which remain poorly understood. The NAD(P)H: quinone oxidoreductase (NQO1)-mediated detoxification of quinones is an essential mechanism for preserving cellular homeostasis, it also serves as a pivotal factor in preventing cancer. The *Nqo1* gene is regulated by the nuclear factor erythroid 2-related factor-2 (NRF2), with the aryl hydrocarbon receptor (AHR) acting as an additional regulator for *Nqo1* gene expression. Therefore, we investigated the effect of ATO on the modulation of NQO1 expression in the absence or presence of the NQO1 inducer, 2,3,7,8-tetrachlorodibenzo-*p*-dioxin (TCDD) in C57BL/6 mice and mouse hepatoma (Hepa-1c1c7) cells.

Methods: C57BL/6 mice were subjected to intraperitoneal injections of ATO at 8 mg/kg, administered alone or concurrently with 15 µg/kg TCDD, for 6 and 24 hours. Similarly, murine Hepa-1c1c7 cells were exposed to increasing ATO concentrations (0.63, 1.25, and 2.5 µM), with or without 1 nM TCDD, over 6 and 24 hours.

Results: Our results show that ATO increased the hepatic expression of NQO1 in C57BL/6 mice as well as Hepa-1c1c7 cells, in the presence and absence of TCDD, at the mRNA, protein, as well as activity levels. Furthermore, ATO increased the nuclear translocation of both NRF2 and AHR transcription factors. Mechanistically, ATO exposure has increased the antioxidant response element (ARE)-driven reporter gene activity.

Conclusion: ATO exposure is found to upregulate the NQO1 enzyme through a transcriptional mechanism via AHR- and NRF2-dependent mechanisms, offering valuable insights into its therapeutic mechanisms. **Support:** This work was supported by the Natural Sciences and Engineering Research Council of Canada (NSERC) Discovery Grant [RGPIN 250139] to A.O.S.E., S.R.E. is a recipient of the Egyptian government scholarship.

References: 1- Annu Rev Pharmacol Toxicol, 2023, 20;63:341-358; 2- EXCLI J, 2021, 12;20:1184-1242.

RM-581, an aminosteroid derivative, reduces proliferation of prostate cancer (PCa) cells

Atsuhiko Yoshizawa¹, Mitali Pandey¹, René Maltais², Donald Poirier², Michael E. Cox¹, Kishor M. Wasan¹

¹Vancouver Prostate Centre, Dept. of Urologic Sciences, University of British Columbia, Vancouver, BC V6H 3Z6 Canada, ²Laboratory of Medicinal Chemistry, Endocrinology & Nephrology Unit, CHU de Québec Research Center- Université Laval, Québec, QC G1V 4G2, Canada

Purpose: Prostate cancer (PCa), the most common cancer to affect Canadian men, requires androgens in its early stages and initial treatments include androgen ablation therapies. However, in one-third cases, a castrate resistant (CRPC) metastatic form emerges. Despite the arrival of novel promising therapies for CRPC such as androgen receptor signaling inhibitors, some patients develop resistance to these treatments too. Thus, there exists an urgent need for new therapeutic agents to improve treatment of CRPC. RM-581, an aminosteroid derivative, exhibits potent anticancer activity¹. In this study we investigate the effects of RM-581 on the proliferation of different PCa cell lines.

Methods: The effect of RM-581 on cell proliferation was tested in RWPE-1, 22Rv1, LNCaP, DU145 & PC3 prostate cancer cell lines. 24 hours after cells were plated, they were incubated with 1.25, 2.5, 5, 10, 20 & 40 µM RM-581. Treatments were performed in triplicates and experiments repeated for an *n* = 3. The Incucyte Live-Cell Analysis System was used to capture high-resolution, bright field images, and record confluence metrics. Its integrated software was used to analyze, graph and plot the data. GraphPad Prism was used for statistical analysis and determination of half-maximal inhibitory concentration (IC₅₀).

Results: Our results indicate that RM-581 reduces proliferation in all PCa cells in a dose- and time-dependent manner. This inhibition is unique to each cell line and not affected by its dependency on androgens. The IC₅₀ of RM-581 for each cell line is reported in Table 1. Cell proliferation curves for RM-581 are reported in Fig. 1. The change in cell confluency at various time-points and doses with the proliferation curve is reported in Fig. 2.

Conclusions: Our findings demonstrate that RM-581 reduces proliferation in PCa cells in a dose- and time-dependent manner. Studies to investigate the potential mechanisms of action are on-going.

References: 1. Eur J Med Chem. 2020 188:111990

Table 1: IC₅₀ of RM-581 in prostate cancer cell lines

Cell line	Androgen dependency	Doubling time (hrs)	RM-581 (μM)
RWPE-1	Dependent	~58	3.0
22Rv1	Dependent	~49	5.8
LNCaP	Dependent	~60	6.7
C4-2 (CRPC derivative of LNCaP)	Independent	~36	3.7
DU145	Independent	~34	1.3
PC3	Independent	~26	8.8

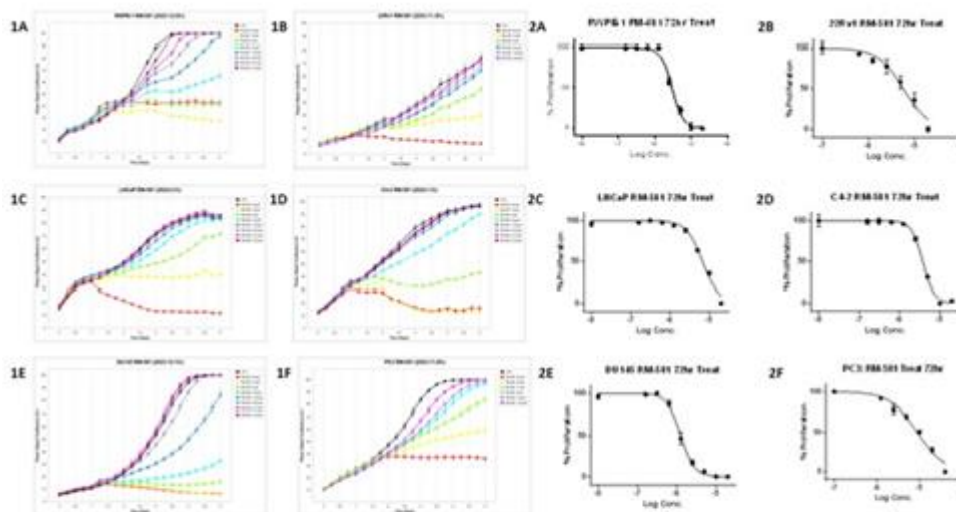


Fig. 1. The IncuCyte® live-cell analysis to study proliferation of prostate cancer cells treated with RM-581, in real-time: 5.00E+03 prostate cancer cells (RWPE-1, 22Rv1, LNCaP, C4-2, DU145 and PC3) were seeded per well of a 96-well plate. 24 hrs post-culture cells were treated with varying concentrations of RM-581 (1.25, 2.5, 5, 10, 20 & 40 μM). High definition (HD) phase-contrast images were acquired and cell proliferation measured in 4 fields/well every 6 hours, for 7 days using the Classic Confluence Analysis Software Module. Untreated cells and those treated with DMSO were used as controls. Real-time viability measurements for each cell line (1A: RWPE-1, 1B: 22Rv1, 1C: LNCaP, 1D: C4-2, 1E: DU145 & 1F: PC3), where data is the mean of 3 independent wells per time point ± SEM, has been plotted against time in days.

Fig. 2. Determination of RM-581 binding kinetics on prostate cancer cells. Six concentrations of RM-581 (1.25, 2.5, 5, 10, 20 & 40 μM) were incubated with 5.00 E+03 prostate cancer cells (RWPE-1, 22Rv1, LNCaP, C4-2, DU145 & PC3) seeded per well, of a 96-well plate for 72 hrs at 37°C. Real-time measurement of cell confluency as described in Fig. 1, was plotted against log₁₀ for each concentration to generate a dose-response curve for every cell line.

Free radical metabolites induce formation of protein radical: Clues for the mechanism of idiosyncratic drug-induced agranulocytosis (IDIAG)

HUAN LIU¹, Dinesh Babu², Arno Siraki¹

¹Faculty of Pharmacy and Pharmaceutical Sciences, Katz Group-Rexall Centre for Pharmacy and Health Research, University of Alberta, Edmonton, Alberta, T6G 2E1 Canada, ²Li Ka Shing Applied Virology Institute, University of Alberta, Edmonton, AB, T6G 2E1, Canada

Purpose: Myeloperoxidase (MPO) is the most abundantly expressed protein by human neutrophils. MPO can oxidize xenobiotics to reactive free radicals. Radical-mediated protein oxidation may produce protein radical formation. The study aims to investigate whether MPO-mediated metabolites of drugs that are associated with idiosyncratic drug-induced agranulocytosis (IDIAG), metabolism can form protein radicals in human neutrophils. We hypothesize that the enzymatic oxidation of clozapine, chlorpromazine, and metamizole (dipyrone) by MPO will produce reactive metabolites and consequently induce protein radicals in human neutrophils, which may be linked to the risk of IDIAG.

Methods: The human leukemia (HL-60) cell line resembles promyeloblasts, which highly express MPO. Cytotoxicity screening of clozapine, chlorpromazine, and metamizole was assessed by Cell Counting Kit-8 (CCK-8). Electron paramagnetic resonance (EPR) and liquid chromatography-mass spectrometry (LCMS) analyses are to investigate MPO-metabolized drug generated radical metabolites. Protein radicals were trapped by DMPO (5,5-dimethyl-1-pyrroline N-oxide), and immunoblots were utilized to detect DMPO-protein adducts.

Results: The IC₅₀ of clozapine in HL-60 cells was 40.99 μ M and the IC₅₀ of chlorpromazine was 20.82 μ M. Dipyrone interferes with the absorbance of WST-8 formazan, rendering the CCK-8 assay ineffective for detecting cytotoxicity. The anti-DMPO protein band appeared around 44 kDa in the treatment of clozapine, chlorpromazine, and metamizole in HL-60 cells. The level of DMPO-protein adducts with the treatment of chlorpromazine and metamizole produced intense anti-DMPO recognition, whereas less anti-DMPO recognition was observed with clozapine.

Conclusion: These findings revealed a correlation between protein radical formation and the three drugs used in this study that have a risk of IDIAG. The biological effect of protein radicals requires further exploration, and studies in neutrophils are also required.

Western blot analysis of metabolite effect on protein adsorption to PEO gold surfaces

Aishwarya Pawar¹, Mehdi Ghaffari Sharaf¹, Larry Unsworth¹

¹University of Alberta, Edmonton, Alberta

Purpose: Non-specific protein adsorption at the material-blood interface is well known to affect the host response to blood-contacting biomaterials. Polyethylene oxide (PEO) is commonly employed to minimize non-specific protein adsorption, but almost all studies rely upon the use of blood from healthy patients despite the fact they are applied to the unhealthy. Chronic kidney disease (CKD) patients show a remarkable difference in blood composition due to retained metabolites, some strongly bound by blood proteins (i.e., Protein-bound Uremic Toxins (PBUTs)). There is a dearth in the literature regarding the effect of metabolite accumulation in the blood compartment on protein adsorption to PEO films. The effect of common CKD metabolites on the adsorbed proteome was evaluated for PEO films.

Method: Au (200 nm)-Cr (50 nm)-Si wafers were cleaned (basic piranha) and modified using CH₃O-PEO to obtain chain densities of 0.5 to 0.8 chain/nm². PEO films were characterized using XPS and spectroscopic ellipsometry. Surfaces were incubated in platelet-poor human plasma with and without 31 common CKD metabolites, and adsorbed proteome was evaluated using Immunoblots.

Results: Increased metabolite composition and concentration in the plasma sample led to a significant increase in intensity in the immunoblot band for all proteins, with the maximum increase observed for fibrinogen, albumin, IgG, and complement C3. However, some anticoagulant proteins - Protein C, Protein S, and Plasminogen were completely absent, indicating no anticoagulant solid activity by samples.

Conclusion: Metabolites affect protein conformation and enzymatic function. Thus, it is unknown whether the increased protein presence at the blood-biomaterial interface directly affects increased biological function or is only a result of protein denaturation. The effect of metabolites on blood proteins and their interactions with engineered surfaces should not be overlooked when considering the design of blood-contacting materials.

PC12 Cells as A Model for Studying Parkinson's Disease and Treatment

Kaiwen Liu, Taylor C. Skinner, John T. Weber

School of Pharmacy, Memorial University, St. John's, Newfoundland and Labrador

Purpose: Parkinson's disease is a neurodegenerative disorder associated with degeneration of dopaminergic neurons. This *in vitro* study is aimed at investigating the toxic effects of glutamate and 6-hydroxydopamine (6-OHDA) in a rat PC12 pheochromocytoma cell line that is known to differentiate into dopaminergic neurons upon exposure to nerve growth factors.

Methods: Rat PC12 pheochromocytoma cells were cultured in DMEM media followed by the introduction of nerve growth factor (NGF) to promote differentiation into dopaminergic neuron phenotype for 2 days. The cells were subsequently incubated with glutamate or 6-OHDA of different concentrations for 24 hours. On day 4, the cells were stained with propidium iodide (PI) and DAPI and observed under a fluorescence microscope.

Results: After 2 days of incubation with NGF, some cells showed certain morphological changes (e.g., neurite growth, cell size increase). This indicates the effectiveness of NGF. After the cells were challenged with glutamate or 6-OHDA of different concentrations, PI staining showed increased cell death in glutamate or 6-OHDA treated cells compared to the control group while DAPI staining showed less cell survival in treated cells.

Conclusion: Although only some PC12 cells showed morphological changes upon NGF incubation, this does not affect how they respond to glutamate or 6-OHDA challenges. The cytotoxic effect of glutamate and 6-OHDA on the PC12 cell line certainly make it an ideal model to study potential treatments for Parkinson's disease *in vitro*, including extracts from natural products.

Kaiwen Liu is a recipient of a CSPS National Undergraduate Student Research Program Award

52 - Safety assessment of gold nanoparticles used to enhance radiofrequency ablation

Michelle Vargas Fernández¹, Wenjun Zhang¹, Michael Moser¹, Ildiko Badea¹

¹University of Saskatchewan

Purpose Radiofrequency ablation (RFA) is a minimally invasive technique for treating advanced hepatocellular carcinoma (HCC) stages [1]. Despite promising results, inducing uniform cell death in large tumours (>5cm) requires a multidisciplinary approach. This study aims to improve the current technique by increasing tissue conductivity with gold nanoparticles (AuNPs) of ~50 nm functionalized by two cationic molecules: poly-L-lysine (PLL) and the gemini surfactant 16-7N(GK)-16 (GS).

Methods Cytotoxic effect of AuNPS+PLL and AuNPS+PBS in HepG2 cells were studied using the ATP (CellTiter-Glo™ 2.0 Assay kit (Promega). Tumor spheroids (1×10^5 cells/spheroid) were grown for 10-days and were treated with AuNPS+PLL, and AuNPS+GS. 24 hours post-treatment, cell viability was assessed through a Live/Dead assay kit and imaged with a confocal microscope Nikon ECLIPSE Ti2.

Results A concentration of 7.75×10^9 particles/ml showed the safest profile in HepG2 cells in both cases: (7.75×10^9 vs. 3.88×10^9 , ANOVA, Tukey's Multiple Comparison Test $p = 0.9702$ for first assay and 7.75×10^9 vs. 6.05×10^7 , $p = 0.3858$ in second assay), suggesting its preferential use due to its lower likelihood of adverse effects. ATP assay showed non-significant death of cells: Dilution factor of 0.25 (0.250 vs. 0.125 ANOVA, Tukey's Multiple Comparison Test, $p = 0.9999$ and 0.250 vs. 0.125 ANOVA, Tukey's Multiple Comparison Test, $p = 0.9841$) for both assay cases. Confocal microscopy showed that AuNPs coated with PLL or GS maintained cell viability in HepG2 spheroids in the proliferative cells and inner core.

Conclusions The ATP assay proved to be a reliable assay for the current experimental conditions. Both PLL and GS provide safe coating maintaining HepG2 cell viability. These findings represent the foundation of functional studies evaluating the increase in tumour conductivity, leading to the successful ablation of large tumours.

References

[1] Ni Y, Mulier S, Miao Y, Michel L, Marchal G. A review of the general aspects of radiofrequency ablation. *Abdom Imaging*. 2005 Jul-Aug;30(4):381-400. doi: 10.1007/s00261-004-0253-9. PMID: 15776302.

Sexual Dimorphism in Cardiac CYP Enzymes and HETEs in Pressure Overload-Induced Cardiac Hypertrophy

Samar H. Gerges¹, Sara A. Helal¹, Heidi L. Silver², Jason R.B. Dyck², Ayman O.S. El-Kadi¹

¹Faculty of Pharmacy and Pharmaceutical Sciences, University of Alberta, Edmonton, Alberta, Canada, ²Department of Pediatrics, Faculty of Medicine and Dentistry, University of Alberta, Edmonton, Alberta, Canada

Purpose: Cardiac hypertrophy is a risk factor for heart failure and death, and is usually less common in women than in men (1). Cytochrome P450 (CYP) enzymes in the heart metabolize arachidonic acid into hydroxyeicosatetraenoic acids (HETEs), which have hypertrophic effects (2). In this study, we investigated sex-specific differences in pressure overload-induced cardiac hypertrophy and its effect on cardiac CYP enzymes and HETE levels.

Methods: Adult male and female Sprague-Dawley rats were subject to sham or abdominal aortic constriction (AAC) surgeries. 5-weeks post-surgery, cardiac function was assessed by echocardiography. The mRNA and protein levels of hypertrophic markers and CYP enzymes were measured by real-time PCR (RT-PCR) and Western blot. Heart tissue HETE levels and formation rate were measured by liquid chromatography-tandem mass spectrometry.

Results: Our results show significant sex-specific differences in AAC-induced cardiac hypertrophy. Echocardiography showed stronger hypertrophy in male rats compared to female rats. Several hypertrophic markers were significantly increased in male AAC rats like atrial natriuretic peptide (ANP), skeletal muscle α -actin (ACTA1), and β/α -myosin heavy chain (MHC), while only β/α -MHC was increased in female AAC rats compared to sham. CYP1B1, CYP4A, and CYP4F were significantly increased only in male AAC, but not in female AAC rats. The formation rates of all HETEs and the basal 12-HETE level were significantly increased in male AAC rats compared to male sham rats, while 5-, 9-, and 15-HETE formation were significantly decreased in female AAC rats compared to female sham rats.

Conclusion: Male rats developed stronger AAC-induced cardiac hypertrophy compared to female rats, that was associated with a significant increase in cardiac CYP hydroxylases and HETEs.

This work was supported by a grant from the Canadian Institutes of Health Research [CIHR PS 168846] to A.O.S.E-K. S.H.G. is the recipient of Alberta Innovates Graduate Student Scholarship.

References: (1) J Cardiovasc Transl Res 2020 13(1):73-84. (2) Drug Metab Rev 2013 45(2):173-195.

Identification and validation of an antibody to visualize protein restoration in the LumA luciferase reporter mouse model for genome editing.

Nadine Ramsden¹, Jackie Ho¹, Alexandra Birkenshaw¹, Tyler Thomson¹, Lin-Hua Zhang¹, Alexander D. Smith¹, Colin Ross¹

¹University of British Columbia

Purpose: We have developed a luminescent transgenic mouse model (LumA) that encodes a firefly luciferase transgene harbouring a premature stop codon, which results in a non-functional protein. When repaired by gene editing, the stop codon is removed, restoring luminescent activity. This allows for in vivo bioimaging to efficiently evaluate the efficacy and biodistribution of base editors and delivery vectors, such as lipid nanoparticles (LNPs). Unfortunately, bioimaging does not allow for cell-specific characterization. To overcome this limitation, we sought to identify an antibody that recognizes the functional luciferase protein present in positive controls and base-edited LumA mice, but not the truncated version in untreated mice.

Methods: Four antibodies were assessed via western blot for suitability to detect the restoration of functional luciferase following base editor correction in treated mice: this required binding the full luciferase protein, but not the truncated, unedited protein. The best performing antibodies were then used to develop an immunofluorescence protocol for histological examination of murine liver tissues.

Results: The superior antibody was a recombinant rabbit anti-luciferase antibody (abcam 185924). It had no non-specific banding in western blots and clearly indicated the presence of the functional luciferase protein in both luciferase-expressing controls and base edited LumA mice, but not in untreated LumA mice. Other antibodies exhibited multiple non-specific bands.

Conclusion: Western blotting and immunofluorescence provide the means to examine biodistribution and protein restoration at a histological level, and further immunofluorescence experiments are currently underway. The identification of a specific antibody to detect editing in this model provides a crucial tool to characterize base editing efficiency and LNP formulations. Examining protein restoration provides an important window into cellular distribution and the phenotypic effects of gene editors delivered in vivo.

Acknowledgements: NR was the recipient of the 2024 CSPA National Undergraduate Student Research Program Award.

26 - An Optimized Chiral Liquid Chromatography - Electrospray Ionization-Tandem Mass Spectrometry (LC-ESI-MS/MS) Ionization Method for the Enantioselective Determination of Underived Epoxyeicosatrienoic acids (EETs).

Fadumo Isse¹, Sara Helal¹, Ahmed El-Sherbeni², Dion R. Brocks¹, Ayman El-Kadi¹

¹University of Alberta, Edmonton, Canada, ²Tanta University, Tanta, Egypt

Purpose: Cytochrome P450 (CYPs) are become the hotspot of the research involving cardiovascular disease as CYP metabolic pathway of AA results in vasodilator and anti-inflammatory eicosanoids called epoxyeicosatrienoic acids (EETs) (1). The current reported chiral LC-MS/MS assays have either a long run time (about 100 min) (2) or there is a derivatization step involved in the process of EET quantification, adding further complexity (3), therefore, the objective of current assay was to develop and validate a

chiral assay for quantitation of underived EET enantiomers using Liquid Chromatography Mass Spectrometry (LC-MS/MS) with a short run time.

Methods: A specific mass transition was scanned for each EET regio-isomer by obtaining a unique multiple reaction monitoring (MRM). MS parameters such as the collision energy and the ionization polarity were optimized. The operational condition for liquid chromatography involved using suitable mobile phases consisting of organic phase: acetonitrile, methanol, and isopropyl alcohol. EETs separation was performed using a chiral reverse phase **REFLEC C-AMYLOSE** column and a gradient elution method. Other optimized parameters include flow rate, injection volume and the condition state of column.

Results: The method achieved efficient separation of the two enantiomers for each 4 regio-isomer EETs. The linearity of the calibration curves over the range used (10-600 ng/ml) was > 0.99 . The intra-run percent error and coefficient of variation (CV) were $\leq \pm 15 \%$. The inter-run percent error and coefficient of variation (CV) were $\leq \pm 15 \%$, and $\leq 15 \%$, respectively. The lowest quality control CV was $< 20 \%$. The run time was 20 minutes.

Conclusion: This LC-ESI-MS/MS chiral assay shows promise for measuring underived EETs with a short run time. The method was found to be accurate and precise in measuring the spiked standard EETs.

References

1. Spector AA, Fang X, Snyder GD, Weintraub NL. Epoxyeicosatrienoic acids (EETs): metabolism and biochemical function. *Prog Lipid Res.* 2004;43(1):55-90.
2. Kiss L, Bier J, Röder Y, Weissmann N, Grimminger F, Seeger W. Direct and simultaneous profiling of epoxyeicosatrienoic acid enantiomers by capillary tandem column chiral-phase liquid chromatography with dual online photodiode array and tandem mass spectrometric detection. *Anal Bioanal Chem.* 2008;392(4):717-26.
3. Mesaros C, Lee SH, Blair IA. Analysis of epoxyeicosatrienoic acids by chiral liquid chromatography/electron capture atmospheric pressure chemical ionization mass spectrometry using $[^{13}\text{C}]$ -analog internal standards. *Rapid Commun Mass Spectrom.* 2010;24(22):3237-47.

Potential role of lipophagy inhibition for anticancer effects of glycolysis-suppressed pancreatic ductal adenocarcinoma cells

Zhang Zhiheng¹, Aoki Haruna¹, Umezawa Keitaro², Kranrod Joshua³, Miyazaki Natsumi¹, Oshima Taichi¹, Hirao Takuya⁴, Miura Yuri², Seubert John³, Ito Kousei¹, Aoki Shigeki¹

¹Chiba University, ²Tokyo Metropolitan Institute of Gerontology, ³University of Alberta, ⁴International University of Health and Welfare

Although increased aerobic glycolysis is common in various cancers, pancreatic ductal adenocarcinoma (PDAC) cells can survive a state of glycolysis suppression. We aimed to identify potential therapeutic targets in glycolysis-suppressed PDAC cells. By screening anticancer metabolic compounds, we identified SP-2509, an inhibitor of lysine-specific histone demethylase 1A (LSD1), which dramatically decreased the growth of PDAC cells (PANC-1, PK-1, and KLM-1 cell lines) and showed an anti-tumoral effect in tumor-bearing mice. Another LSD1 inhibitor, OG-L002, could also suppress PDAC cell growth. However, the anticancer effects of these compounds on PDAC cells were unrelated to LSD1. To investigate how PDAC cells survive in a glycolysis-suppressed condition, we conducted proteomic analyses. These results combined with our previous findings suggested that glucose-starvation causes PDAC cells to enhance mitochondrial oxidative phosphorylation. In particular, mitochondrial fatty acid metabolism was identified as a key factor contributing to the survival of PDAC cells under glycolysis suppression. We further demonstrated that SP-2509 and OG-L002 disturbed fatty acid metabolism and induced lipid droplet accumulation through the inhibition of lipophagy, but not bulk autophagy. These findings indicate a significant potential association of lipophagy inhibition and anticancer effects in glycolysis-suppressed PDAC cells, offering ideas for new therapeutic strategies for PDAC by dual inhibition of glycolysis and fatty acids metabolism.

Investigating the mechanism of myeloperoxidase-mediated toxicity of the industrial contaminant, 6-PPD, in vitro

Steven Lockhart¹, Arno Siraki¹, Newton Tran¹, Dinesh Babu², Lusine Tonoyan³, Béla Reiz⁴

¹Faculty of Pharmacy & Pharmaceutical Sciences, Katz Group-Rexall Centre for Pharmacy and Health Research, University of Alberta, Edmonton, Alberta, T6G 2E1, Canada, ²Faculty of Medicine & Dentistry - Medical Microbiology and Immunology Dept, University of Alberta, Alberta, Canada, ³Applied Pharmaceutical Innovation, Edmonton AB, T6G 2E1, ⁴Department of Chemistry, 11227 Saskatchewan Drive, University of Alberta, Edmonton, Alberta, T6G 2G2, Canada

PurposeA product of the industrial contaminant, 6-PPD (N-[1,3-Dimethylbutyl]-N'-phenyl-p-phenylenediamine), has been recently reported as highly toxic to coho salmon and potentially toxic to other aquatic organisms. The potential toxicity of 6-PPD in humans, however remains unknown. The enzyme myeloperoxidase (MPO) in neutrophils, is known to produce free radicals and oxidized metabolites from xenobiotics therefore its role in 6-PPD-mediated toxicity was investigated.

MethodsUV-visible spectroscopy and liquid chromatography-mass spectrometry (LC/MS) were performed to investigate the MPO mediated oxidation of 6-PPD and identify possible metabolites in the absence/presence of glutathione (GSH). 6-PPD's cytotoxicity, effect on mitochondrial membrane potential (MMP), and GSH depleting ability in the HL-60 cell line, a MPO-rich human leukemia cell line, were assessed. Electron paramagnetic resonance (EPR) and DMPO spin-trap was applied to capture the possible radical products in the presence of GSH.

ResultsUV-Vis analysis of MPO-catalyzed oxidation of 6-PPD demonstrated changes in 6-PPD spectrum, whereas GSH addition altered the spectrum indicating possible GSH conjugation. LC/MS showed the formation of multiple products, including GSH-6-PPD conjugates, and a GSH-4-hydroxydiphenylamine conjugate (a known 6-PPD degradant) which could potentially induce cytotoxicity. 6-PPD demonstrates a positive concentration dependent relationship with cytotoxicity whereas GSH level was decreased by 6-PPD in HL-60 cells. With increasing 6-PPD levels, MMP decreased which suggest cellular mitochondrial depolarization occurred. EPR spin-trapping demonstrated a concentration-dependent relationship between 6-PPD and GS radical signal intensity in the presence of H₂O₂. Spin-trapping of mitochondrial radical also shows a positive relationship with 6-PPD's concentration.

Conclusion6-PPD's oxidation can induce radical products formation and GSH conjugation in the presence of MPO. Furthermore, 6-PPD induces toxicity, disrupts MMP and depletes GSH in MPO-rich HL-60 cells. Our results suggest that MPO could be an activator of 6-PPD's toxicity in humans. A potential relationship between 6-PPD's oxidative metabolites and toxicity mechanism requires deeper investigation to determine its toxicity in mammals, including humans.

Increased interleukin-1 receptor antagonist (IL-1Ra) in human islets protects beta cells from amyloid-mediated apoptosis - Implications in type 2 diabetes and islet transplantation

Danish Malhotra¹, Rushie Tyagi¹, Lucy Marzban¹

¹University of Manitoba, Winnipeg, MB

Purpose: Type 2 diabetes (T2D) is characterized by insulin resistance, impaired beta-cell function, and death. Islet amyloid, formed by aggregation of human islet amyloid polypeptide (hIAPP, amylin), contributes to islet inflammation and beta-cell death in T2D. Islet amyloid also forms in cultured and transplanted human islets. We previously showed that amyloid formation promotes interleukin-1 (IL-1) beta production in human islets, which leads to beta-cell upregulation of the Fas cell death receptor and apoptosis. Amyloid-induced IL-1beta production may lead to imbalance between IL-1beta and its natural inhibitor IL-1 receptor antagonist (IL-1Ra), thereby promoting islet inflammation. In this study, we tested if increasing the local production of IL-1Ra can reduce amyloid-mediated beta-cell death.

Methods: Isolated human islets (n=3 donors; purity: >90% assessed by dithizone) were transduced with adeno-IL-1Ra to increase the local expression of IL-1Ra in islets. Transduced islets were cultured in normal (5.5 mM) or elevated (11.1 mM) glucose (to form amyloid) for 5 days. Paraffin-embedded islet sections were used for quantitative immunolabelling for insulin, IL-1beta, thioflavin S (amyloid), TUNEL and caspase-3 (apoptosis). Islet culture medium was collected to assess islet IL-1beta release (by ELISA).

Results: Human islets cultured in normal glucose formed little or no amyloid and had low levels of IL-1beta. However, islets cultured in elevated glucose formed amyloid during culture which was associated with elevated islet IL-1beta levels, and the proportion of TUNEL and caspase-3 positive beta cells. Following culture, adeno-IL-1Ra transduced islets had lower number of TUNEL and caspase-3 positive beta cells than non-transduced islets.

Conclusion: These findings suggest that local elevation of IL-1Ra in human islets can reduce IL-1beta-mediated amyloid-induced beta-cell death. Modulation of islet IL-1beta/IL-1Ra balance may therefore provide a therapeutic strategy to protect human islets from amyloid-mediated beta-cell death in patients with T2D and islet grafts.

Differentiated HL-60 cells as a surrogate model to study NETosis

Othman Eldalal¹, Dinesh Babu¹, Joshua Kranrod¹, John Seubert¹, Ahmad Alammari¹, Ayman El-Kadi¹, Lusine Tonoyan², Arno Siraki¹

¹Faculty of Pharmacy and Pharmaceutical Sciences, College of Health Sciences, University of Alberta, Edmonton, Alberta, Canada,

²Applied Pharmaceutical Innovation, Katz Group-Rexall Centre for Pharmacy and Health Research, University of Alberta, Edmonton, Canada.

Background: Neutrophils serve as key players in the innate immune response, and the differentiated human promyelocytic leukemia cell line (dHL-60) offers a valuable model for understanding neutrophil functions as they behave like human neutrophils. However, the choice of differentiating agents for generating neutrophil-like cells from HL-60 remains a matter of debate. Key considerations include cell phenotypic and functional resemblance to primary neutrophils, including the ability to undergo NETosis, a regulated form of neutrophil cell death through neutrophil extracellular trap (NET) formation.

Purpose: Our aim was to select and characterize an appropriate differentiation agent in order to establish a reliable neutrophil-like cell model using HL-60 cells to investigate NETosis and determine the effects of modulating myeloperoxidase (MPO) activity.

Methods: Dimethylformamide (DMF) and dimethyl sulfoxide (DMSO) were used as differentiation agents, and the cell differentiation was assessed through various assays, including UV-visible spectroscopy, immunoblotting, and electron paramagnetic resonance (EPR) spectroscopy, to measure MPO activity and protein expression, and the respiratory burst. Phorbol myristate acetate (PMA) and Sytox Green and fluorescence microscopy were used to discern the molecular mechanism of NETosis release.

Results: DMF- and DMSO-differentiated HL-60 cells showed a decrease in MPO activity and protein expression, and elevated superoxide formation compared to undifferentiated HL-60 cells, indicating successful cell differentiation with both agents. Fluorescence imaging with Sytox Green staining showed NET formation and cell death following PMA treatment of DMF- and DMSO-differentiated HL-60 cells. Our findings suggest that DMF-differentiated HL-60 cells may offer a suitable model for studying the NADPH oxidase (NOX)-dependent pathway of NETosis, as evidenced by higher superoxide activity compared to DMSO-differentiated HL-60 cells. **Conclusion:** This study emphasizes the critical importance of selecting the appropriate differentiating agents when using dHL-60 cells as a model for investigating neutrophil responses, such as NETosis and MPO modulation.

Efficiency and Microstructural Characterization of Decellularized Porcine Uterine for Regenerative Medicine

Abbas Fazel Anvari-Yazdi¹, Daniel J. MacPhee², Kobra Tahermanesh³, Maryam Ejlali⁴, Ildiko Badea⁵, Xiagbiao Chen⁶

¹Division of Biomedical Engineering, College of Engineering, University of Saskatchewan, Saskatoon, SK, Canada, ²Department of Veterinary Biomedical Sciences, Western College of Veterinary Medicine, University of Saskatchewan, Saskatoon, SK, Canada,

³Department of Obstetrics and Gynecology, College of Medicine, Iran University of Medical Sciences (IUMS), Tehran, Tehran, Iran,

⁴Iran University of Medical Sciences (IUMS), Tehran, Tehran, Iran, ⁵Drug Discovery and Development Research Group, College of Pharmacy and Nutrition, University of Saskatchewan, Saskatoon, SK, Canada, ⁶Department of Mechanical Engineering, University of Saskatchewan, 57 Campus Dr, S7K 5A9 Saskatoon, Canada

Purpose: The development of new treatments for uterine diseases holds significant clinical value. One promising strategy is the use of decellularized uterine extracellular matrix (dUECM) Comprised of growth factors, collagens, elastin, proteoglycans, glycosaminoglycans (GAGs), and laminins, dUECM provides essential cues to recreate the native tissue environment and offers functional support for cellular adhesion and interactions. Therefore, dUECM is a promising material for tissue engineering and 3D bioprinting applications.

Methods: A protocol was developed to decellularize pig uterine tissues for use in research on 3D bioprinting and uterine disease modelling. Uterine tissue was cut into 3cm transversal slices, followed by washing with phosphate-buffered saline for 48 h and treatment with SDS, Triton® X-100 detergents and DNase I enzyme to remove cellular material. The resulting dUECM powder was characterized for DNA content and morphology.

Results: A significant decrease in DNA content post-decellularization was observed indicating the removal of cellular remnants. The quantity of DNA in the native tissue of 9142.67 ± 26.63 ng/mg decreased significantly to 853.21 ± 12.84 ng/mg when treated with detergent and to 34.40 ± 33.34 ng/mg when DNase I was added to the treatment ($P < 0.01$). This reduction was further confirmed by DAPI and H&E staining, which showed the absence of stained nuclei, and gel electrophoresis analysis, which displayed no DNA fragments after treatment with DNase I. Scanning electron microscopy (SEM) demonstrated complete decellularization, with preserved collagen architecture and the absence of cellular debris.

Conclusion: These findings highlight the potential of dUECM in tissue engineering and regenerative medicine, particularly for applications related to uterine diseases. By providing a suitable microenvironment, decellularized matrices offer a platform for developing innovative therapies and models for studying uterine conditions for females This study establishes a foundation for further exploration and development of dUECM-based approaches to address the clinical challenges associated with uterine diseases.

References : [1] Sawkins, Michael J., et al. "ECM hydrogels for regenerative medicine." Extracellular Matrix for Tissue Engineering and Biomaterials (2018): 27-58.; [2] McInnes, A.D.; Moser, M.A.J.; Chen, X. Preparation and Use of Decellularized Extracellular Matrix for Tissue Engineering. J. Funct. Biomater. 2022.

